nature communications

Article

https://doi.org/10.1038/s41467-023-35984-5

Benchmark single-step ethylene purification from ternary mixtures by a customized fluorinated anion-embedded MOF

Received: 28 October 2022

Accepted: 11 January 2023

Published online: 25 January 2023

Check for updates

Yunjia Jiang,[1,4], Yongqi Hu,[1,4], Binquan Luan,[2], Lingyao Wang,[1], Rajamani Krishna,[3], Haofei Ni,[1], Xin Hu[1] & Yuanbin Zhang[1]

Ethylene (C_2H_4) purification from multi-component mixtures by physical adsorption is a great challenge in the chemical industry. Herein, we report a GeF_6^{2-} anion embedded MOF (ZNU-6) with customized pore structure and pore chemistry for benchmark one-step C_2H_4 recovery from C_2H_2 and CO_2. ZNU-6 exhibits significantly high C_2H_2 (1.53 mmol/g) and CO_2 (1.46 mmol/g) capacity at 0.01 bar. Record high C_2H_4 productivity is achieved from C_2H_2/CO_2/C_2H_4 mixtures in a single adsorption process under various conditions. The separation performance is retained over multiple cycles and under humid conditions. The potential gas binding sites are investigated by density functional theory (DFT) calculations, which suggest that C_2H_2 and CO_2 are preferably adsorbed in the interlaced narrow channel with high aff0inity. In-situ single crystal structures with the dose of C_2H_2, CO_2 or C_2H_4 further reveal the realistic host-guest interactions. Notably, rare C_2H_2 clusters are formed in the narrow channel while two distinct CO_2 adsorption locations are observed in the narrow channel and the large cavity with a ratio of 1:2, which accurately account for the distinct adsorption heat curves.

Ethylene (C_2H_4) is the foremost olefin as well as the highest volume product in the petrochemical industry, with an annual production capacity exceeding 214 million tons in 2021[1]. The manufacture of C_2H_4 and C_3H_6 accounts for 0.3% of global energy[2]. Current C_2H_4 production mainly relies on stream cracking of hydrocarbons[3–6]. Alternatively, oxidative coupling of methane (CH_4) has emerged as a promising technique to produce C_2H_4, among which acetylene (C_2H_2) and carbon dioxide (CO_2) are generated as byproducts and need to be deeply removed to produce polymer grade (>99.996%) C_2H_4[7]. Presently, multi-step purification process is adopted for purification of C_2H_4 from C_2H_4/C_2H_2/CO_2 mixtures in industry[8]. C_2H_2 is removed by catalytic hydrogenation using expensive noble-metal catalysts or solvent extraction, which is either energy intensive or associated with pollution[9,10]. CO_2 is removed by chemical adsorption using caustic soda, which causes huge waste of costly solvents[11].

Physical adsorption offers potential to significantly reduce the energy footprint of separation processes[12–21]. Nonetheless, C_2H_4 purification from ternary C_2H_4/C_2H_2/CO_2 mixtures remains an unmet challenge due to the similarity in molecular size and polarity (Supplementary Table 2), although separation of C_2H_2/C_2H_4[22–26] or C_2H_2/CO_2[27–32] binary mixtures has been realized by a plethora of porous materials. Besides, single-step purification of C_2H_4 from ternary C_2H_2/C_2H_4/C_2H_6[33,34] or quaternary C_2H_2/C_2H_4/C_2H_6/CO_2[35] mixtures has also been realized by several porous materials. To date, less than ten materials have been demonstrated to separate C_2H_4 from C_2H_4/C_2H_2/CO_2, including activated carbons, zeolites, covalent organic frameworks

[1]Key Laboratory of the Ministry of Education for Advanced Catalysis Materials, College of Chemistry and Life Sciences, Zhejiang Normal University, Jinhua 321004, China. [2]IBM Thomas J. Watson Research, Yorktown Heights, New York, NY 10598, USA. [3]Van't Hoff Institute for Molecular Sciences, University of Amsterdam, Science Park 904, 1098 XH Amsterdam, the Netherlands. [4]These authors contributed equally: Yunjia Jiang, Yongqi Hu.
e-mail: ybzhang@zjnu.edu.cn

and metal organic framework (MOFs)[36–39]. TIFSIX-17-Ni[36], NTU-65[37], and NTU-67[38] are so far the three optimal materials. TIFSIX-17-Ni[36] exhibits high C_2H_2/C_2H_4 and CO_2/C_2H_4 selectivity due to the negligible uptake of C_2H_4 under ambient condition. However, the capacity of C_2H_2 (3.30 mmol/g) and CO_2 (2.20 mmol/g) is relatively low due to the over-contracted channel. NTU-65[37] can selectively capture C_2H_2 and CO_2 by tuning the gate opening. However, the applied temperature must be at 263 K because lower temperatures lead to the adsorption of all the gases while higher temperatures cause the exclusion of CO_2. NTU-67[38] displays similar C_2H_2 (3.29 mmol/g) and CO_2 (2.04 mmol/g) capacity, but the C_2H_2/C_2H_4 and CO_2/C_2H_4 selectivity is greatly reduced as the C_2H_4 capacity (1.41 mmol/g) is relatively high. Additionally, the separation performance is deteriorated under humid conditions. Therefore, there is still a lack of ideal and stable materials to realize the simultaneous removal of C_2H_2 and CO_2 in $C_2H_2/CO_2/C_2H_4$ mixtures.

In this work, we reported a GeF_6^{2-} anion embedded MOF ZNU-6 (ZNU = Zhejiang Normal University) with large cages (~8.5 Å diameter) connected by narrow interlaced channels (~4 Å diameter) for benchmark one-step C_2H_4 recovery from C_2H_2 and CO_2. ZNU-6 is constructed by $CuGeF_6$ and tri(pyridin-4-yl)amine (TPA) and exhibits excellent chemical stability. Static gas adsorption isotherms showed that ZNU-6 takes up 1.53/8.06 mmol/g of C_2H_2 and 1.46/4.76 mmol/g of CO_2 at 0.01 and 1.0 bar (298 K), respectively. The calculated IAST selectivities for C_2H_2/C_2H_4 (1/99) and CO_2/C_2H_4 (1/99) are 43.8–14.3 and 52.6–7.8 (0.0001–1.0 bar), respectively. The calculated Q_{st} values at near-zero loading for C_2H_2 and CO_2 are 37.2 and 37.1 kJ/mol, indicative of its facility for material regeneration but much higher than that of C_2H_4 (29.0 kJ/mol). Modeling study indicates that there are two potential binding sites for C_2H_2, C_2H_4, and CO_2. One is in the interlaced channel and the other locates in the large cage. Moreover, all gas molecules prefer to be adsorbed in the interlaced channel with higher affinity. The realistic binding sites and host–guest interactions under normal conditions (298 K and 1.0 bar) were further demonstrated by in-situ single crystal structures with the saturated dose of gases. Notably, rare C_2H_2 clusters formed by π···π packing and C-H···C≡C interactions are observed in the interlaced channel with a small proportion of C_2H_2 molecules adsorbed in the large cage additionally. In sharp contrast, only 1/3 of CO_2 molecules are located in the narrow channel while 2/3 of CO_2 molecules are accommodated in the large cavity. This distinct gas distribution is highly consistent with the difference of adsorption heat curves. The practical C_2H_4 purification performance is further demonstrated by dynamic breakthroughs and record high C_2H_4 productivity is achieved from ternary $C_2H_2/CO_2/C_2H_4$ mixtures in a single adsorption process under various conditions. The separation performance is retained over multiple cycles and under humid conditions.

Results

Violet single crystals of ZNU-6 (Supplementary Fig. 1) were produced by layering a MeOH solution of TPA onto an aqueous solution of $CuGeF_6$ (Fig. 1a). X-ray crystal analysis revealed that ZNU-6 [$Cu_6(GeF_6)_6(TPA)_8$] crystallizes in a three-dimensional (3D) framework in the cubic Pm-3n space group. Every unit cell consists of six Cu^{2+} ions, six GeF_6^{2-} anions, and eight tridentate TPA ligands (Supplementary Table 1). The combination of Cu^{2+} and TPA produces a cationic pto network first (Fig. 1b), which determines the main pore size. The network is further embedded by GeF_6^{2-} pillar to give a ith-d topology framework with optimal pore chemistry (Fig. 1c). The frameworks are composed of large icosahedral cage-like pores (~8.5 Å) and interlaced narrow channels (~4 Å) (Fig. 1d–f). Each large cage is surrounded by 12 channels and every interlaced channel connects 4 cages. The adjacent two cages and two channels share the same GeF_6^{2-} anions at the edge. Both large pores and interlaced channels are abundant of Lewis basic F functional sites on the surface for gas binding. Such interconnected large cages and narrow channels are distinct from previous straight 1D channels of anion pillared MOFs (e.g., SIFSIX-1-Cu, SIFSIX-3-Ni). Besides, the narrow channel size may provide kinetic selectivity for C_2H_2 (3.3 Å) and CO_2 (3.3 Å) given their small molecular size compared to C_2H_4 (4.2 Å). Thus, ZNU-6 with abundant functional GeF_6^{2-} binding sites, high porosity for C_2H_2 and CO_2 accommodation and narrow channel for kinetic preference features the promising characteristics for efficient purification of C_2H_4 from ternary $C_2H_2/CO_2/C_2H_4$ mixture.

The intrinsic porosity of ZNU-6 was investigated by N_2 adsorption at 77 K. As shown in Fig. 2a, ZNU-6 exhibited a type I adsorption isotherm. The Brunauer–Emmett–Teller surface area and pore volume were calculated to be 1330.3 m^2/g and 0.554 cm^3/g (Supplementary Fig. 10). The calculated pore size ranges from 8.22 to 10.76 Å with the summit in 9.0 Å, highly close to the pore aperture of ~8.5 Å evaluated from the single crystal structure (Fig. 2a). Then, single-component adsorption isotherms of C_2H_2, CO_2, and C_2H_4 were collected at 298 K (Fig. 2b). At 1.0 bar, the C_2H_2 and CO_2 uptakes are 8.06 and 4.76 mmol/g, higher than those of most APMOFs (Fig. 2c). The capacities are equal to 4.68 and 2.77 gas molecules per GeF_6^{2-} anion. Such high C_2H_2/anion and CO_2/anion uptakes have never been realized in anion pillared MOFs (Supplementary Table S7)[36–38,40–44]. Particularly, C_2H_2/anion and CO_2/anion uptakes in benchmark TIFSIX-17-Ni[36], SIFSIX-17-Ni[36] and NTU-67[38] are only 1.36/0.91, 1.29/0.9 and 2.06/1.28, respectively (Supplementary Fig. 25). So far, isomorphic SIFSIX-Cu-TPA[40] displays the ever highest C_2H_2/anion (4.44) uptake while SIFSIX-1-Cu[41] displays the ever highest CO_2/anion (2.72) uptake. It is worth mentioning that these records have been marginally surpassed by ZNU-6's (Supplementary Fig. 25). Notably, the uptakes of C_2H_2 and CO_2 on ZNU-6 at 0.01 bar are as high as 1.53 and 1.46 mmol/g, superior to those of all the porous materials in the context of ternary $C_2H_2/CO_2/C_2H_4$ separation, such as TIFSIX-17-Ni (1.38/0.32 mmol/g)[36], SIFSIX-17-Ni (0.91/0.20 mmol/g)[36], NTU-67 (0.47/0.65 mmol/g)[38], and TpPa-NO_2 (0.17/0.03 mmol/g)[39]. At 0.1 bar, the capacities of C_2H_2 and CO_2 reach up to 4.64 and 2.21 mmol/g (Fig. 2b), even higher than the uptakes of many porous materials at 1 bar and 298 K, for example, TIFSIX-17-Ni (3.30/2.20 mmol/g)[36]. In the meantime, the C_2H_4 uptakes on ZNU-6 at 0.01 and 0.1 bar are only 0.15 and 1.07 mmol/g, much lower than those of C_2H_2 and CO_2 under the same conditions. The C_2H_2, CO_2, and C_2H_4 adsorption isotherms were further collected at 278 and 308 K (Fig. 2d). The adsorption capacities of C_2H_2 and CO_2 at 1 bar increase to 8.74 and 6.26 mmol/g at 278 K. As selectivity is also an important parameter to assess the separation performance, we further calculated the C_2H_2/C_2H_4 and CO_2/C_2H_4 selectivities on ZNU-6 using ideal adsorbed solution theory (IAST) after fitting isotherms into dual site Langmuir or single site Langmuir equation with excellent accuracy. The IAST selectivity for 1/99 C_2H_2/C_2H_4 is 43.8–14.3 (Fig. 2e), higher than those of NTU-67 (8.1)[38] and TpPa-NO_2 (5.9)[39]. The IAST selectivities for 1/99 CO_2/C_2H_4 mixture is also as high as 52.6-7.8 (Fig. 2e). Besides, both C_2H_2/C_2H_4 and CO_2/C_2H_4 selectivity on ZNU-6 is improved with the pressure decrease or the increase of C_2H_4 ratios (from 90% to 99%) in the binary mixtures (Supplementary Figs. 13, 14), indicating ZNU-6 is favored for trace C_2H_2 and CO_2 capture from bulky C_2H_4 mixtures. Apart from the IAST selectivity, the Henry coefficients were also calculated to evaluate the Henry's selectivity of ZNU-6 (Supplementary Figs. 15–17), the Henry's selectivity for C_2H_2/C_2H_4 and CO_2/C_2H_4 is 8.2 and 7.8, respectively, superior to those of NTU-67 (2.4/4.2)[38] and TpPa-NO_2 (4.0/1.8)[39] (Supplementary Tables 4, 5). We further calculated the isosteric enthalpy of adsorption (Q_{st}) for ZNU-6 by using the Clausius-Clapeyron equation. Q_{st} values at near-zero loading for C_2H_2, CO_2, and C_2H_4 are 37.2, 37.1, and 29.0 kJ/mol (Fig. 2f), respectively, indicative of the preferred affinity of C_2H_2 and CO_2 over C_2H_4. Notably, the Q_{st} values for C_2H_2 and CO_2 on ZNU-6 are only modestly high and slightly lower than those of many top-performing materials in the context of C_2H_4 purification, such as SIFSIX-17-Ni (44.2/40.2 kJ/mol)[36], TIFSIX-17-Ni (48.3/37.8 kJ/mol)[36], and NTU-67 (44.1/41.5 kJ/mol)[38]. Such moderate Q_{st} endows facile regeneration of ZNU-6 under mild conditions.

https://doi.org/10.1038/s41467-023-35984-5

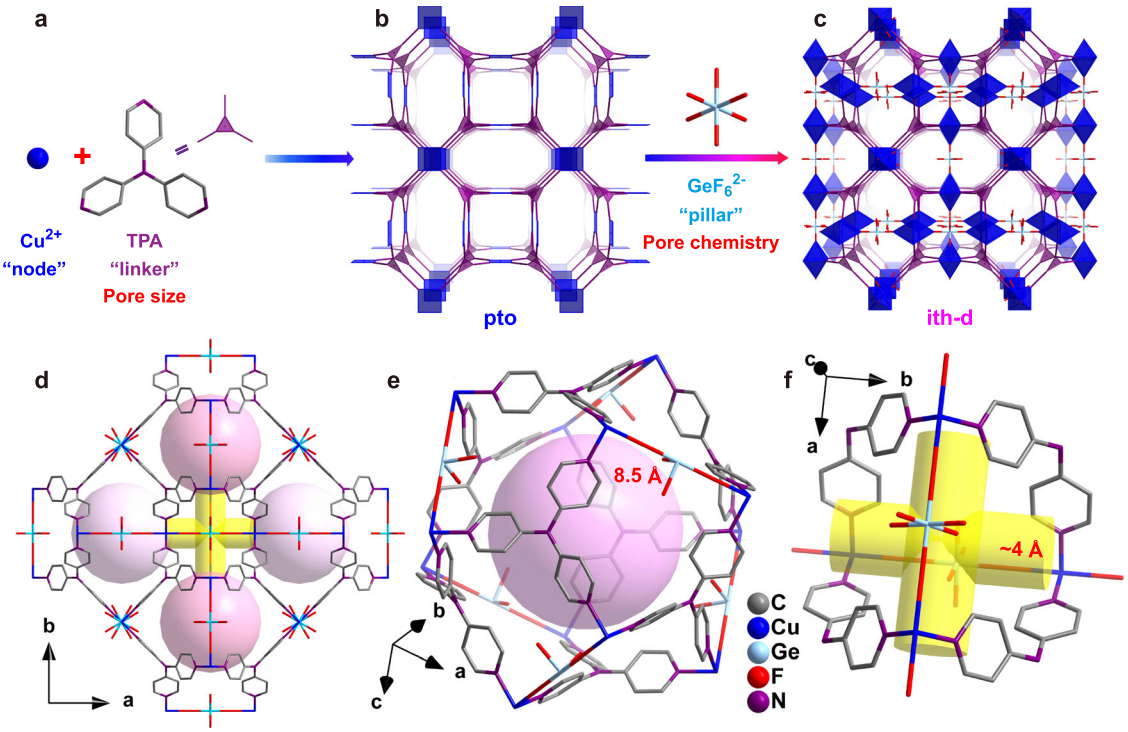

Fig. 1 | Porous structure of ZNU-6. a–c Exquisite control of pore size/shape and pore chemistry in ZNU-6 from pillared (3,4)-connected pto network to GeF_6^{2-} embedded ith-d topology framework; **d** Overview of ZNU-6 structure with cage-like pores and interlaced channels. **e** Structure and size of the cage-like pore. **f** Structure and size of the interlaced channel connecting four cages.

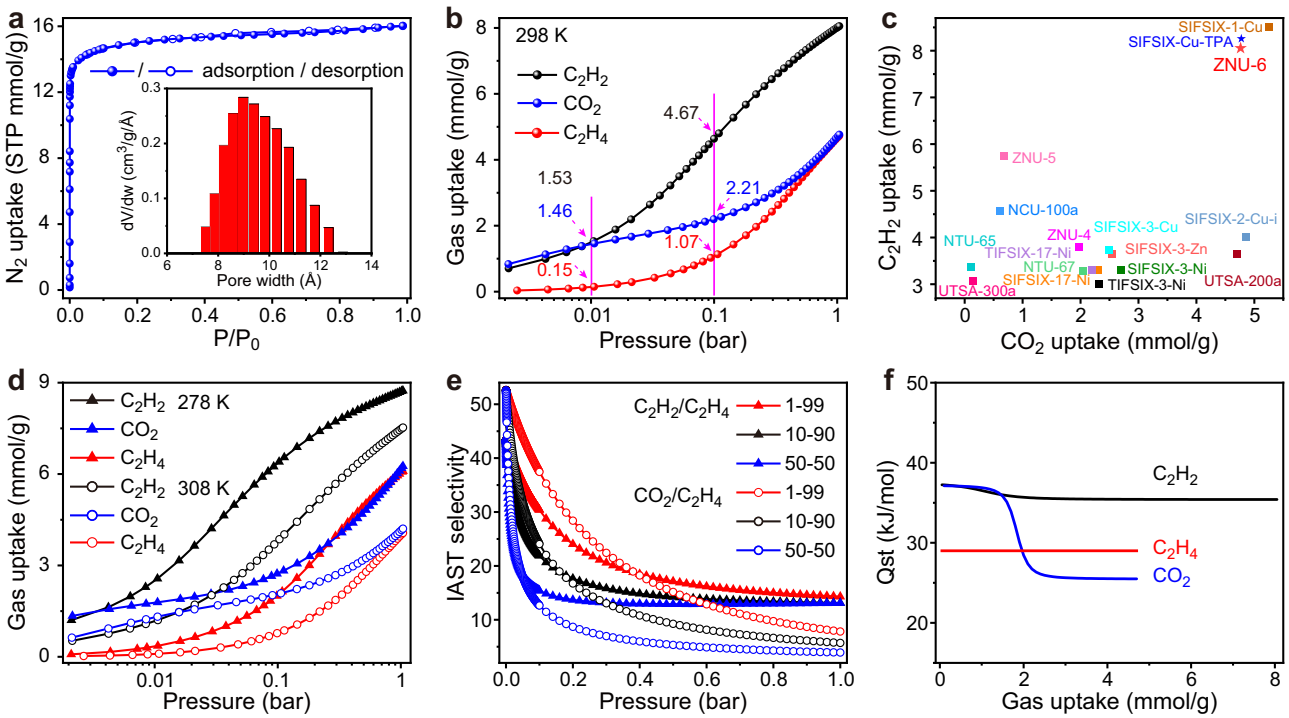

Fig. 2 | The sorption performance. a N_2 adsorption and desorption isotherms for ZNU-6 and the calculated pore size distribution. **b** C_2H_2, CO_2, and C_2H_4 adsorption isotherms of ZNU-6 at 298 K. **c** Comparison of the saturated C_2H_2 and CO_2 uptake (1 bar, 298 K) among anion pillared MOFs. **d** C_2H_2, CO_2, and C_2H_4 adsorption isotherms of ZNU-6 at 278/308 K. **e** C_2H_2/C_2H_4 and CO_2/C_2H_4 IAST selectivity of ZNU-6 at 298 K. **f** Q_{st} of C_2H_2, CO_2, and C_2H_4 in ZNU-6. Source data are provided as a Source Data file.

https://doi.org/10.1038/s41467-023-35984-5

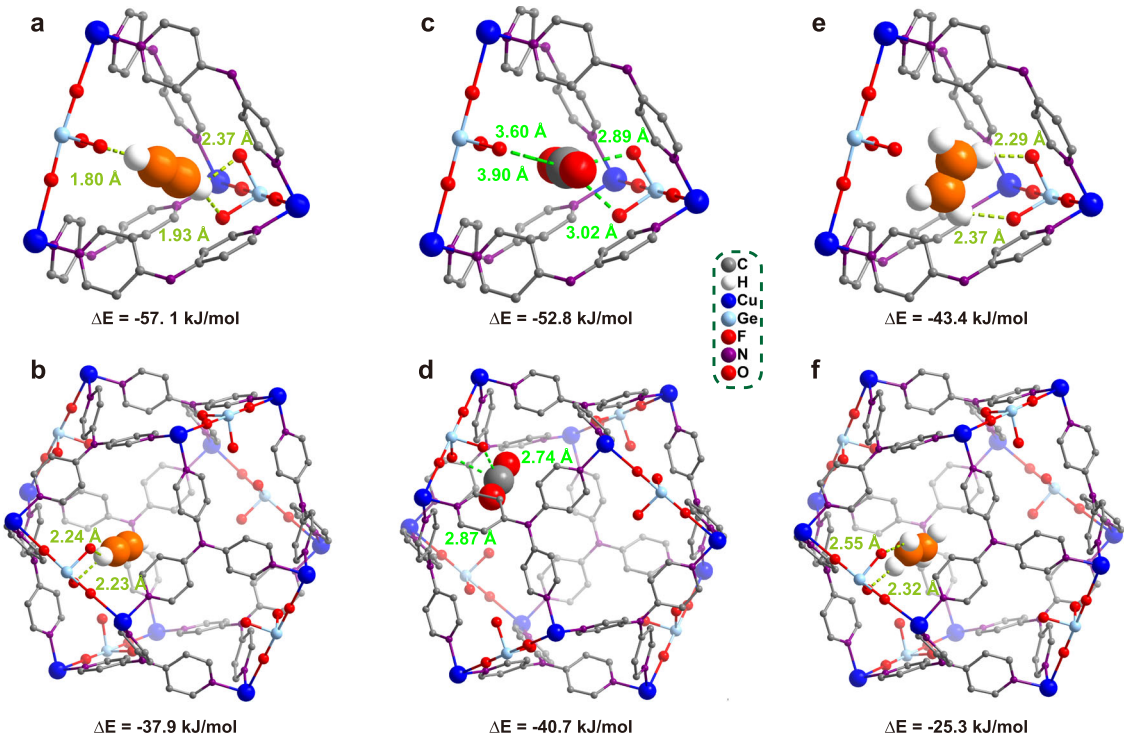

Fig. 3 | The DFT optimized gas adsorption configuration. Binding sites I, II of C_2H_2 (**a, b**), CO_2 (**c, d**), and C_2H_4 (**e, f**).

To gain more insights into the gas adsorption behavior, density functional theory (DFT)-based calculations (see Method section) were applied to identify the adsorption configuration and binding energies of C_2H_2, CO_2, and C_2H_4. For all gases, two different binding sites were observed. Site I is in the interlaced channel and Site II is in the large cavity (Fig. 3). For C_2H_2 in Site I, the two hydrogen atoms interact strongly with three F atoms with the distances of 1.80, 1.93, and 2.37 Å. The calculated binding energy is 57.1 kJ/mol (Fig. 3a). As for C_2H_2 adsorbed in Site II, only one hydrogen atom can interact with the adjacent F atoms with the distance of 2.23 and 2.24 Å, and the corresponding binding energy decreases to 37.9 kJ/mol (Fig. 3b), indicating that C_2H_2 is preferentially adsorbed in the narrow channel. The same results are also observed for CO_2 and C_2H_4, the binding energies in the channel are much higher than those in the large cage. In Site I, CO_2 is trapped by two strong and two weak electrostatic F···C=O interactions in the distance of 2.89, 3.02, 3.60, and 3.90 Å, the binding energy is 52.8 kJ/mol (Fig. 3c); C_2H_4 is adsorbed via two F···H interactions (2.29 and 2.37 Å) with the binding energy of 43.3 kJ/mol (Fig. 3e). In Site II, the binding energy of CO_2 drops to 40.7 kJ/mol with the number of electrostatic F···C=O interactions (2.74 and 2.87 Å) decreasing to two (Fig. 3d); the binding energy of C_2H_4 reduces to 25.3 kJ/mol with the length of F···H extending to 2.55 and 2.32 Å (Fig. 3f). In addition, it is notable that either in Site I or II, the binding energy of C_2H_2 or CO_2 is superior to that of C_2H_4, confirming that the adsorption of C_2H_2 or CO_2 in ZNU-6 is more preferable than that of C_2H_4.

Although DFT calculations have identified two different binding sites for each gas, it is still difficult to understand the distinct adsorption heat curves. Therefore, we further studied the in-situ structures of ZNU-6 with gas loading (Fig. 4). We found that averagely 25.78 C_2H_2, 18 CO_2, or 13.07 C_2H_4 molecules can be adsorbed per unit cell of ZNU-6 (Supplementary Table 1), corresponding to 4.3 C_2H_2, 3.0 CO_2, and 2.2 C_2H_4 molecules for each GeF_6^{2-} anion, which are close to the saturated values from gas adsorption isotherms (4.63 C_2H_2, 2.77 CO_2, and 2.75 C_2H_4). Both of C_2H_2 and CO_2 have two binding sites, i.e., Site I in the interlaced channel and Site II in the large cage. Notably, the amount of C_2H_2 molecules distributed to the two locations is 3.8 and 0.5 per GeF_6^{2-} anion while that for CO_2 is 1 and 2 per GeF_6^{2-} anion (Fig. 4a, b). Such different gas distribution can precisely account for the C_2H_2 Q_{st} curve with a modest decrease and the CO_2 Q_{st} curve with a sharp decrease along the gas loading. Specifically, C_2H_2 molecules adsorbed in Site I bind to F atoms on the surface of the channels via multiple cooperative hydrogen bonds (C-H···F = 1.97–2.55 Å), and the others in Site II interact F atoms via single H···F hydrogen bond with the distance of 2.51 Å (Fig. 4a and Table 1). Besides, the C_2H_2 molecules in Site I aggregate to form a stacked gas cluster by π···π packing and C-H···C≡C interactions, which has rarely been observed previously. Regarding CO_2, it is trapped by F···C=O electrostatic interaction in Site I and II (Fig. 4b). The only difference is that the C···F distance is 2.64 Å in Site I and 2.80 Å in Site II (Table 1). From the single crystal structure, two different CO_2 molecules that are very close and opposite to each other in the narrow channel (site I) are observed. However, these two CO_2 molecules cannot exist in the same narrow channel at the same time and thus both CO_2 molecules display the occupancy of 50%. In Site II, the C atom of CO_2 is ordered while the O atoms are disordered to two perpendicular positions with the occupancy of 50% for each configuration. Besides, the linear CO_2 molecules are slightly bent due to the strong attraction from GeF_6^{2-} anion. The bent angle of 157.5° (in Site I) and 170.8° (in Site II) are consistent with the interaction strength. In term of C_2H_4, only one site in the narrow channel is found. The C atoms of C_2H_4 molecule are ordered while the H atoms are disordered. The distances of C-H···F interactions between C_2H_4 and framework are 2.31–2.64 Å (Fig. 4c and Table 1). Considering the slight lower C_2H_4/GeF_6^{2-} ratio observed in the single crystal structure, there should be some C_2H_4 molecules adsorbed in the large cage. However, due to the probable disorder of C_2H_4 molecules over the whole cage, the C_2H_4 molecules in Site II were not solved. Nonetheless, this uniform adsorption configuration is consistent with the flat Q_{st} curve for C_2H_4.

Apart from the C_2H_2, CO_2, or C_2H_4 molecules, some water molecules were also identified in the framework (Supplementary Fig. 4). As there is still a lot of space in the large cavity after saturated adsorption of C_2H_2, CO_2, or C_2H_4 gases at 100 kPa, the water adsorption behavior probably occurred during the single crystal measurement, which is

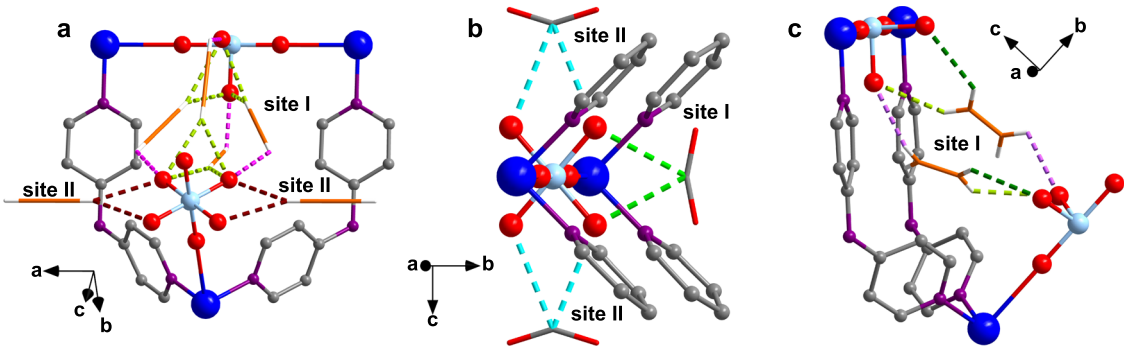

Fig. 4 | Single crystal structure of gas-loaded ZNU-6. a C_2H_2 @ ZNU-6 [$Cu_6(GeF_6)_6(TPA)_8$ $(C_2H_2)_{25.78}$]; **b** CO_2 @ ZNU-6 [$Cu_6(GeF_6)_6(TPA)_8$ $(CO_2)_{18}$]; **c** C_2H_4 @ ZNU-6 [$Cu_6(GeF_6)_6(TPA)_8$ $(C_2H_4)_{13.07}$].

exposed to air. Interestingly, these water molecules are distant from GeF_6^{2-}, indicating that these H_2O molecules do not occupy the binding sites for the targeted gases. Instead, some unique interactions are observed between the gas molecules and water molecules, e.g., O-H···C=O hydrogen bonds between CO_2 and H_2O. Notably, our resolved single crystal structures show completely different C_2H_2 and CO_2 adsorption configurations from those of isomorphic SIFSIX-Cu-TPA for C_2H_2/CO_2 separation in Wu's work[39].

Motivated by the high adsorption capacity and selectivity in single-component adsorption as well as the in-situ single crystal structure analysis, breakthrough experiments were conducted for C_2H_2/C_2H_4, CO_2/C_2H_4, and $C_2H_2/CO_2/C_2H_4$ mixtures. The results showed that highly efficient separations can be accomplished by ZNU-6 for all the gas mixtures under various conditions. For 1/99 C_2H_2/C_2H_4 mixtures, C_2H_4 is eluted at 12 mins while C_2H_2 is detected until 192 min. For 10/90 CO_2/C_2H_4 mixtures, C_2H_4 and CO_2 are detected at 12 and 43.5 min, respectively (Fig. 5a). For 1/1/98 $C_2H_2/CO_2/C_2H_4$ mixtures, C_2H_2 and CO_2 broke out simultaneously and 64.42 mol/kg of polymer grade C_2H_4 is produced by single adsorption process (Fig. 5b). The productivity is improved to 80.89 mol/kg when decreasing the temperature to 283 K (Supplementary Fig. 46). The CO_2 breakthrough time becomes shortened with the increase of CO_2 ratio, which is 72 and 52 min for 1/5/94 (Figs. 5c) and 1/9/90 (Fig. 5d) $C_2H_2/CO_2/C_2H_4$ mixtures. The polymer grade C_2H_4 productivity is 21.37 and 13.81 mol/kg, respectively. As most reported C_2H_4 productivity from $C_2H_2/CO_2/C_2H_4$ mixtures are compared under 1/9/90, a comparison plot of the C_2H_4 productivity and dynamic C_2H_2 capacity from 1/9/90 $C_2H_2/CO_2/C_2H_4$ mixtures is presented in Fig. 5e. ZNU-6 displays the record high C_2H_4 productivity and second highest C_2H_2 dynamic capacity. The C_2H_4 productivity of ZNU-6 is >2.5 folds of the previous benchmark of NTU-67 (5.42 mol/kg)[38]. C_2H_4 productivity with the unit of mol/kg/h is also calculated for comparison (Supplementary Table S10). ZNU-6 with the productivity of 15.93 mol/kg/h is the highest reported value.

In view of the importance of the recyclability and stability of porous materials for practical applications, the water and thermal stability of ZNU-6 was investigated. There was no noticeable loss in the CO_2 adsorption capacity after six cycles of adsorption/desorption experiments (Supplementary Fig. 26). Long time soaking of ZNU-6 in water or polar organic solvents such as DMSO, DMF and MeCN did not change the porous structure of ZNU-6, as demonstrated by the PXRD patterns as well as the gas adsorption isotherms (Supplementary Fig. 7). Thermogravimetric analysis (TGA) and temperature varied PXRD indicated ZNU-6 is stable below 200 °C (Supplementary Figs. 8, 9). Breakthroughs under humid conditions or over four cycles preserved nearly the identical separation performance (Fig. 5f). Although many water molecules can be adsorbed in ZNU-6, as described in in-situ crystals and water adsorption isotherms (Supplementary Fig. 27), the presence of humid has negligible influence on the separation performance (Fig. 5f). This is probably due to the co-adsorption of water and target gases as well as the fast $C_2H_2/CO_2/C_2H_4$ diffusion kinetics (Supplementary Fig. 29–31).

Table 1 | The distances of the host–guest interactions

Crystals	Site I	Site II
25.78 C_2H_2 @ ZNU-6	1.97/2.55 Å (C-H···F)	2.51 Å (C-H···F)
18 CO_2 @ ZNU-6	2.64 Å (C···F)	2.80 Å (C···F)
13.07 C_2H_4 @ ZNU-6	2.31/2.54/2.64 Å (C-H···F)	-

Discussion

In conclusion, we reported a GeF_6^{2-} anion embedded metal organic framework ZNU-6 with optimal pore structure and pore chemistry for benchmark one-step C_2H_4 purification by simultaneous removal of C_2H_2 and CO_2. ZNU-6 exhibits remarkably high C_2H_2 and CO_2 capacity under both low and high pressures. The C_2H_2/anion and CO_2/anion uptakes are the highest among all the anion pillared MOFs. 64.42, 21.37, 13.81 mol/kg polymer grade C_2H_4 can be produced from $C_2H_2/CO_2/C_2H_4$ (1/1/98, 1/5/94, 1/9/90) mixtures, all superior to the previous benchmarks. The separation performance is sustained over multiple cycles or under humid conditions. The potential gas binding sites are investigated by DFT calculation, which indicate that C_2H_2 and CO_2 are preferentially adsorbed in the interlaced narrow channel with high affinity. In-situ single crystal structures with the dose of C_2H_2, CO_2 or C_2H_4 further reveal the realistic host–guest interactions, accounting for the distinct shapes of the adsorption heat curves. In general, our work highlights the significance of regulating pore structure and pore chemistry in porous materials to construct multiple cooperative functionalities for gas separation.

Methods

Synthesis of ZNU-6

To a 5 mL long thin tube was added a 1 mL of aqueous solution with $Cu(NO_3)_2{\cdot}3H_2O$ (~1.3 mg) and $(NH_4)_2GeF_6$ (~1.0 mg). 2 mL of MeOH/H_2O mixture (v:v = 1:1) was slowly layered above the solution, followed by a 1 mL of MeOH solution of TPA (~1.0 mg). The tube was sealed and left undisturbed at 298 K. After ~1 week, purple single crystals were obtained.

Preparation of gas loaded ZNU-6

The crystalline sample of ZNU-6 was filled into a glass tube and heated at 120 °C under vacuum for 24 h. After the sample cooling down, CO_2, C_2H_2, or C_2H_4 was introduced into the sample respectively with Builder SSA 7000 (Beijing) instrument until the pressure reach to 1 bar at 298 K and the state is maintained for another hour. Then, the crystals were picked out, covered with the degassed oil, and single crystal X-ray diffraction measurements were then carried out at 298 K as soon as possible.

https://doi.org/10.1038/s41467-023-35984-5

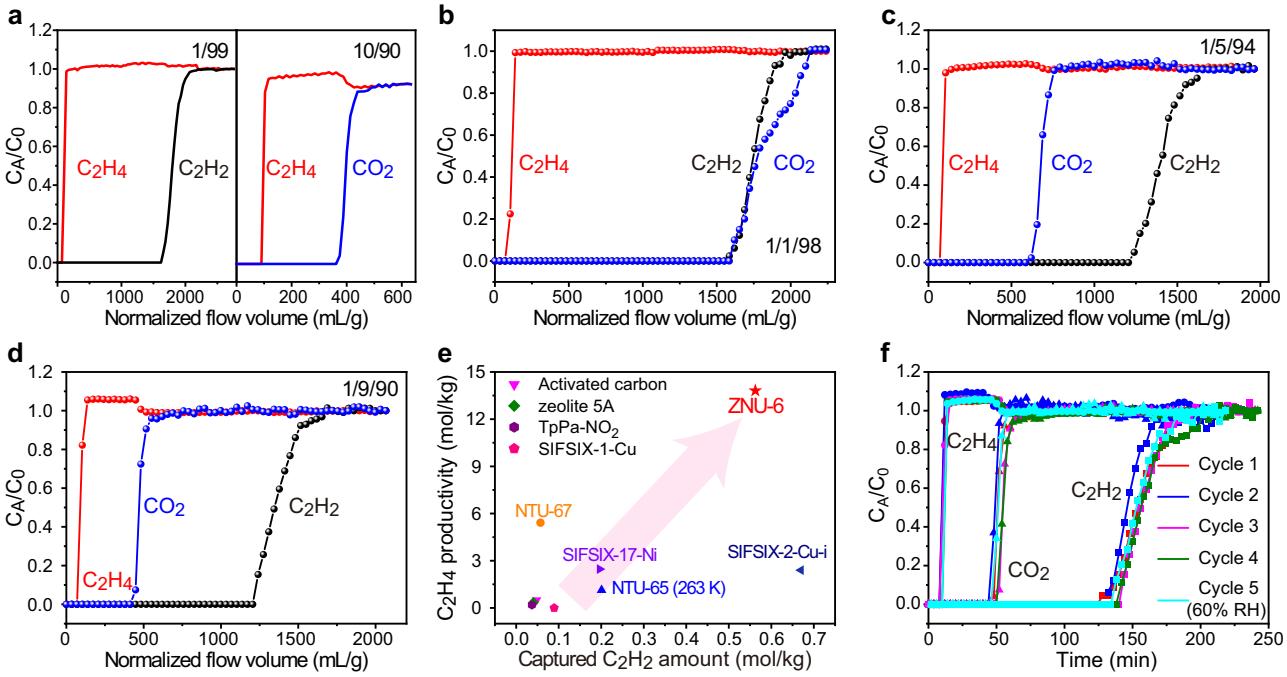

Fig. 5 | C_2H_4 purification. Experimental breakthrough curves of ZNU-6 for binary mixture **a** C_2H_2/C_2H_4 (1/99) and CO_2/C_2H_4 (10/90) at 298 K. Experimental breakthrough curves of ZNU-6 for ternary mixture **b** $C_2H_2/CO_2/C_2H_4$ (1/1/98), **c** $C_2H_2/CO_2/C_2H_4$ (1/5/94), and **d** $C_2H_2/CO_2/C_2H_4$ (1/9/90). **e** Comparison of the captured C_2H_2 amount and C_2H_4 productivity from $C_2H_2/CO_2/C_2H_4$ (1/9/90) ternary mixture. **f** Five cycles of experimental breakthrough curves of ZNU-6 for $C_2H_2/CO_2/C_2H_4$ (1/9/90) at 298 K (1–4: dry condition, 5: humid condition). Source data are provided as a Source Data file.

Single-crystal X-ray diffraction

Single-crystal X-ray diffraction studies were conducted on the BrukerAXS D8 VENTURE diffractometer equipped with a PHOTON-100/CMOS detector (GaKα, $\lambda = 1.34139$ Å). Indexing was performed using APEX2. Data integration and reduction were completed using SaintPlus 6.01. Absorption correction was performed by the multi-scan method implemented in SADABS. The space group was determined using XPREP implemented in APEX2.1 The structure was solved with SHELXS-97 (direct methods) and refined on F2 (nonlinear least-squares method) with SHELXL-97 contained in APEX2, WinGX v1.70.01, and OLEX2 v1.1.5 program packages. All non-hydrogen atoms were refined anisotropically. The contribution of disordered solvent molecules was treated as diffuse using the Squeeze routine implemented in Platon.

Powder X-ray diffraction

Powder X-ray diffraction (PXRD) data were collected on the SHIMADZU XRD-6000 diffractometer (Cu Kα$\lambda = 1.540598$ Å) with an operating power of 40 kV, 30 mA and a scan speed of 4.0°/min. The range of 2θ was from 5° to 50°.

Thermal gravimetric analysis

Thermal gravimetric analysis was performed on the TGA STA449F5 instrument. Experiments were carried out using a platinum pan under nitrogen atmosphere which conducted by a flow rate of 60 mL/min nitrogen gas. The data were collected at the temperature range of 50 °C to 600 °C with a ramp of 10 °C /min.

The static gas/vapor adsorption equilibrium measurements

The static gas adsorption equilibrium measurements were performed on the Builder SSA 7000 instrument. The water vapor adsorption equilibrium measurements were performed on the BeiShiDe DVS instrument. Before measurements, the sample of ZNU-6 (~100 mg) was evacuated at 25 °C for 2 h firstly, and then at 120 °C for 12 h until the pressure dropped below 7 μmHg. The sorption isotherms were collected at 77 K, 278, 298, and 308 K on activated samples. The experimental temperatures were controlled by liquid nitrogen bath (77 K) and water bath (278, 298, and 308 K), respectively.

Breakthrough experiments

The breakthrough experiments were carried out on a dynamic gas breakthrough equipment. The experiments were conducted using a stainless steel column (4.6 mm inner diameter × 50 mm length). The weight of ZNU-6 powder packed in the columns were 0.5806 g. The column was activated at 75 °C for 2 h under vacuum, and then raised to 120 °C for overnight. The mixed gas of C_2H_2/C_2H_4 (1/99, v/v), CO_2/C_2H_4 (10/90, v/v), or $C_2H_2/CO_2/C_2H_4$ (1/9/90, 1/5/94, 1/1/98, 5/5/90, v/v/v) was then introduced. $C_2H_2/CO_2/C_2H_4$ mixtures are produced by mixing three pure gases or mixing binary mixture with pure gas. Every flowrate was calibrated by self-made soap film flowmeter. Outlet gas from the column was monitored using gas chromatography (GC-9860-5CNJ) with the thermal conductivity detector TCD. After the breakthrough experiment, the sample was regenerated with an Ar flow of 5 mL min^{-1} under 120 °C for 8 h or under vacuum at 120 °C for 8 h.

Fitting of experimental data on pure component isotherms

The unary isotherms for C_2H_2 and CO_2 measured at three different temperatures 278 K, 298 K, and 308 K in ZNU-6 were fitted with excellent accuracy using the dual-site Langmuir model, where we distinguish two distinct adsorption sites A and B:

$$q = \frac{q_{sat,A} b_A p}{1 + b_A p} + \frac{q_{sat,B} b_B p}{1 + b_B p} \tag{1}$$

In Eq (S1), the Langmuir parameters b_A,b_B are both temperature dependent

$$b_A = b_{A0} \exp\left(\frac{E_A}{RT}\right); b_b = b_{B0} \exp\left(\frac{E_B}{RT}\right) \tag{2}$$

In Eq. (2), E_A,E_B are the energy parameters associated with sites A, and B, respectively.

The corresponding unary isotherms for C_2H_4 measured at three different temperatures 278 K, 298 K, and 308 K in ZNU-6 were fitted with excellent accuracy using the single-site Langmuir model.

$$q = \frac{q_{sat,A} b_A p}{1 + bp} \tag{3}$$

The unary isotherm fit parameters for C_2H_2, CO_2, and C_2H_4 are provided in Table S1.

IAST calculations

The adsorption selectivity for separation of binary mixtures of species 1 and 2 is defined by

$$S_{ads} = \frac{q_1/q_2}{p_1/p_2} \tag{4}$$

where q_1, q_2 are the molar loading (units: mol kg^{-1}) in the adsorbed phase in equilibrium with a gas mixture with partial pressures p_1, p_2 in the bulk gas.

Calculation of isosteric heat of adsorption (Q_{st})

The isosteric heat of adsorption, Q_{st}, is defined as

$$Q_{st} = -RT^2 \left(\frac{\partial \ln p}{\partial T}\right)_q \tag{5}$$

where the derivative in the right member of Eq. (5) is determined at constant adsorbate loading, q. The calculations are based on the Clausius-Clapeyron equation.

Density functional theory calculation

In this work, the DFT-based calculations were carried out using the CP2K package[45]. The Perdew-Burke-Ernzerhof (PBE) exchange functional[46], Gaussian plane wave (PAW) pseudopotentials[47] and DZVP basis sets[48] for carbon, oxygen, fluorine, nitrogen, germanium and copper atoms, were used to describe the exchange–correlation interactions and electron–ion interaction, respectively. At the same time, the PBE-D3 method[49] with Becke–Jonson damping for all atoms and Hubbard U corrections for the open-shell 3d transition metal (Cu) was used for geometry optimizations. The U value of 5.0 eV was used in this study. In all calculations, the net charges of simulation systems were set to zero. The adsorption energy can be obtained from formula below:

$$E_{ads} = E_{adsorbate+substrate} - E_{substrate} - E_{adsorbate} \tag{6}$$

where $E_{adsorbate+substrate}$ and $E_{substrate}$ were the total energies of the substrate with and without adsorbate, and $E_{adsorbate}$ was the energy of the adsorbate.

Data availability

The authors declare that the data supporting the findings of this study are available within the article and Supplementary Information. The X-ray crystallographic data related to ZNU-6 have been deposited at the Cambridge Crystallographic Data Centre (CCDC), under deposition numbers 2192744–2192747, respectively. These data can be obtained free of charge from the CCDC via www.ccdc.cam.ac.uk/data_request/cif. The data that support the findings of this study are available from the corresponding author. Besides, Source data are provided with this paper.

References

1. Fernández, L. Global production capacity of ethylene 2018–2021, https://www.statista.com/statistics/1067372/global-ethylene-production-capacity/ (2022).
2. Sholl, D. S. & Liverly, R. P. Seven chemical separations to change the world. *Nature* **532**, 435–437 (2016).
3. Wang, Q. et al. One-step removal of alkynes and propadiene from cracking gases using a multi-functional molecular separator. *Nat. Commun.* **13**, 2955 (2022).
4. Suo, X. et al. Synthesis of ionic ultramicroporous polymers for selective separation of acetylene from ethylene. *Adv. Mater.* **32**, 1907601 (2020).
5. Li, J. et al. Metal-organic framework containing planar metal-binding sites: efficiently and cost-effectively enhancing the kinetic separation of C_2H_2/C_2H_4. *J. Am. Chem. Soc.* **141**, 3807–3811 (2019).
6. Sahoo, R. et al. C_{2s}/C_1 hydrocarbon separation: the major step towards natural gas purification by metal-organic frameworks (MOFs). *Coord. Chem. Rev.* **442**, 213998 (2021).
7. Farrell, B. L. et al. A viewpoint on direct methane conversion to ethane and ethylene using oxidative coupling on solid catalysts. *ACS Catal.* **6**, 4340–4346 (2016).
8. Chen, K.-J. et al. Synergistic sorbent separation for one-step ethylene purification from a four-component mixture. *Science* **366**, 241–246 (2019).
9. Zhang, R. et al. The cost-effective Cu-based catalysts for the efficient removal of acetylene from ethylene: the effects of Cu valence state, surface structure and surface alloying on the selectivity and activity. *Chem. Eng. J.* **351**, 732–746 (2018).
10. Huang, Y. et al. Separation of light hydrocarbons with ionic liquids: a review. *Chin. J. Chem. Eng.* **27**, 1374–1382 (2019).
11. Ren, T. et al. Olefins from conventional and heavy feedstocks: energy use in steam cracking and alternative processes. *Energy* **31**, 425–451 (2006).
12. Chai, Y. et al. Control of zeolite pore interior for chemoselective alkyne/olefin separations. *Science* **368**, 1002–1006 (2020).
13. Li, H. et al. Porous metal-organic frameworks for gas storage and separation: status and challenges. *EnergyChem* **1**, 100006 (2019).
14. Adil, K. et al. Gas/vapour separation using ultra-microporous metal-organic frameworks: insights into the structure/separation relationship. *Chem. Soc. Rev.* **46**, 3402–3430 (2017).
15. Yang, L. et al. Energy-efficient separation alternatives: metal-organic frameworks and membranes for hydrocarbon separation. *Chem. Soc. Rev.* **49**, 5359–5406 (2020).
16. Wang, H. & Li, J. Microporous metal-organic frameworks for adsorptive separation of C5-C6 alkane isomers. *Acc. Chem. Res* **52**, 1968–1978 (2019).
17. Barnett, B. R. et al. Recent progress towards light hydrocarbon separations using metal-organic frameworks. *Trends Chem.* **1**, 159–171 (2019).
18. Zhao, X. et al. Metal-organic frameworks for separation. *Adv. Mater.* **30**, 1705189 (2018).
19. Zeng, H. et al. Orthogonal-array dynamic molecular sieving of propylene/propane mixtures. *Nature* **595**, 542–548 (2021).
20. Zhang, P. et al. Ultramicroporous material based parallel and extended paraffin nano-trap for benchmark olefin purification. *Nat. Commun.* **13**, 4928 (2022).
21. Jiang, Y. et al. Comprehensive pore tuning in an ultrastable fluorinated anion cross-linked cage-like MOF for simultaneous benchmark propyne recovery and propylene purification. *Angew. Chem. Int. Ed.* **61**, e202200947 (2022).
22. Peng, Y.-L. et al. Robust ultramicroporous metal-organic frameworks with benchmark affinity for acetylene. *Angew. Chem. Int. Ed.* **57**, 10971–10975 (2018).

23. Zhang, Y. et al. Rational design of microporous MOFs with anionic boron cluster functionality and cooperative dihydrogen binding sites for highly selective capture of acetylene. *Angew. Chem. Int. Ed.* **59**, 17664–17669 (2020).
24. Lin, R.-B. et al. Optimized separation of acetylene from carbon dioxide and ethylene in a microporous material. *J. Am. Chem. Soc.* **139**, 8022–8028 (2017).
25. Zhang, Z.-Q. et al. Hexafluorogermanate (GeFSIX) anion-functionalized hybrid ultramicroporous materials for efficiently trapping acetylene from ethylene. *Ind. Eng. Chem. Res.* **57**, 7266–7274 (2018).
26. Ke, T. et al. Molecular sieving of C_2-C_3 alkene from alkyne with tuned threshold pressure in robust layered metal-organic frameworks. *Angew. Chem. Int. Ed.* **59**, 12725–12730 (2020).
27. Yang, L. et al. Adsorption site selective occupation strategy within a metal-organic framework for highly efficient sieving acetylene from carbon dioxide. *Angew. Chem. Int. Ed.* **60**, 4570–4574 (2021).
28. Niu, Z. et al. A MOF-based ultra-strong acetylene nano-trap for highly efficient C_2H_2/CO_2 separation. *Angew. Chem. Int. Ed.* **60**, 5283–5288 (2021).
29. Zhang, L. et al. Benchmark C_2H_2/CO_2 Separation in an Ultra-Microporous Metal-Organic Framework via Copper(I)-Alkynyl Chemistry. *Angew. Chem. Int. Ed.* **60**, 15995–16002 (2021).
30. Wang, L. et al. Interpenetration symmetry control within ultra-microporous robust boron cluster hybrid MOFs for benchmark purification of acetylene from carbon dioxide. *Angew. Chem. Int. Ed.* **60**, 22865–22870 (2021).
31. Di, Z. et al. Cage-like porous materials with simultaneous High C_2H_2 storage and excellent C_2H_2/CO_2 separation performance. *Angew. Chem. Int. Ed.* **60**, 10828–10832 (2021).
32. Lou, W. et al. Screening Hoffman-type metal organic frameworks for efficient C_2H_2/ CO_2 separation. *Chem. Eng. J.* **452**, 139296 (2023).
33. Xu, Z. et al. A robust Th-azole framework for highly efficient purification of C_2H_4 from a $C_2H_4/C_2H_2/C_2H_6$ mixture. *Nat. Commun.* **11**, 3163 (2020).
34. Gu, X.-W. et al. Immobilization of lewis basic sites into a stable ethane-selective mof enabling one-step separation of ethylene from a ternary mixture. *J. Am. Chem. Soc.* **144**, 2614–2623 (2022).
35. Cao, J.-W. et al. One-step ethylene production from a four-component gas mixture by a single physisorbent. *Nat. Commun.* **12**, 6507 (2021).
36. Mukherjee, S. et al. Amino-functionalised hybrid ultra-microporous materials that enable single-step ethylene purification from a ternary mixture. *Angew. Chem. Int. Ed.* **60**, 10902–10909 (2021).
37. Dong, Q. et al. Tuning gate-opening of a flexible metal-organic framework for ternary gas sieving separation. *Angew. Chem. Int. Ed.* **59**, 22756–22762 (2020).
38. Dong, Q. et al. Shape- and size-dependent kinetic ethylene sieving from a ternary mixture by a trap-and-flow channel crystal. *Adv. Funct. Mater.* **32**, 2203745 (2022).
39. Xiong, X.-H. et al. Nitro-decorated microporous covalent organic framework (TpPa-NO_2) for selective separation of C_2H_4 from a C_2H_2/ C_2H_4/CO_2 mixture and CO_2 capture. *ACS Appl. Mater. Interfaces* **14**, 32105–32111 (2022).
40. Li, H. et al. An unprecedented pillar-cage fluorinated hybrid porous framework with highly efficient acetylene storage and separation. *Angew. Chem. Int. Ed.* **60**, 7547–7552 (2021).
41. Cui, X. et al. Pore chemistry and size control in hybrid porous materials for acetylene capture from ethylene. *Science* **353**, 141–144 (2016).
42. Li, B. et al. An ideal molecular sieve for acetylene removal from ethylene with record selectivity and productivity. *Adv. Mater.* **29**, 1704210 (2017).
43. Xu, N. et al. A TIFSIX pillared MOF with unprecedented zsd topology for efficient separation of acetylene from quaternary mixtures. *Chem. Eng. J.* **450**, 138034 (2022).
44. Wang, J. et al. Optimizing pore space for flexible-robust metal-organic framework to boost trace acetylene removal. *J. Am. Chem. Soc.* **142**, 9744–9751 (2020).
45. Hutter, J. et al. $_{CP}2_K$: atomistic simulations of condensed matter systems. *WIREs Comput. Mol. Sci.* **4**, 15–25 (2014).
46. Perdew, J. P. et al. Generalized gradient approximation made simple. *Phys. Rev. Lett.* **77**, 3865–3868 (1996).
47. Hartwigsen, C. et al. Relativistic separable dual-space Gaussian pseudopotentials from H to Rn. *Phys. Rev. Lett.* **58**, 3641–3663 (1998).
48. VandeVondele, J. et al. Gaussian basis sets for accurate calculations on molecular systems in gas and condensed phases. *J. Chem. Phys.* **127**, 114105 (2007).
49. Klimeš, J. et al. Perspective: Advances and challenges in treating van der Waals dispersion forces in density functional theory. *J. Chem. Phys.* **137**, 120901 (2012).

Acknowledgements

This work was supported by the National Natural Science Foundation of China (Nos. 21908193 and 22205207) and Jinhua Industrial Key Project (2021A22648). We thank the help of Dr. Yunlei Peng from CUP.

Author contributions

Y.J. and Y.H. contributed equally to this work. Y.Z. designed and guided the project. Y.J. and Y.H. designed and synthesized the materials, performed the majority of the structural characterization, collected gas sorption data and conducted breakthrough experiments. B. L. conducted the DFT calculations. L.W. and H.N. collected X-ray diffraction data and solved the structures. R.K. performed the IAST and Q_{st} calculation. Y.J. and Y.Z. draft the paper. X.H. provided important advice and revised the paper. All authors contributed to the discussion of results and commented on the paper.

Competing interests

The authors declare no competing interests.

Additional information

Supplementary information The online version contains supplementary material available at https://doi.org/10.1038/s41467-023-35984-5.

Correspondence and requests for materials should be addressed to Yuanbin Zhang.

Peer review information *Nature Communications* thanks Zhang-Wen Wei, Soumya Mukherjee and the other, anonymous, reviewer(s) for their contribution to the peer review of this work. Peer reviewer reports are available.

Supplementary information

Benchmark Single-Step Ethylene Purification from Ternary Mixtures by a Customized Fluorinated Anion Embedded MOF

Jiang et al

I General Information and Procedures

Unless otherwise noted, all the reactions were performed under air without N_2 or Ar protection. All reagents were used as received without purification unless stated otherwise.

Chemicals: Tri(pyridin-4-yl)amine (TPA, 99%), $Cu(NO_3)_2 \cdot 3H_2O$ (99%) and $(NH_4)_2GeF_6$ (99.99%) were purchased from Energy Chemical. C_2H_2 (99.9%), C_2H_4 (99.9%), CO_2 (99.99%), N_2 (99.9999%), He (99.9999%), Ar (99.9999%), C_2H_2/C_2H_4 (1:99), CO_2/C_2H_4 (10:90), C_2H_2/CO_2 (50:50) were purchased from Datong Co., Ltd.

II Characterization (SCXRD, PXRD, TGA, IR)

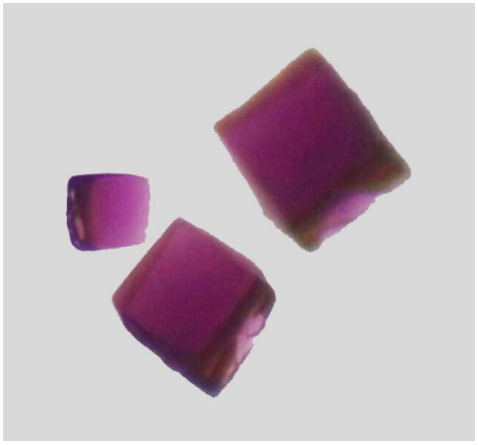

Supplementary Figure 1. Photography of the single crystals of **ZNU-6**.

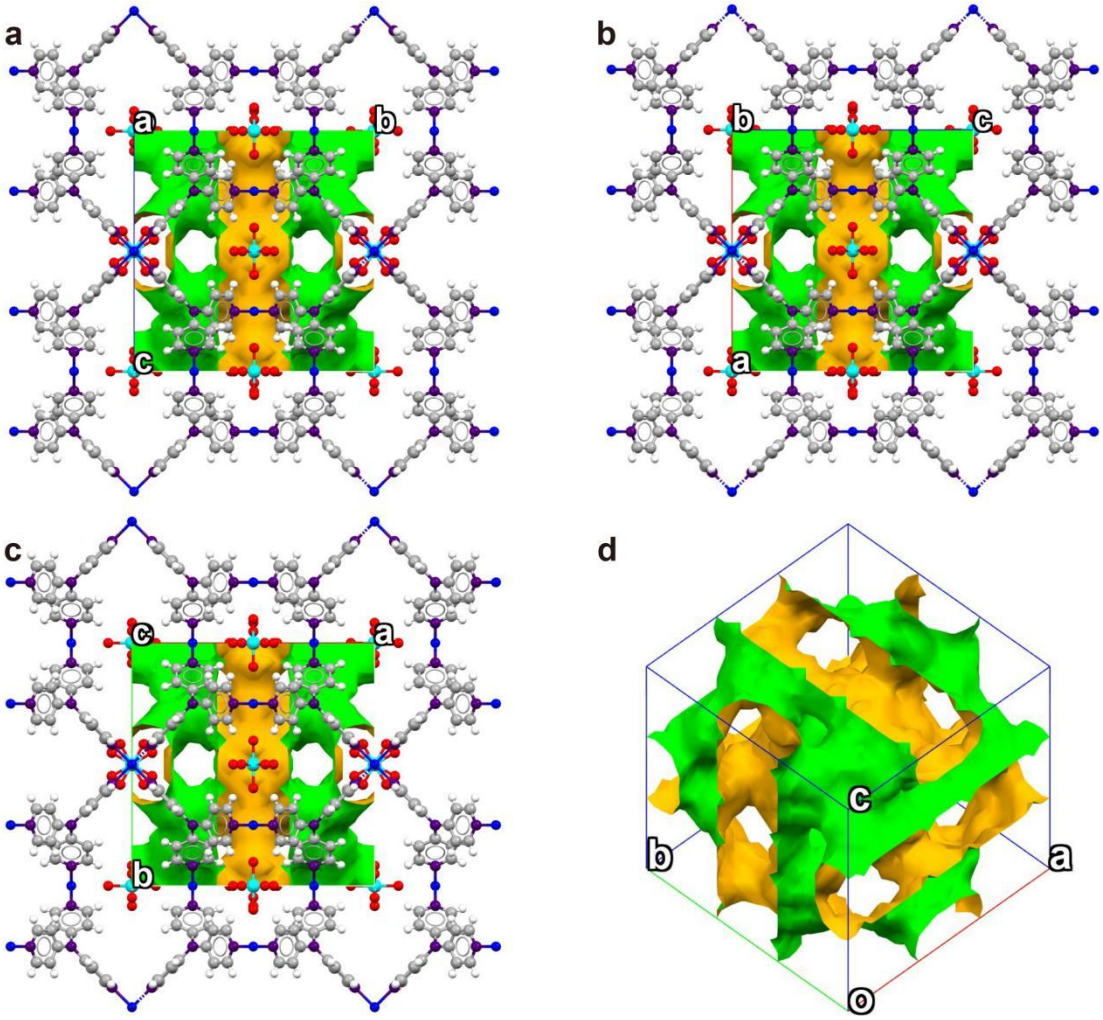

Supplementary Figure 2. 2 × 2 × 2 packing diagrams of **ZNU-6** viewed along the crystallographic *a*-, *b*-, and *c*-axis (a, b, c) and 1 × 1 × 1 packing diagrams of **ZNU-6** with pore surface in green representing the inside and yellow the outside determined using a probe with the radius of 1.2 Å by PLATON.

Supplementary Table 1. Single crystal data of as synthesized ZNU-6, activated ZNU-6, ZNU-6·C_2H_2, ZNU-6·C_2H_4 and ZNU-6·CO_2

		ZNU-6 as synthesized	ZNU-6·C_2H_2	ZNU-6·C_2H_4	ZNU-6·CO_2
cell	a=b=c	17.5352(3)	17.5343(3)	17.5392(3)	17.5395(2)
	α=β=γ	90°	90°	90°	90°
Temperature		298 K	298 K	298 K	298 K
Space group		Pm-3n	Pm-3n	Pm-3n	Pm-3n
Hall group		-P4n23	-P4n23	-P4n23	-P4n23
Formula		$C_{20}H_{16}CuF_6GeN_{5.33}Cu(GeF_6)(TPA)_{1.33}$	$C_{20}H_{16}CuGeF_6N_{5.33}\cdot 4.296C_2H_2Cu(GeF_6)(TPA)_{1.33}(C_2H_2)_{4.296}$	$C_{20}H_{16}CuGeF_6N_{5.33}\cdot 2.178C_2H_4Cu(GeF_6)(TPA)_{1.33}(C_2H_4)_{2.178}$	$C_{20}H_{16}CuGeF_6N_{5.33}\cdot 3CO_2Cu(GeF_6)(TPA)_{1.33}(CO_2)_3$
MW		581.21	701.29	660.38	767.85
density		1.074	1.296	1.219	1.418
Data completeness		0.988	0.985	0.967	0.971
R		0.1146	0.1460	0.1314	0.1451
wR2		0.2588	0.3304	0.2816	0.2970
S		0.986	1.201	1.059	1.002
CCDC. No		2192744	2192745	2192746	2192747

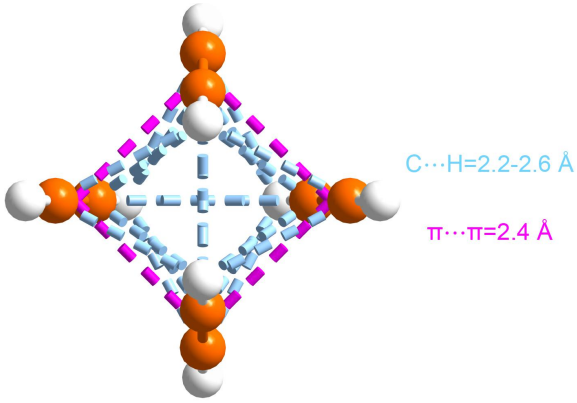

Supplementary Figure 3. The adsorption configuration of C_2H_2 moleucles inside the norrow channel (site I) of ZNU-6 with the formation of rare C_2H_2 clusters.The C-H interaction and π···π packing distance is highlighted.

There are two kinds of interactions between C_2H_2 molecules in the site I. One is the C···H interactions, whose distances are between 2.2 and 2.6 Å, and the other is π···π interactions between C≡C bonds, which are all in the distance of 2.4 Å.

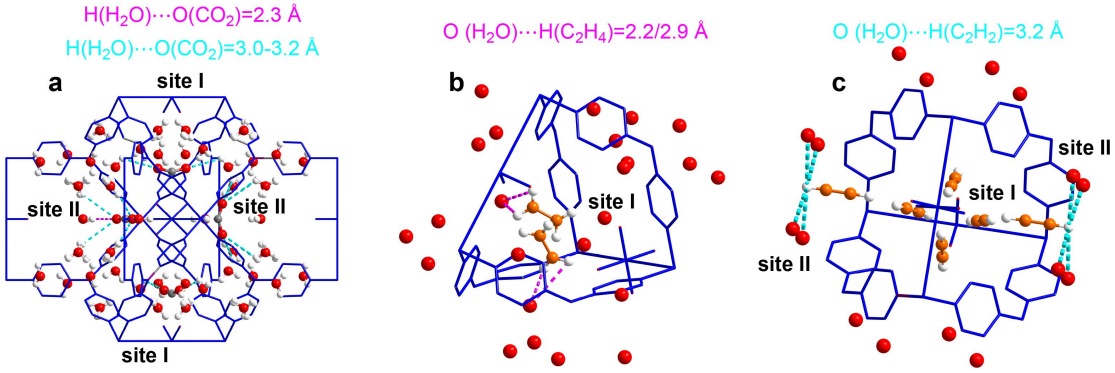

Supplementary Figure 4. Single crystals structure of gas loaded ZNU-6. **a**. $CuGeF_6C_{20}H_{16}N_{5.33}$ $(CO_2)_3$ $(H_2O)_{3.274}$. **b**. $CuGeF_6C_{20}H_{16}N_{5.33}$ $(C_2H_4)_{2.178}$ $(O)_{1.137}$. **c**. $CuGeF_6C_{20}H_{16}N_{5.33}$ $(C_2H_2)_{4.296}$ $(O)_{0.517}$.

Due to the serious disorder of H atoms of H_2O molecules, we haven't solve the H atoms in C_2H_2 and C_2H_4 loaded ZNU-6. In CO_2 loaded crystal, besides 18 CO_2 molecules, there are 19.644 water molecules in each unit cell (sum formula $Cu_6Ge_6F_{36}C_{120}H_{96}N_{32}$). As to C_2H_4 loaded crystals, there are 13.068 C_2H_4 molecules and 6.822 H_2O molecules in an unit cell. In the C_2H_2 loaded crystals, the number of H_2O (3.102) is much lower than that of CO_2 or C_2H_4 loaded crystals. These H_2O vapor molecules don't occupy the adsorption site of targeted gas molecules. Instead, some weak interactions between H_2O and targeted gas molecules were observed. As shown above, The distances of H (H_2O) and O (CO_2) are 2.3-3.2 Å, those of O (H_2O) and H (C_2H_4) are 2.2 and 2.9 Å, and those of O (H_2O) and H (C_2H_2) are 3.2 Å.

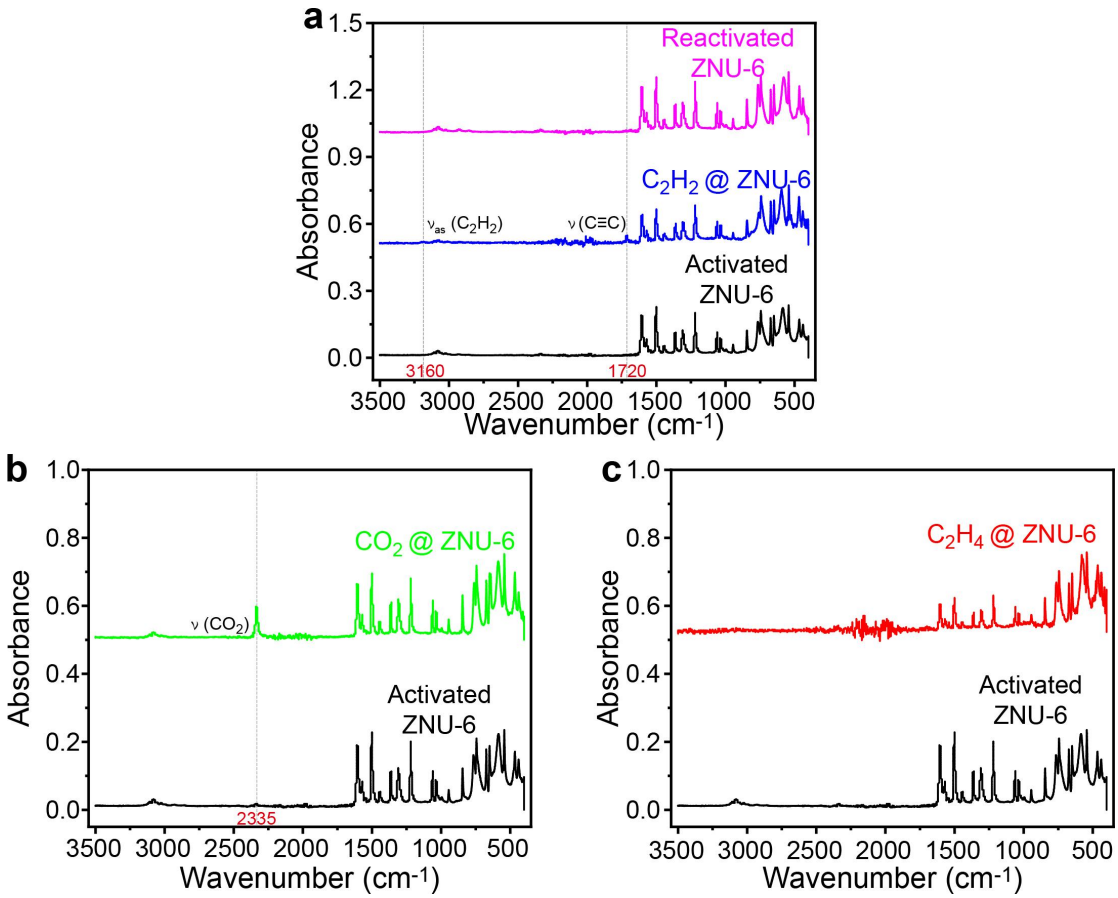

Supplementary Figure 5. In-situ IR spectra for **a.** activated ZNU-6 (black), -C_2H_2@ZNU-6 (blue) and re-activated ZNU-6 (purple); **b.** activated ZNU-6 (black) and CO_2@ZNU-6 (green); **c.** activated ZNU-6 (black) and C_2H_4@ZNU-6 (red).

All the IR spectroscopic data are recorded in a Nicolet iS5 ATR-FTIR spectrometer. The samples of gas-loaded crystals were prepared by the method described in **Preparation of gas loaded ZNU-6** in manuscript.

As shown in the Supplementary Figure 5, new and obvious stretching bands that belong to C_2H_2 and CO_2 are observed in the C_2H_2 and CO2 dosed single crystals. The $\nu_{as}(C_2H_2)$ and $\nu(C{\equiv}C)$ stretching band of adsorbed C_2H_2 down-shifted to 3160 and 1720 cm^{-1} respectively with reference to the gas-phase value at 3287 and 2500-1900 cm^{-1}, indicating the existence of guest-host interactions. Similarity, $\nu(CO_2)$ band also undergoes a downward shift from gas-phase value 2349 cm^{-1} to 2335 cm^{-1}, showing the interactions between CO_2 and framework. In contrast, the stretching band of C_2H_4 is not obvious in C_2H_4@ZNU-6.

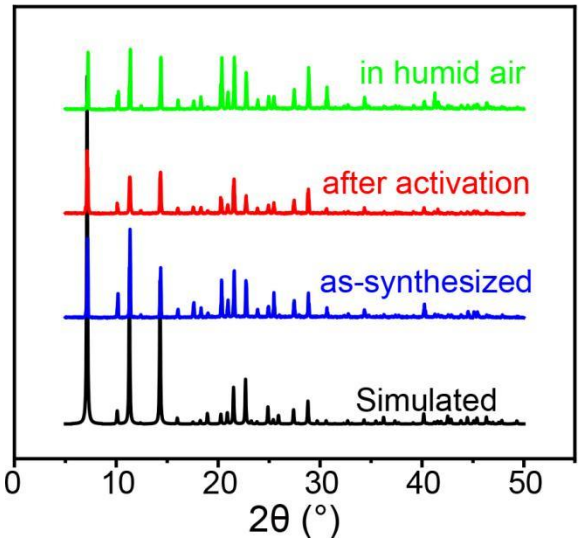

Supplementary Figure 6. PXRD patterns of **ZNU-6**.

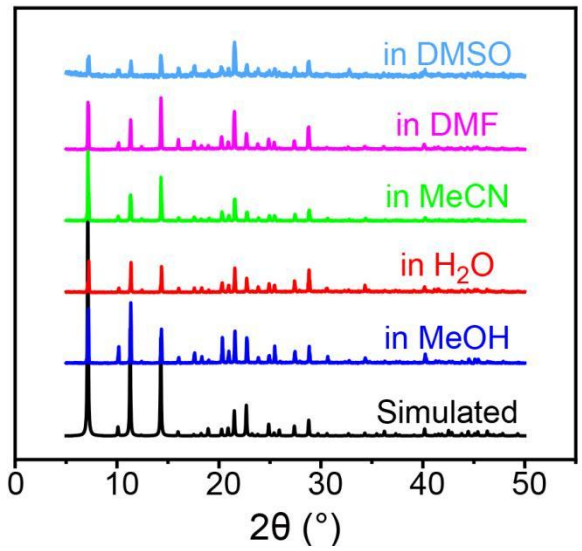

Supplementary Figure 7. PXRD patterns of **ZNU-6** after soaking in solvents for 6 months.

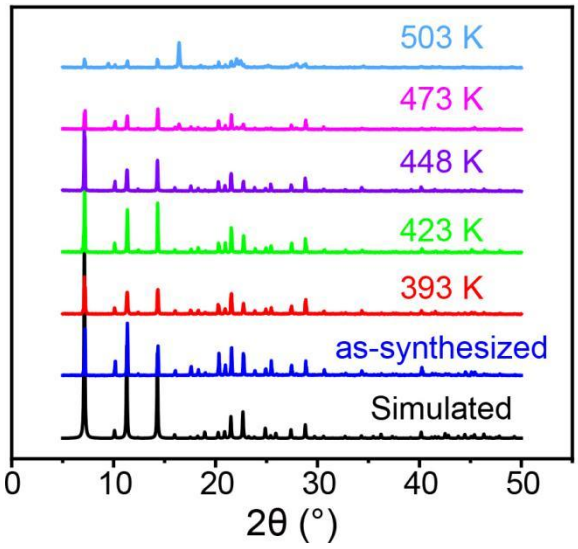

Supplementary Figure 8. PXRD patterns of **ZNU-6** after treatment under different temperatures.

Experimental method: The fresh samples of **ZNU-6** were evacuated at 25 ºC for 2 h firstly, and then evacuated at the corresponding temperature (393/423/448/473/503 K) for 40 mins. After cooling to room temperature, PXRD data were collected.

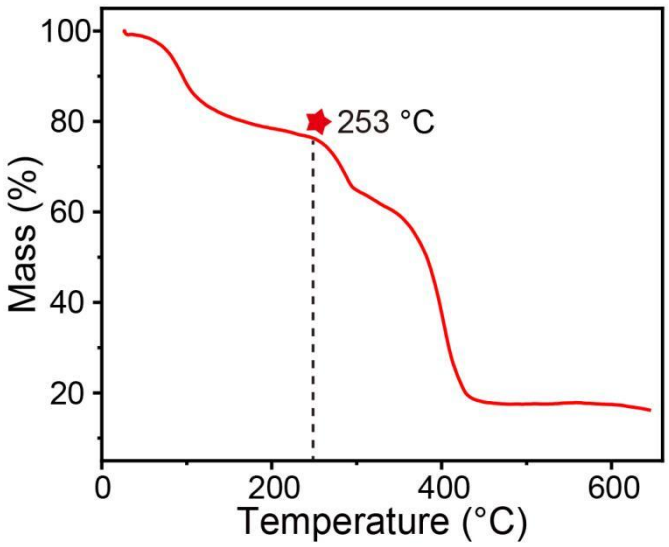

Supplementary Figure 9. TGA curve of **ZNU-6**. The weight loss before 110 ºC is because of the loss of MeOH and water from the sample. The weight keeps consistent until ~253 ºC.

III Adsorption data, Selectivity and Q_{st}

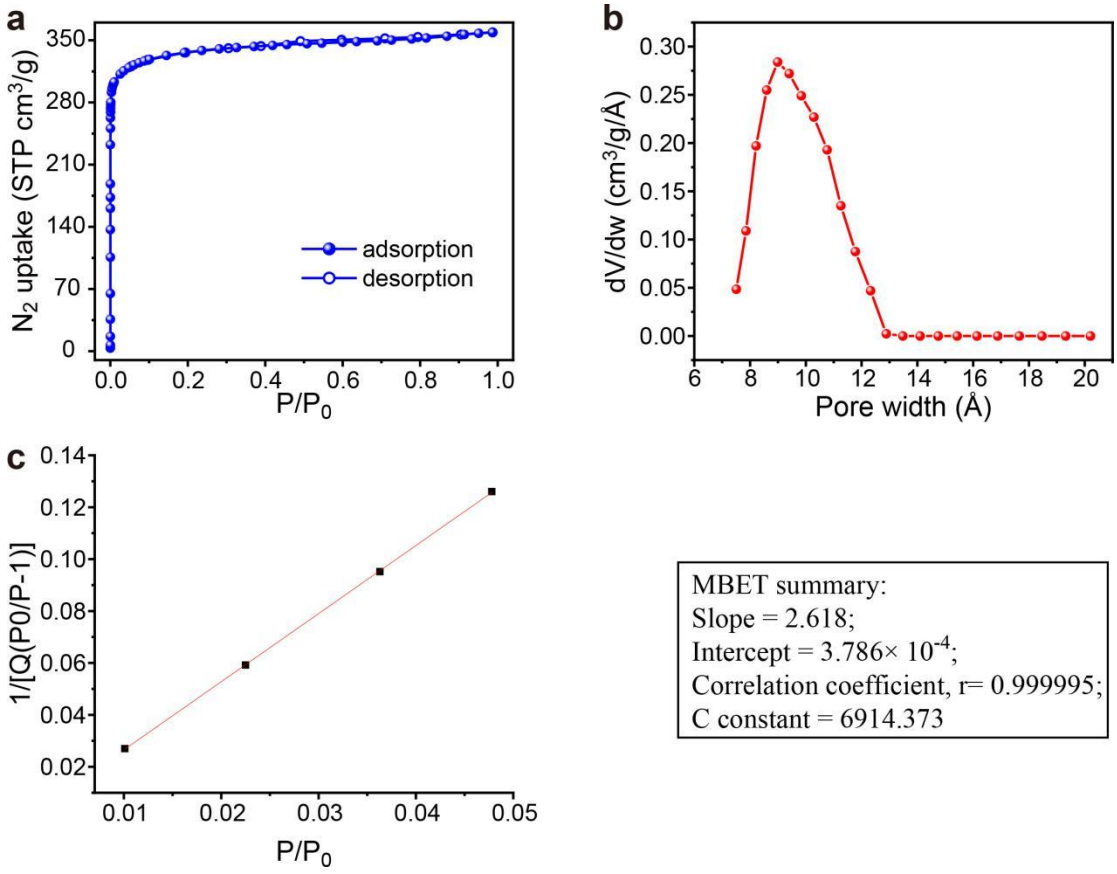

Supplementary Figure 10. Pore size distribution (b) of **ZNU-6** calculated from 77 K N_2 adsorption isotherms (a, c).

The BET surface area calculated from the N_2 adsorption isotherms under the pressure range of P/P_0 = 0.01-0.05 (for micropores) is 1330.3 m^2/g.

The total pore volume calculated from the N_2 adsorption isotherms is 0.554 cm^3/g.

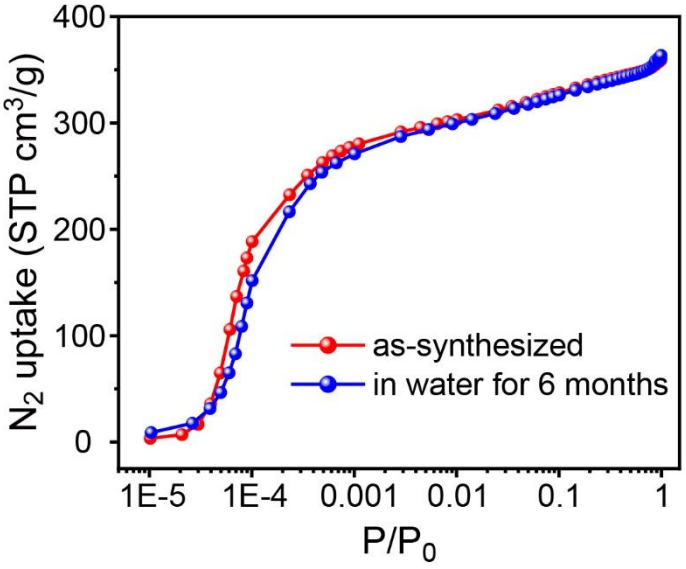

Supplementary Figure 11. The adsorption isotherm of N_2 at 77 K on as-synthesized **ZNU-6**, and **ZNU-6** after soaking in water for 6 months.

Analysis: The overlapping of the N_2 adsorption isotherms suggests its good stability towards water.

Supplementary Table 2. Comparison of C_2H_2, C_2H_4 and CO_2.

Gas molecules	Kinetic Diameter (Å)	Molecular size (Å^3)	Boiling point (K)	Polarizability ($\times 10^{-25}$ cm^3)
C_2H_2	3.3	3.32 x 3.34 x 5.70	189.3	33.3-39.3
C_2H_4	4.2	3.28 x 4.18 x 4.84	169.5	42.5
CO_2	3.3	3.18 x 3.33 x 5.36	194.7	25.93

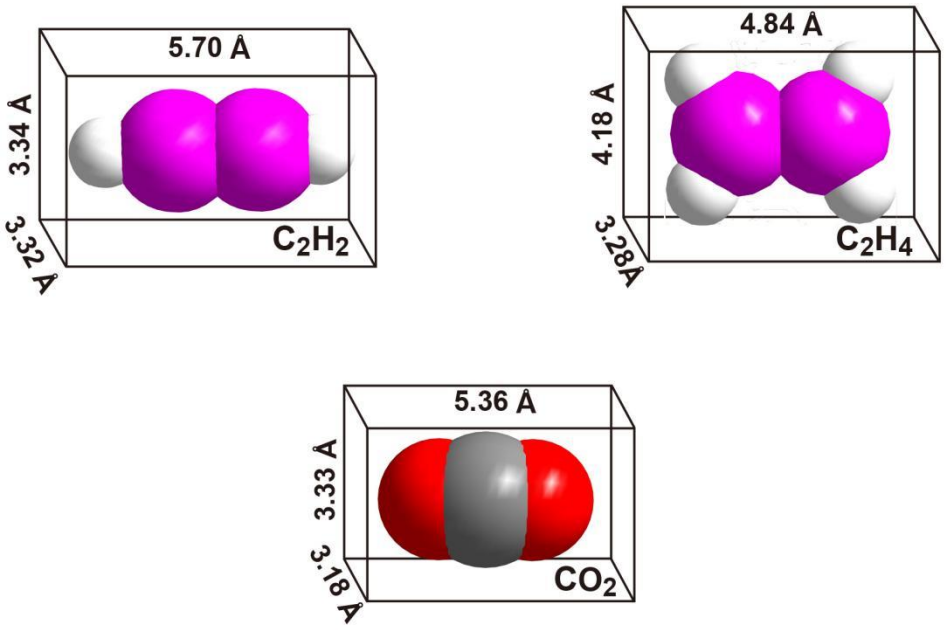

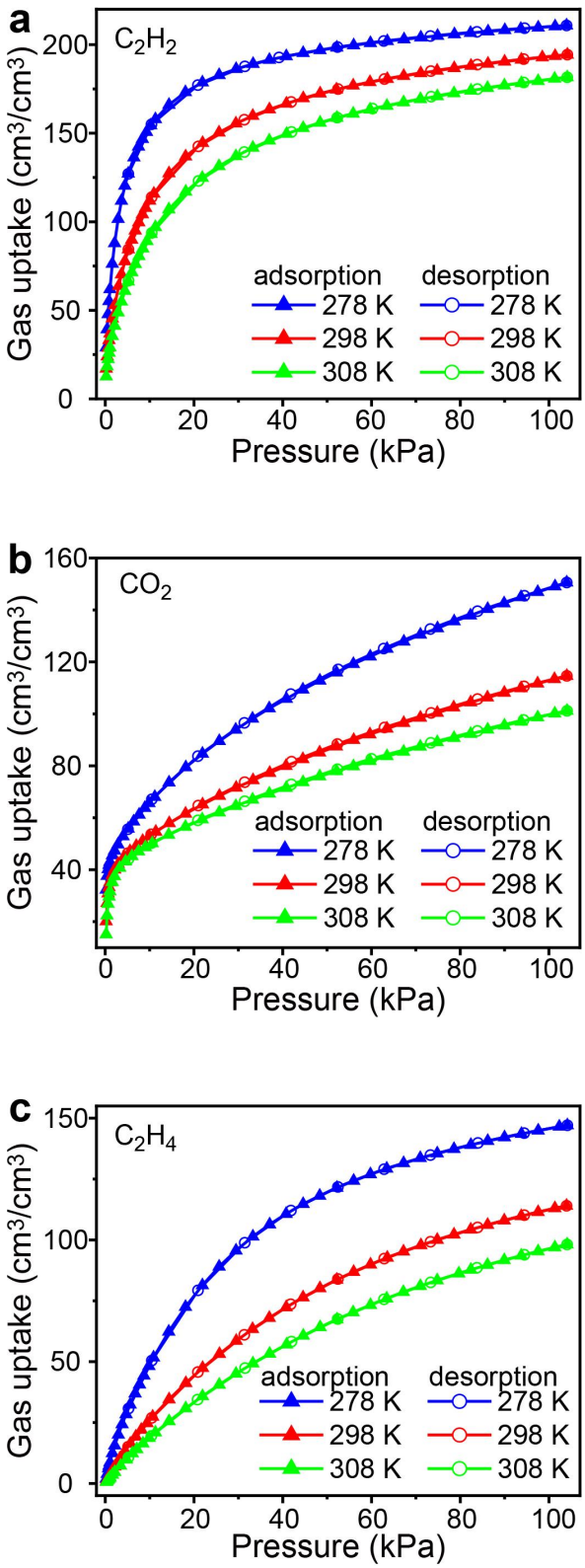

Supplementary Figure 12. The adsorption and desorption isotherms of C_2H_2 (a), CO_2(b), and C_2H_4 (c) on **ZNU-6** at 278, 298, and 308 K.

Supplementary Table 3. Dual-site Langmuir parameter fits for C_2H_2, CO_2 adsorption isotherms and single-site Langmuir parameter fit for C_2H_4 adsorption isotherms in ZNU-6.

	Site A			Site B		
	$\frac{q_{A,sat}}{\text{mol/kg}}$	$\frac{b_{A0}}{\text{Pa}^{-1}}$	$\frac{E_A}{\text{kJ mol}^{-1}}$	$\frac{q_{B,sat}}{\text{mol/kg}}$	$\frac{b_{B0}}{\text{Pa}^{-1}}$	$\frac{E_B}{\text{kJ mol}^{-1}}$
C_2H_2	1.2	1.067E-09	37.5	7.6	5.015E-11	35.4
CO_2	7.7	2.01E-10	25.5	1.8	1.06E-10	37.2
C_2H_4	7.6	1.339E-10	29			

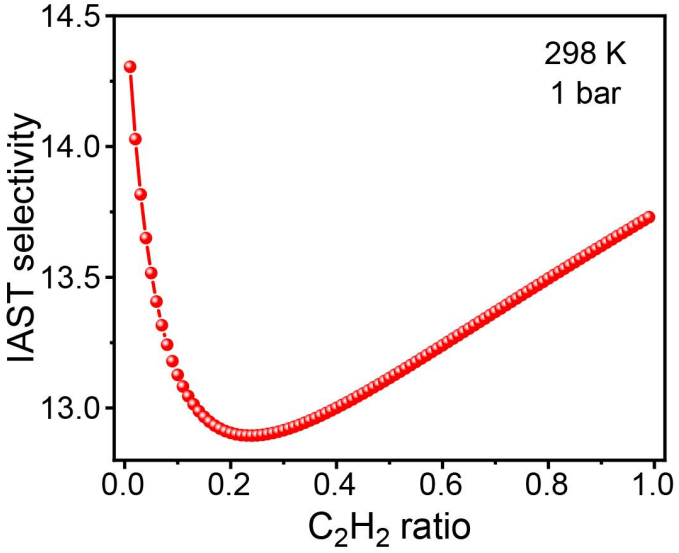

Supplementary Figure 13. IAST selectivity of **ZNU-6** towards gas mixtures of C_2H_2/C_2H_4 with different ratios at 298 K and 1 bar.

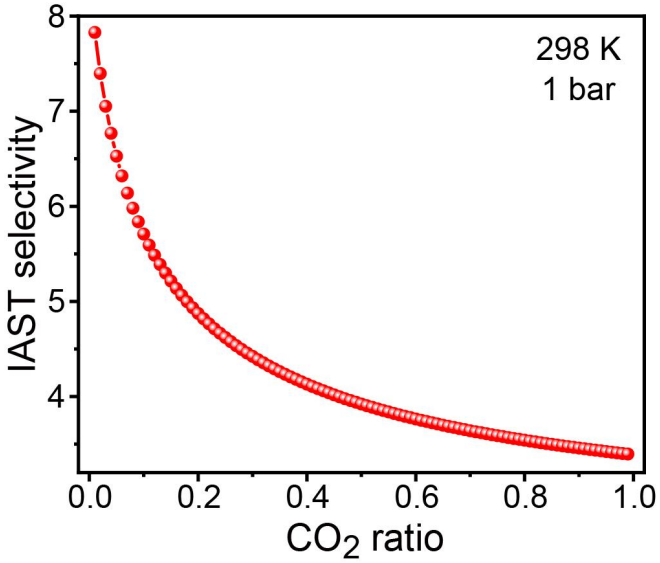

Supplementary Figure 14. IAST selectivity of **ZNU-6** towards gas mixtures of CO_2/C_2H_4 with different ratios at 298 K and 1 bar.

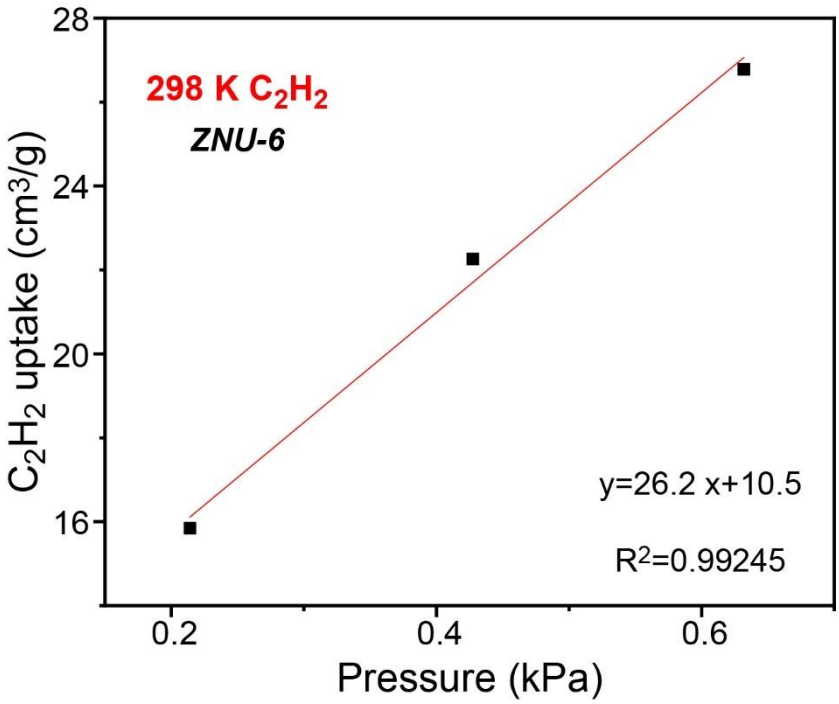

Supplementary Figure 15.. C_2H_2 adsorption isotherm of **ZNU-6** at 298 K fitted with Henry's equation at low pressure (0.2 kPa-0.7 kPa).

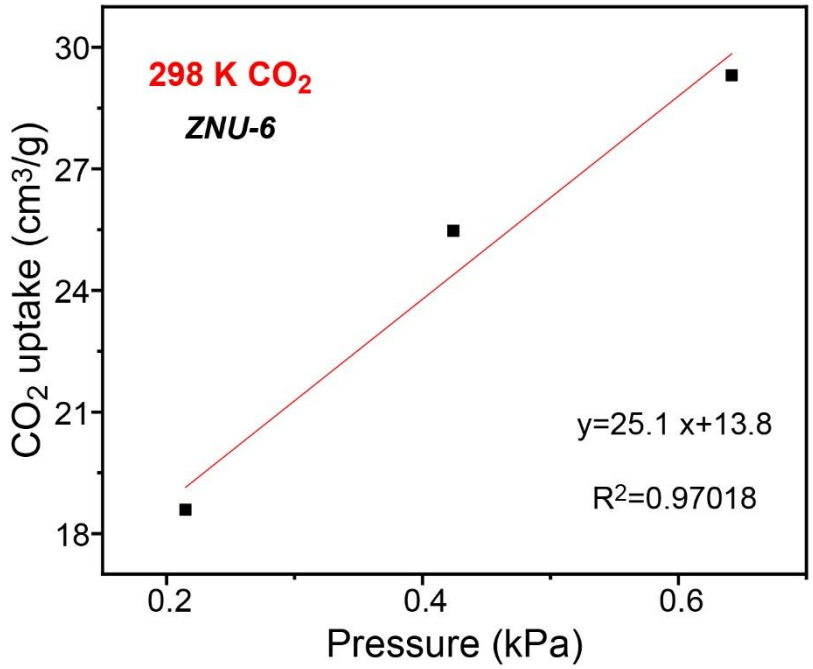

Supplementary Figure 16. CO_2 adsorption isotherm of **ZNU-6** at 298 K fitted with Henry's equation at low pressure (0.2 kPa-0.7 kPa).

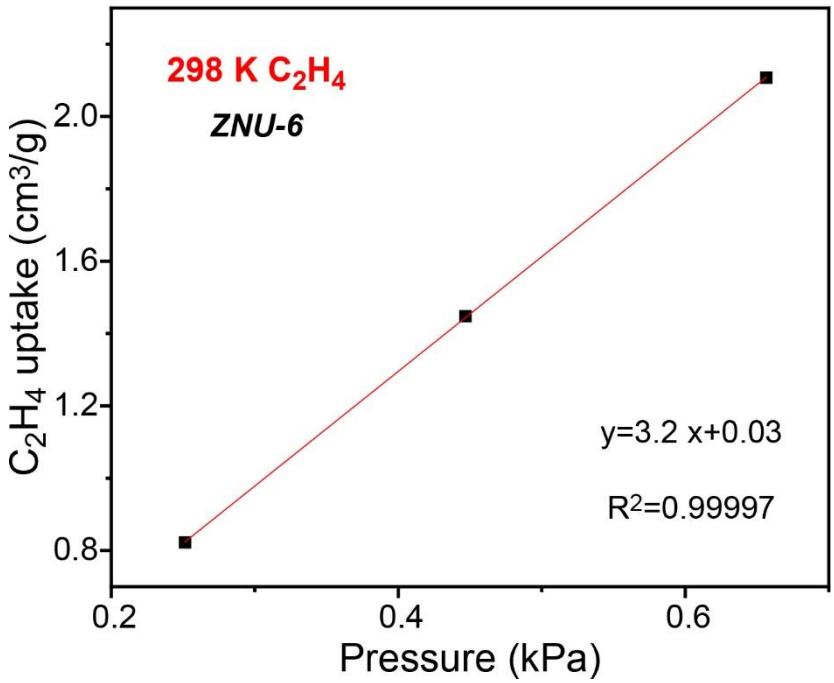

Supplementary Figure 17. C_2H_4 adsorption isotherm of **ZNU-6** at 298 K fitted with Henry's equation at low pressure (0.2 kPa-0.7 kPa).

Supplementary Table 4. Summary of Henry constant and Henry's selectivity of ZNU-6

	Henry constant ($cm^3\ g^{-1}\ kPa^{-1}$)
C_2H_2	26.2
CO_2	25.1
C_2H_4	3.2
C_2H_2/C_2H_4 Henry's selectivity	**8.2**
CO_2/C_2H_4 Henry's selectivity	**7.8**

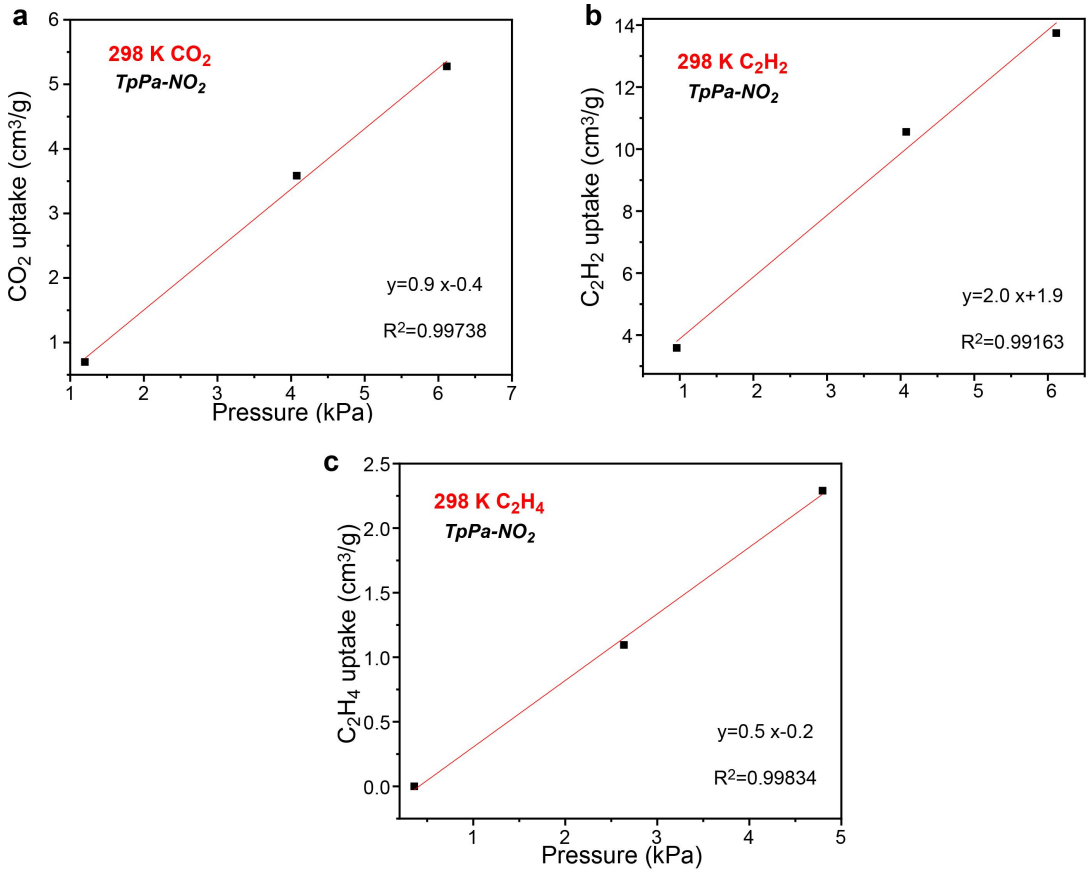

Supplementary Figure 18. $CO_2/C_2H_2/C_2H_4$ adsorption isotherm of **TpPa-NO₂** at 298 K fitted with Henry's equation at low pressure (0-7 kPa). Data of adsorption was from Reference 1.

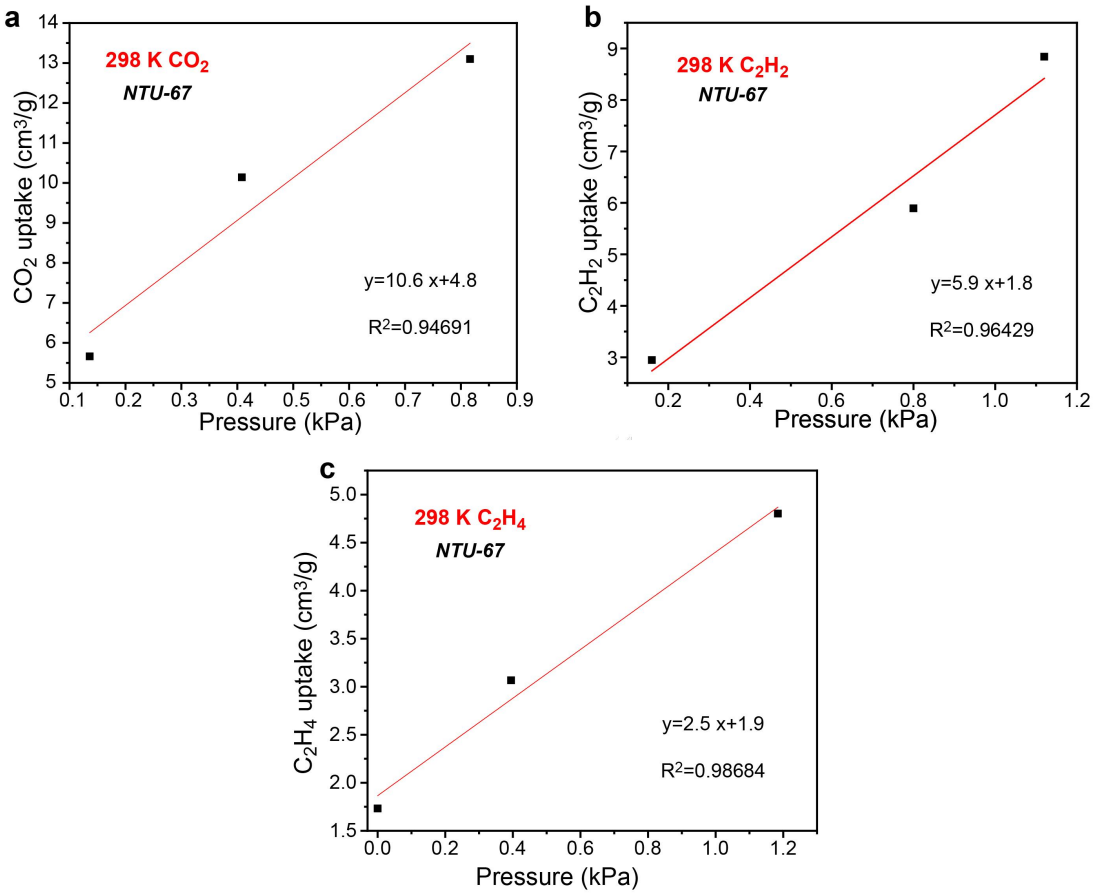

Supplementary Figure 19. $CO_2/C_2H_2/C_2H_4$ adsorption isotherm of **NTU-67** at 298 K fitted with Henry's equation at low pressure (0-1.2 kPa). Data of adsorption was from Reference 2.

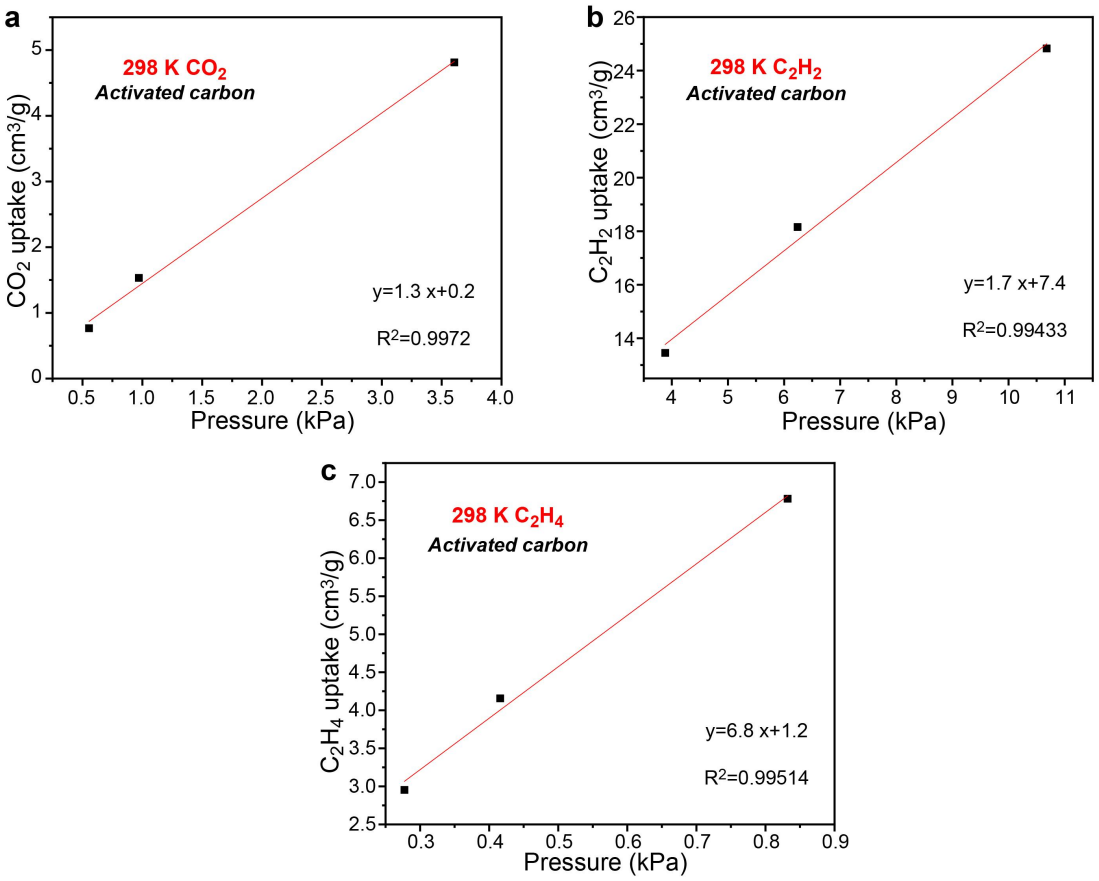

Supplementary Figure 20. $CO_2/C_2H_2/C_2H_4$ adsorption isotherm of activated carbon at 298 K fitted with Henry's equation at low pressure (0-11.0 kPa). Data of adsorption was from Reference 2.

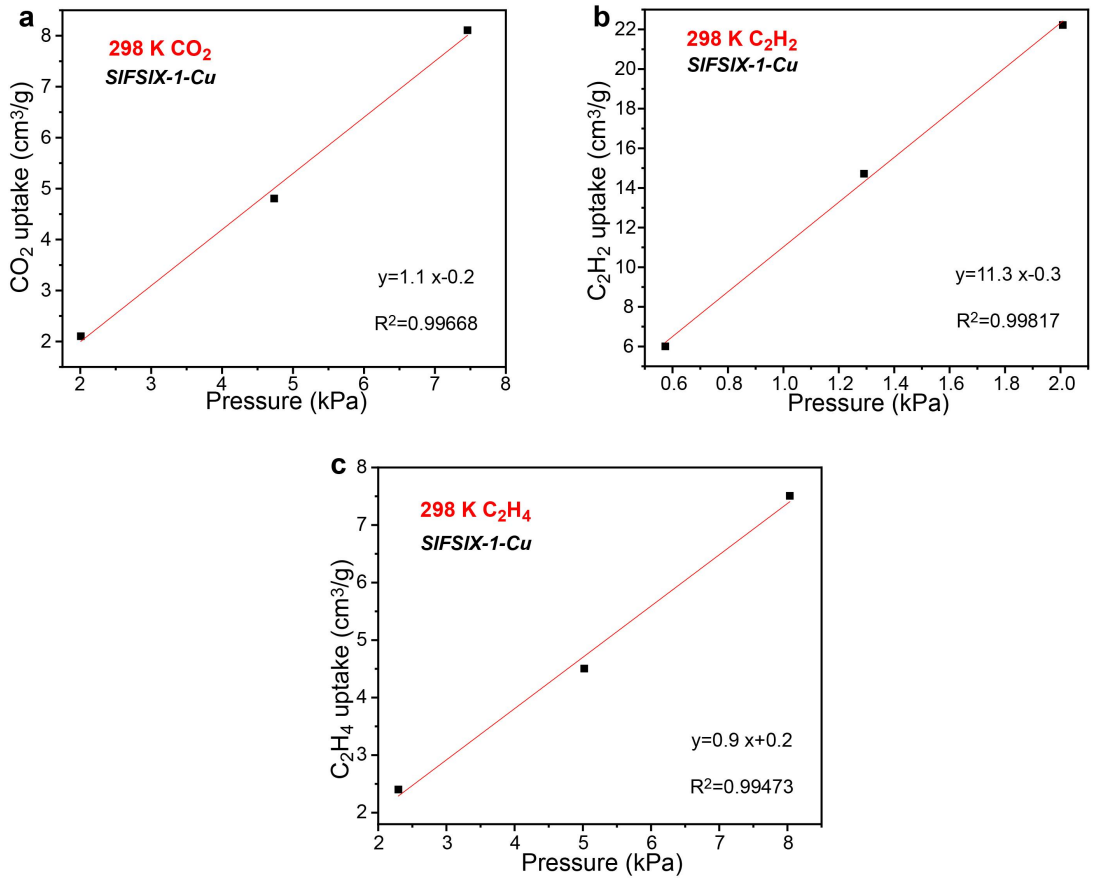

Supplementary Figure 21. $CO_2/C_2H_2/C_2H_4$ adsorption isotherm of SIFSIX-1-Cu at 298 K fitted with Henry's equation at low pressure (0-8.0 kPa). Data of adsorption was from Reference 2.

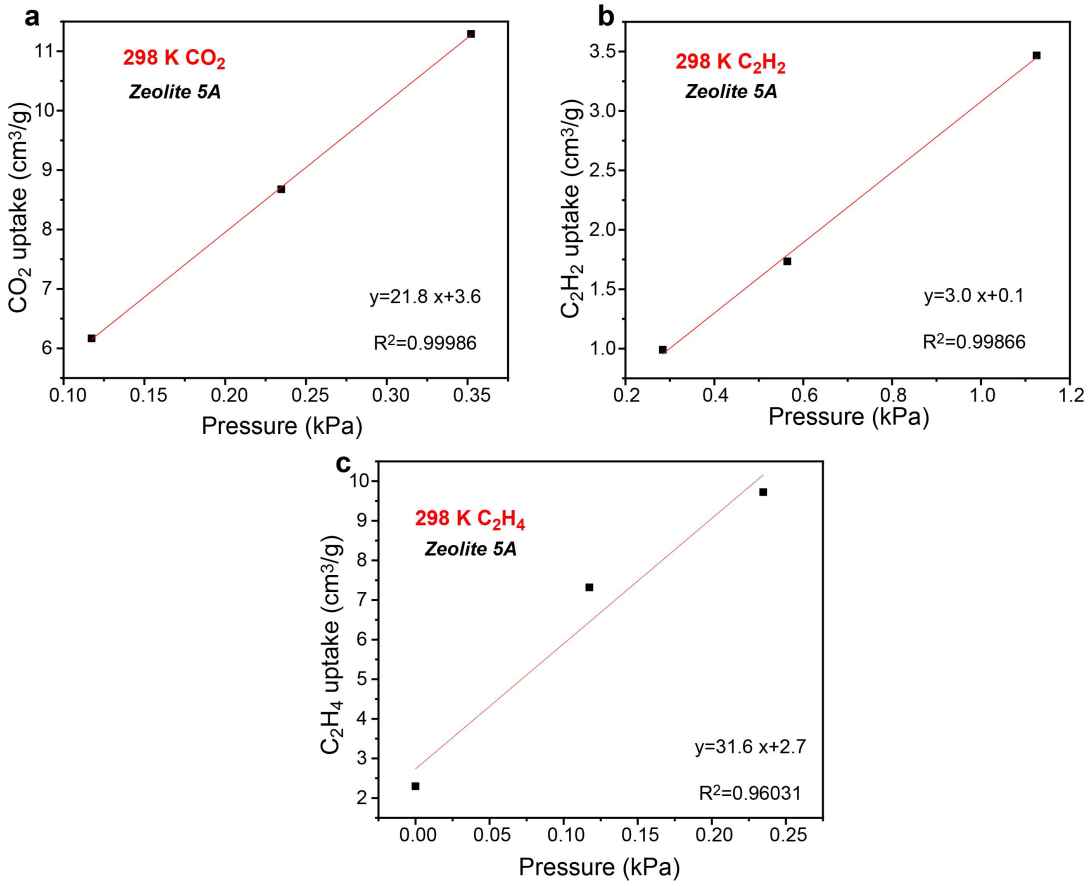

Supplementary Figure 22. $CO_2/C_2H_2/C_2H_4$ adsorption isotherm of Zeolite 5A at 298 K fitted with Henry's equation at low pressure (0-1.2 kPa). Data of adsorption was from Reference 2.

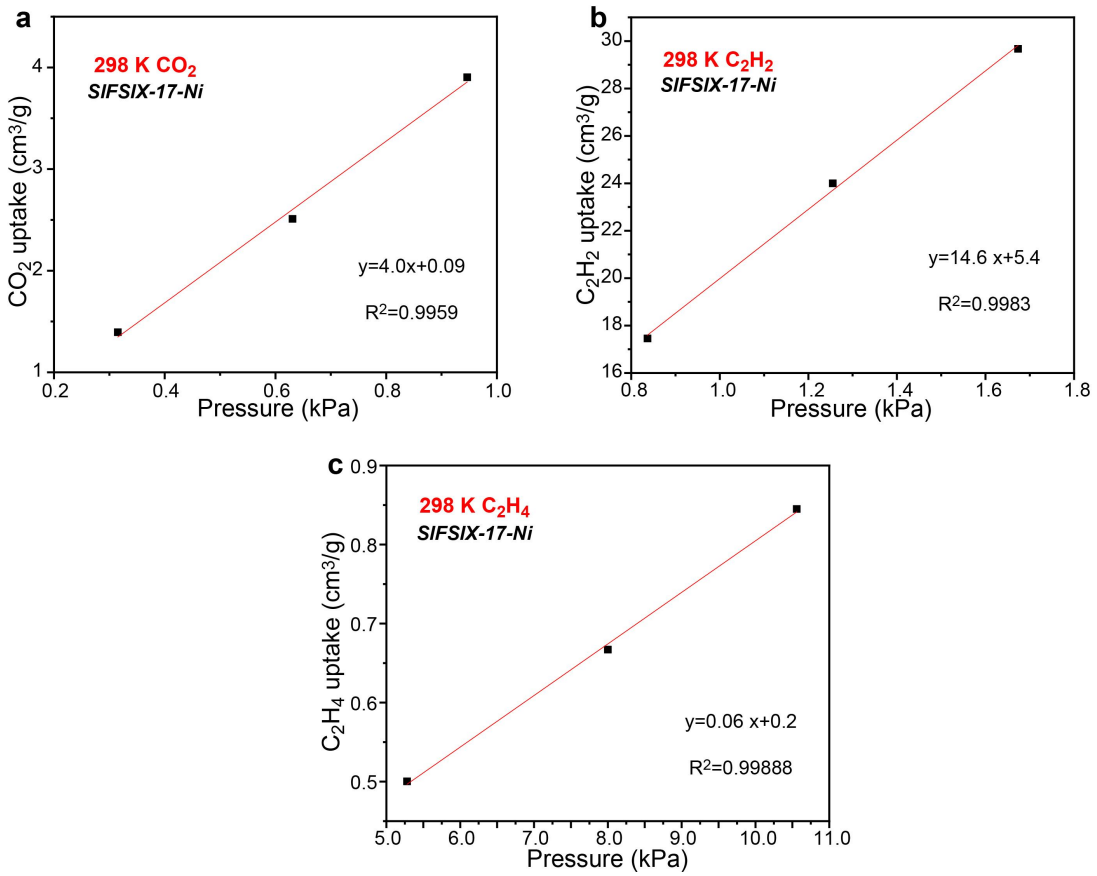

Supplementary Figure 23. $CO_2/C_2H_2/C_2H_4$ adsorption isotherm of SIFSIX-17-Ni at 298 K fitted with Henry's equation at low pressure (0-1.8 kPa). Data of adsorption was from Reference 3.

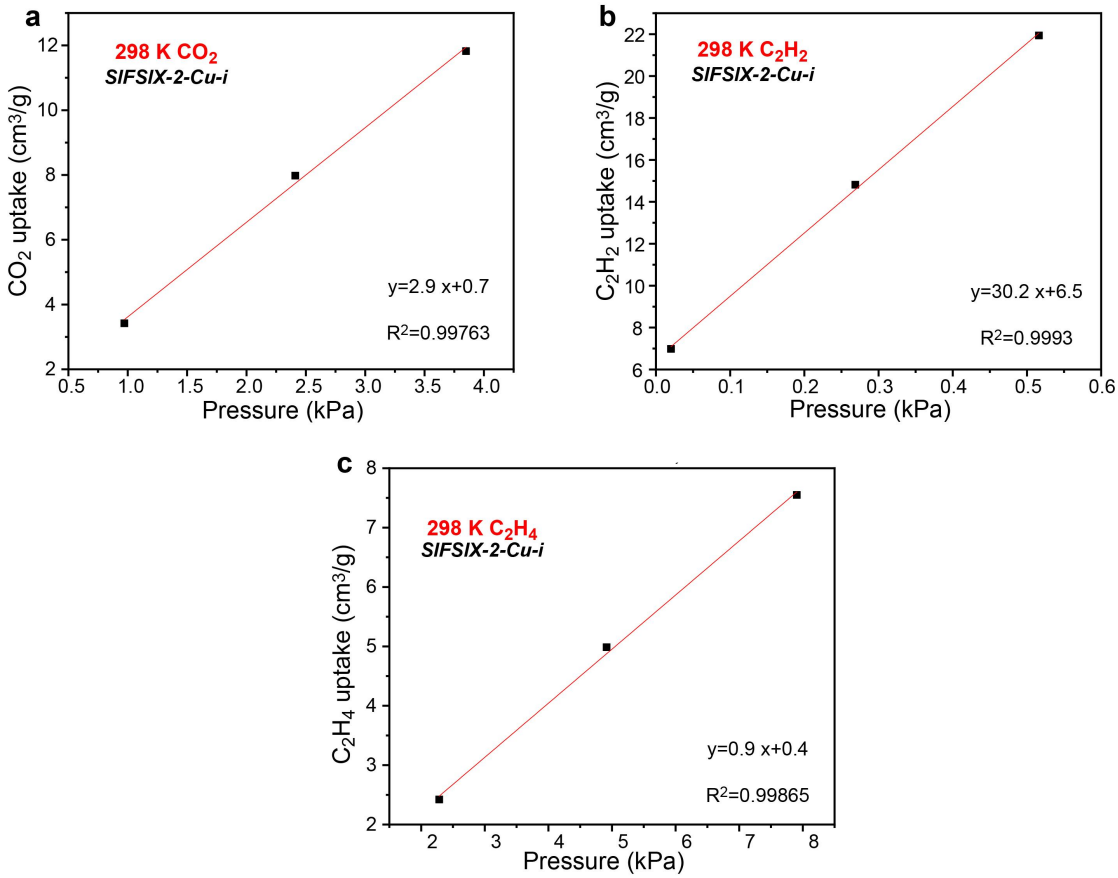

Supplementary Figure 24. $CO_2/C_2H_2/C_2H_4$ adsorption isotherm of SIFSIX-2-Cu-i at 298 K fitted with Henry's equation at low pressure (0-0.6 kPa). Data of adsorption was from Reference 2.

Supplementary Table 5. Comparison of Henry constants and Henry's selectivity among absorbents used in single-step C_2H_4 purification from ternary gas mixture.

	C_2H_2 Henry constant ($cm^3\ g^{-1}\ kPa^{-1}$)	CO_2 Henry constant ($cm^3\ g^{-1}\ kPa^{-1}$)	C_2H_4 Henry constant ($cm^3\ g^{-1}\ kPa^{-1}$)	C_2H_2/C_2H_4 Henry's selectivity	CO_2/C_2H_4 Henry's selectivity
TpPa-NO_2	2.0	0.9	0.5	4.0	1.8
NTU-67	5.9	10.6	2.5	2.36	4.24
Activated carbon	1.7	1.3	6.8	0.25	0.19
SIFSIX-1-Cu	11.3	1.1	0.9	12.56	1.22
Zeolite 5A	3.0	21.8	31.6	0.09	0.69
SIFSIX-17-Ni	14.6	4.0	0.06	243.33	66.67
SIFSIX-2-Cu-i	30.2	2.9	0.9	33.56	3.22
ZNU-6	**26.2**	**25.1**	**3.2**	**8.19**	**7.84**

Supplementary Table 6. Comparison of saturated C_2H_2 and CO_2 uptake (298 K, 1 bar).

	C_2H_2 uptake cm^3/g (cm^3/cm^3)	CO_2 uptake cm^3/g (cm^3/cm^3)	Ref
TIFSIX-3-Ni	67.2	52.0	3
SIFSIX-3-Ni	73.9	60.5	3-5
SIFSIX-17-Ni	73.9	51.5	3
SIFSIX-3-Zn	81.5	57.1	4-6
TIFSIX-17-Ni	73.9	49.3	3
SIFSIX-3-Cu	83.5	56.0	4, 6
UTSA-300a	68.9	3.3	7
NTU-67	73.7	45.7	2
NTU-65	75.4	2.3	8
UTSA-200a	81.8	105.5	9, 10
SIFSIX-2-Cu-i	89.6	108.6	4, 10, 11
ZU-62	82.2	/	12
ZNU-4	85.1	44.1	13
NCU-100a	102.3	13.7	14
ZNU-5	128.6	15.2	15
SIFSIX-1-Cu (ρ=0.864 g/cm^3)	190.4 (164.5)	117.6 (101.6)	4
SIFSIX-Cu-TPA (ρ=0.995 g/cm^3)	185.0 (184.1)	107.0 (106.5)	16
ZNU-6	**180.44 (193.8)**	**106.7 (114.6)**	**This work**

Supplementary Table 7. Comparison of C_2H_2 and CO_2 uptake per anion among anion pillared MOFs.

	Molecule formula	Molecular weight	C_2H_2/anion ratio	CO_2/anion ratio	Ref.
TIFSIX-3-Ni	$Ni(TiF_6)(C_4H_4N_2)_2$	379.95	1.14	0.88	3
SIFSIX-3-Ni	$Ni(SiF_6)(C_4H_4N_2)_2$	360.96	1.19	0.97	3-5
SIFSIX-17-Ni	$Ni(SiF_6)(C_4H_5N_3)_2$	390.98	1.29	0.9	3
SIFSIX-3-Zn	$Zn(SiF_6)(C_4H_4N_2)_2$	367.64	1.34	0.93	4-6
TIFSIX-17-Ni	$Ni(TiF_6)(C_4H_5N_3)_2$	410.76	1.36	0.91	3
SIFSIX-3-Cu	$Cu(SiF_6)(C_4H_4N_2)_2$	365.80	1.37	0.92	4,6
UTSA-300a	$Zn(SiF_6)(C_{10}H_8SN_2)_2$	583.95	1.8	0.09	7
NTU-67	$Cu(SiF_6)(C_{12}H_{10}N_4)_2$	626.12	2.06	1.28	2
NTU-65	$Cu(SiF_6)(C_{12}H_{10}N_4)_2$	626.12	2.11	0.06	8
UTSA-200a	$Cu(SiF_6)(C_{10}H_8N_4)_2$	574.04	2.10	2.71	9-10
SIFSIX-2-Cu-i	$Cu(SiF_6)(C_{12}H_8N_2)_2$	565.78	2.27	3.06	4,10-11
ZU-62	$Cu(NbOF_5)(C_{12}H_8N_2)_2$	627.86	2.31	/	12
ZNU-4	$Cu(TiF_6)(C_{12}H_{10}N_4)_2$	645.88	2.45	1.27	13
NCU-100a	$Cu(SiF_6)(C_{10}H_{14}N_2O_3S)_2$	690.21	3.15	0.42	14
ZNU-5	$Cu(TiF_6)(C_{12}H_{10}N_4)_2$	645.88	3.71	0.44	15
SIFSIX-1-Cu	$Cu(SiF_6)(C_{10}H_8N_2)_2$	517.78	4.40	2.72	4
SIFSIX-Cu-TPA	$Cu(SiF_6)(C_{15}H_{12}N_4)_{1.33}$	536.67	4.44	2.57	16
ZNU-6	**$Cu(GeF_6)(C_{15}H_{12}N_4)_{1.33}$**	**581.21**	**4.68**	**2.77**	**This work**

Guest/anion ratio=$Q_{gas} \times M \div 22.4 \div 1000$

Qgas: the gas uptake of APMOFs, mL/g

M: Molecular weight of crystals, g/mol

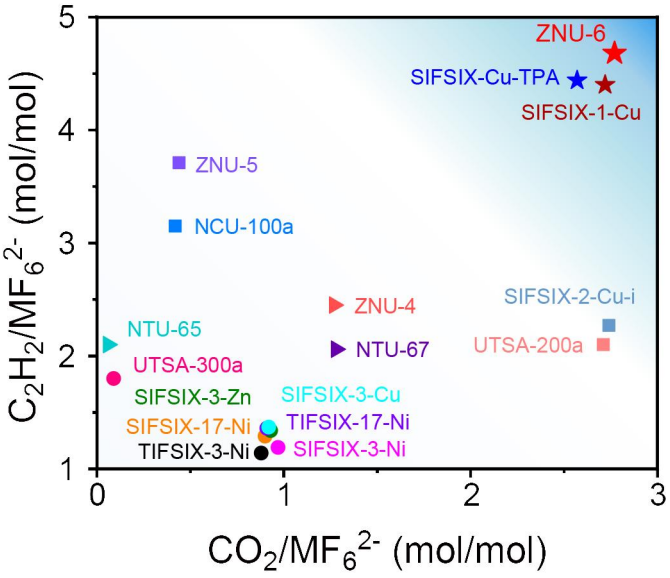

Supplementary Figure 25. Comparison of the saturated C_2H_2 and CO_2 uptake (1 bar, 298 K) among anion pillared MOFs.

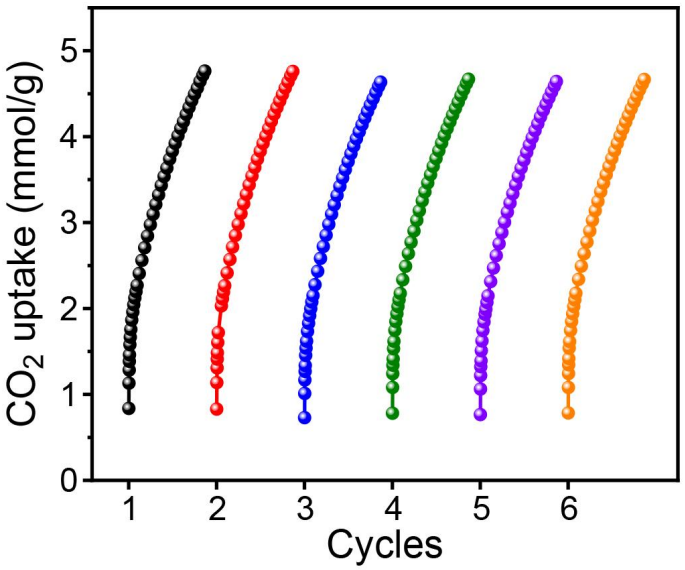

Supplementary Figure 26. Six cycles of CO_2 adsorption of **ZNU-6** at 298 K.

The reactivation condition between 5th and 6th cycle: Under vacuum, at room temperature for 3 hours.

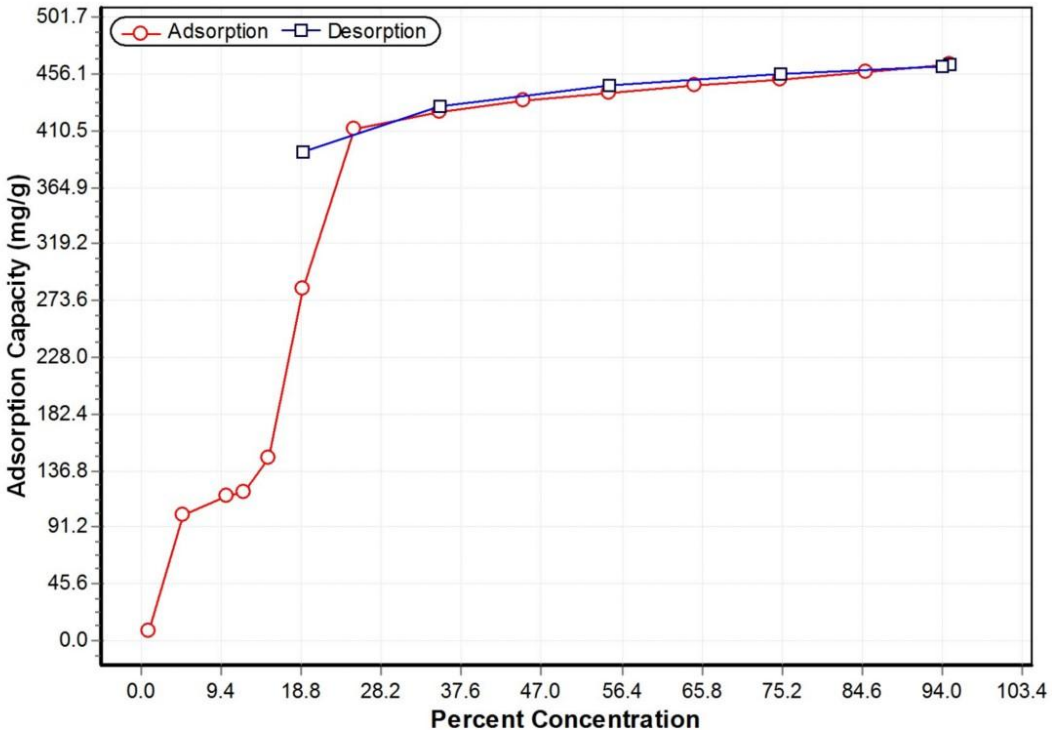

Supplementary Figure 27. H_2O adsorption isotherms of **ZNU-6** at 298 K.

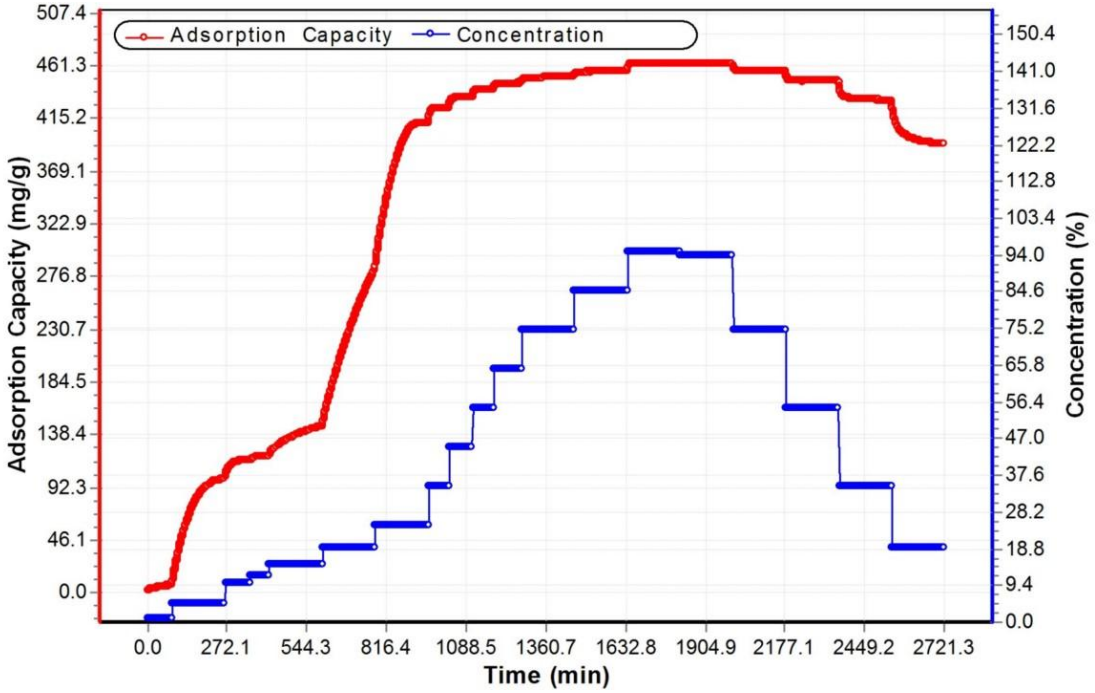

Supplementary Figure 28. H_2O adsorption capacity-time curve (adsorption kinetics) of **ZNU-6** at 298 K.

IV Kinetic studies

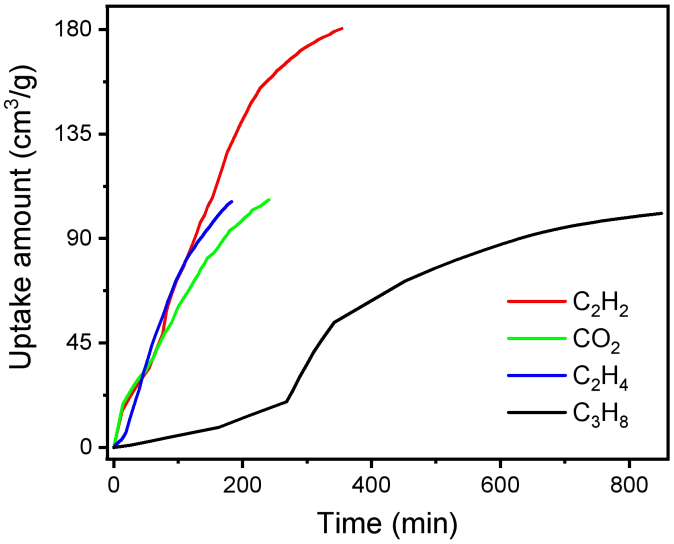

Supplementary Figure 29. Time-dependent adsorption curves of C_2H_2, CO_2, C_2H_4 and C_3H_8.

Analysis: Despite the narrow channel size in ZNU-6, the diffusion of C_2H_2, CO_2 and C_2H_4 are very fast. The measurements are finished within 350 min to reach saturated uptake. When compared, C_3H_8 with larger molecular size is less kinetic-favoured, the measurement takes over 800 min under the same conditions.

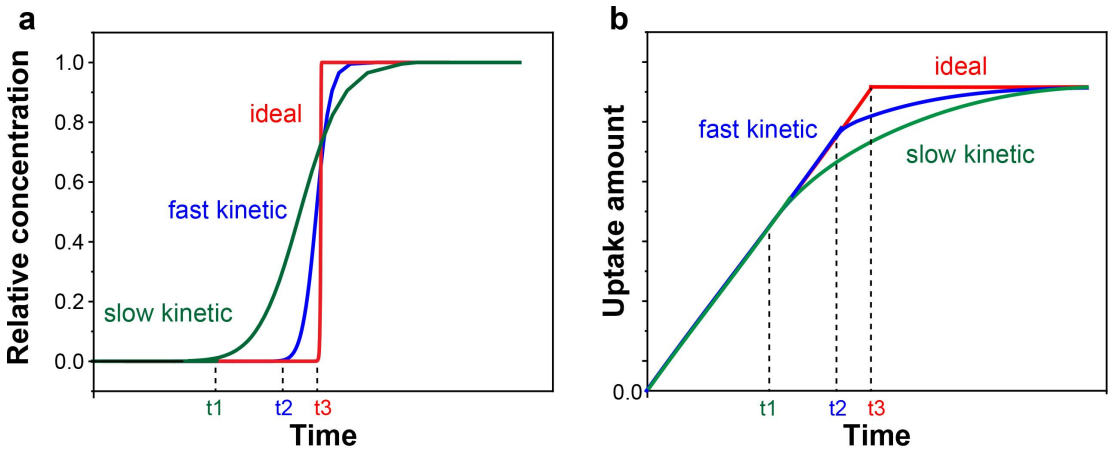

Supplementary Figure 30. Typical breakthrough curves (a) and the calculated kinetic curves therefrom.

1. Ideal materials (red curves) feature nearly vertical breakthrough curves, which is almost impossible to realize in real system due to the lateral diffusion as well as the diffusion between the particles in the fixed bed.

2. Materials with fast kinetic (blue curves) feature very sharp breakthrough curves, indicating the gas diffusion within the pores are very fast. The breakthrough phenomenon occurs when the material is nearly get saturated.

3. Materials with slow kinetic (green curves) feature relatively flat breakthrough curves. Due to the slow diffusion within the pores, tested gas flows through the space between particles instead of diffusion into the pores to be captured. Thus, the breakthrough phenomenon occurs when the material is far from gas-saturation.

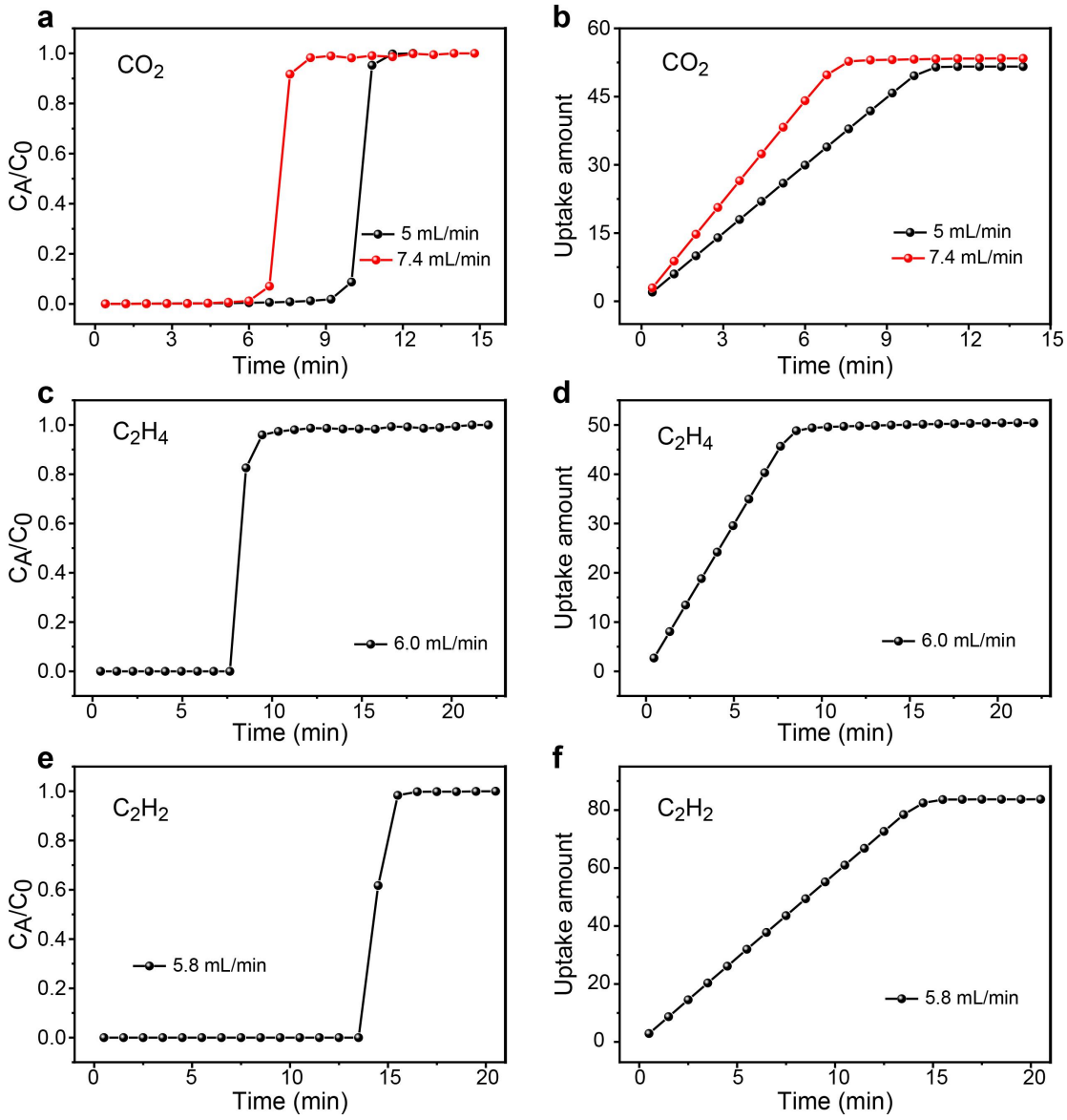

Supplementary Figure 31. Experimental breakthrough curves of pure gases in ZNU-6 and the calculated kinetic curves therefrom (a, b) CO_2; (c, d) C_2H_4; (e, f) C_2H_2.

The breakthrough curves of C_2H_2, CO_2 and C_2H_4 increase sharply after the gas break out, and the corresponding kinetic curves rises rapidly, indicating that ZNU-6 has fast kinetic for CO_2, C_2H_4 and C_2H_2 adsorption. Notably, the flow rate of > 5mL/min is relatively fast for breakthrough experiments; most breakthrough experiments reported in published papers were performed at ~ 2 mL/min. Thus, the retained sharp breakthrough curves under such high flowrate fully confirm the fast diffusion of CO_2, C_2H_4 and C_2H_2 in the pores of ZNU-6, which is very advantageous for practical applications

Experimental method: The column packed with ZNU-6 was activated completely firstly, and then pure CO_2, C_2H_4 or C_2H_2 was introduced at a specific flow rate. The measure range of our flowmetre is 0-10 sccm. The real flowrate is calibrated by self-made soapfilm flowmetre. The displayed and real flowrate is shown in Supplementary Table S8.

Supplementary Table 8. Comparison of the displayed and calibrated actual flowrate.

	Displayed flow rate (mL/min)	Actual flow rate (mL/min)
CO_2	6.8	5.0
CO_2	10.0	7.4
C_2H_4	10.0	6.0
C_2H_2	10.0	5.8

V Breakthrough experiments

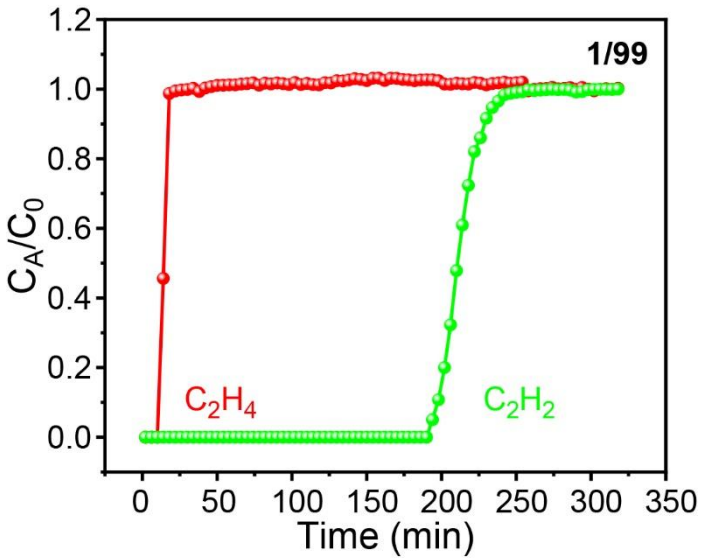

Supplementary Figure 32. Experimental breakthrough curves of **ZNU-6** for C_2H_4/C_2H_2 (1/99).

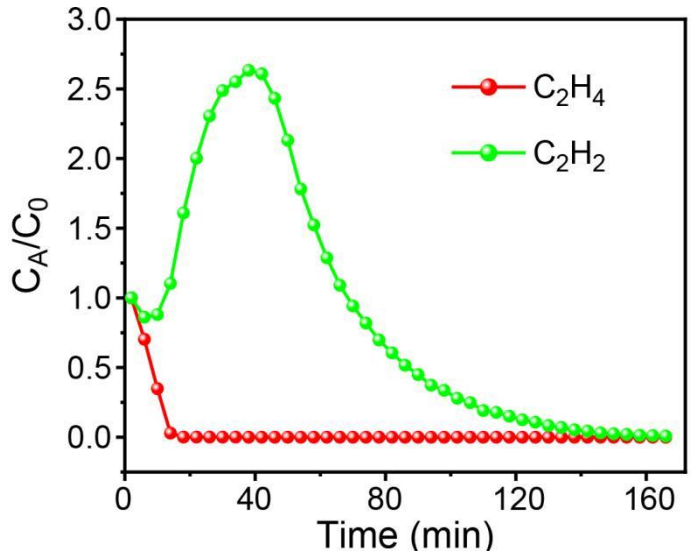

Supplementary Figure 33. Experimental dynamic desorption curves of **ZNU-6** after breakthrough experiment of C_2H_2/C_2H_4 (1/99). Desorption conditions: Ar flow rate 10 mL/min at 75 °C.

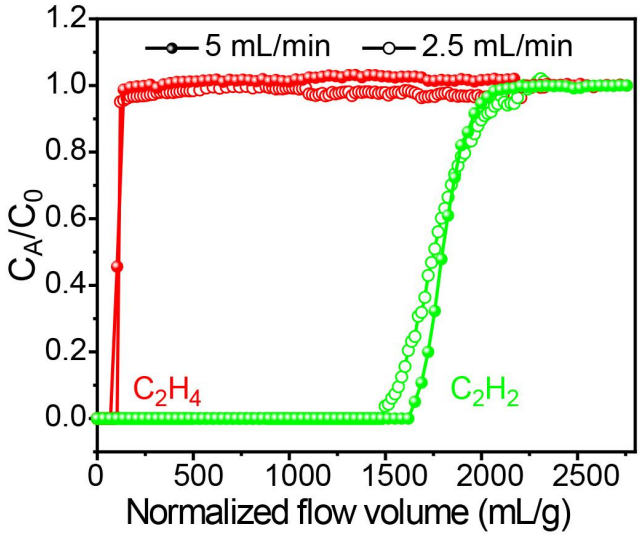

Supplementary Figure 34. Experimental breakthrough curves of **ZNU-6** for C_2H_2 /C_2H_4 (1/99) at different flow rate.

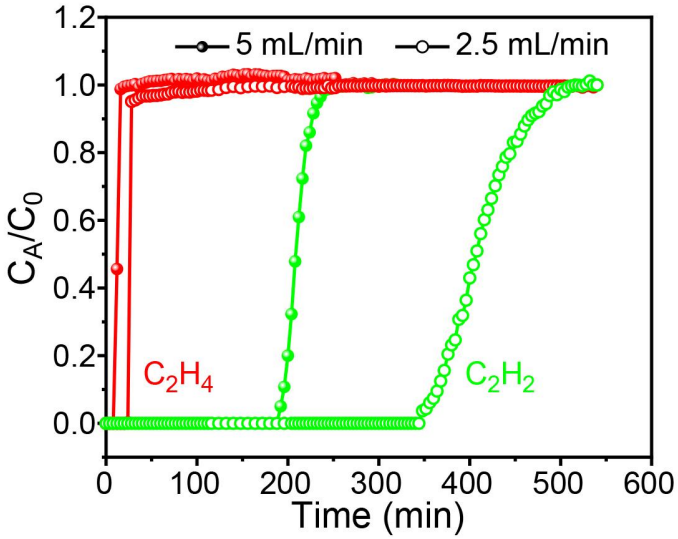

Supplementary Figure 35. Experimental breakthrough curves of **ZNU-6** for C_2H_2/C_2H_4 (1/99) at different flow rate.

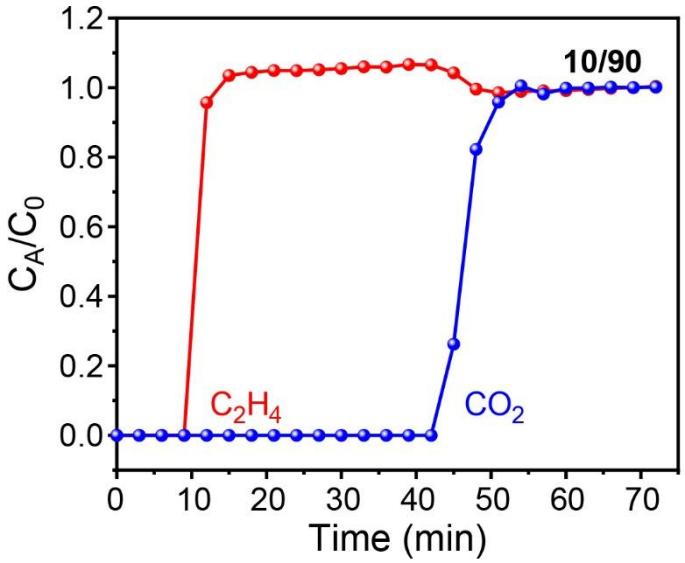

Supplementary Figure 36. Experimental breakthrough curves of **ZNU-6** for CO_2/C_2H_4 (10/90).

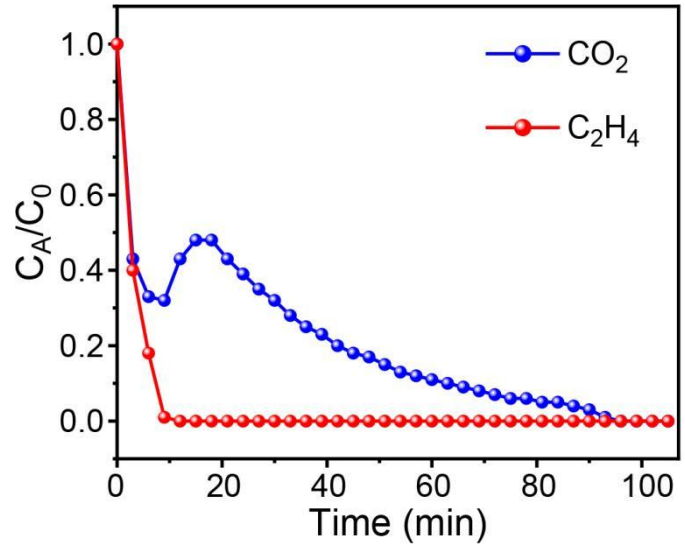

Supplementary Figure 37. Experimental dynamic desorption curves of **ZNU-6** after breakthrough experiment of CO_2/C_2H_4 (10/90). Desorption conditions: Ar flow rate 10 mL/min at 75 °C.

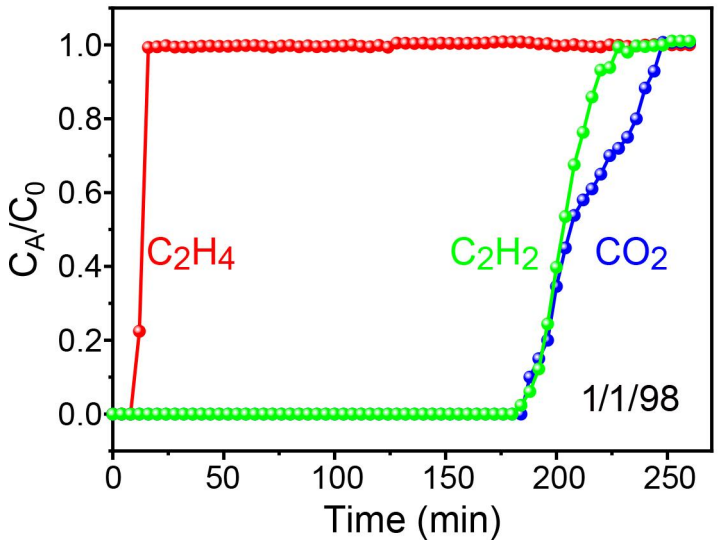

Supplementary Figure 38. Experimental breakthrough curves of **ZNU-6** for $C_2H_2/CO_2/C_2H_4$ (1/1/98). Flow rate: 5 mL/min.

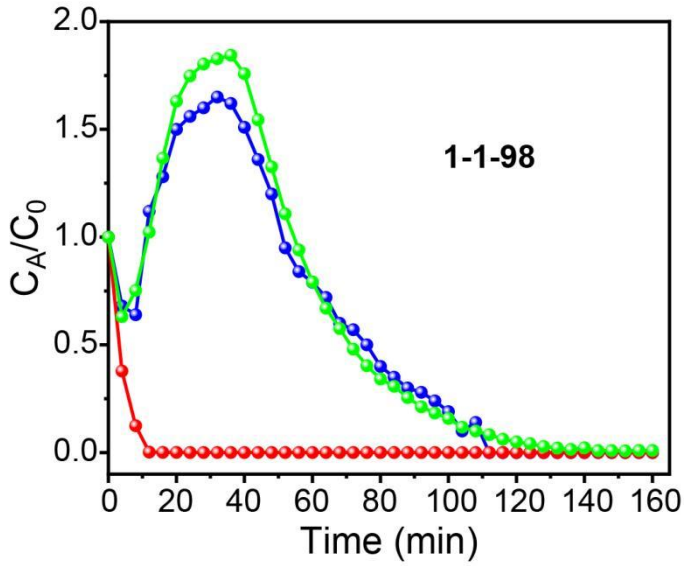

Supplementary Figure 39. Experimental dynamic desorption curves of **ZNU-6** after breakthrough experiment of $C_2H_2/CO_2/C_2H_4$ (1/1/98). Desorption conditions: Ar flow rate 10 mL/min at 75 °C.

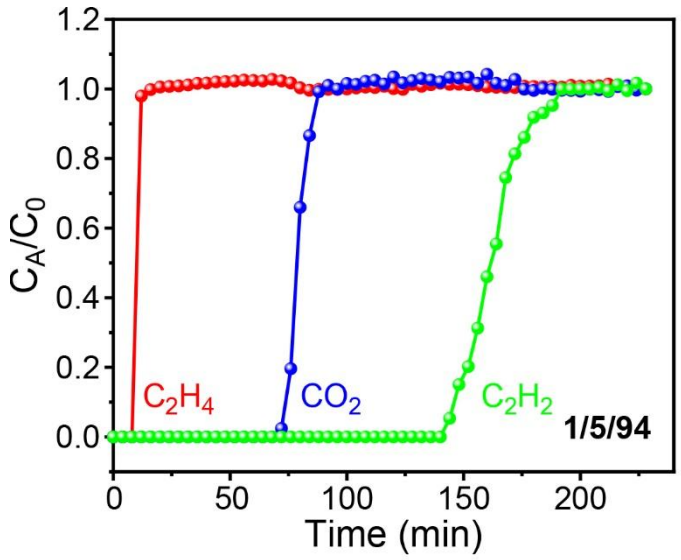

Supplementary Figure 40. Experimental breakthrough curves of **ZNU-6** for $C_2H_2/CO_2/C_2H_4$ (1/5/94). Flow rate: 5 mL/min.

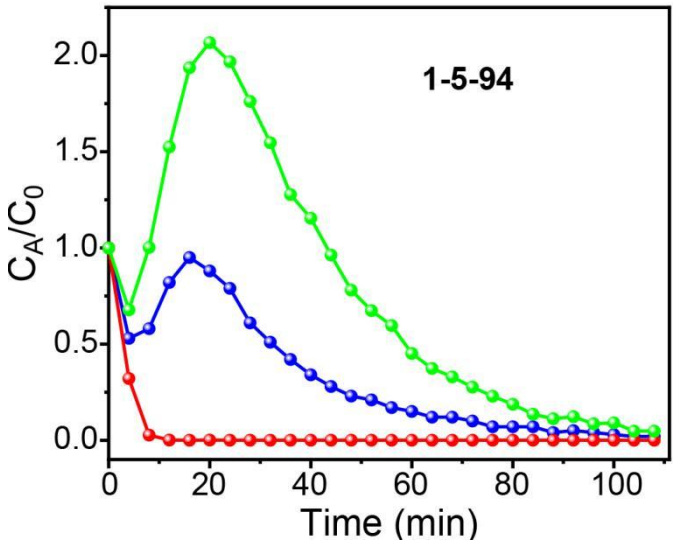

Supplementary Figure 41. Experimental dynamic desorption curves of **ZNU-6** after breakthrough experiment of $C_2H_2/CO_2/C_2H_4$ (1/5/94). Desorption conditions: Ar flow rate 10 mL/min at 75 °C.

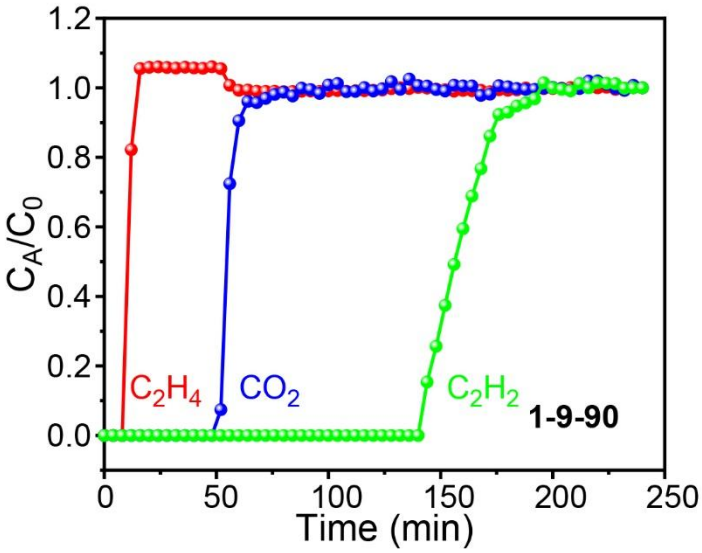

Supplementary Figure 42. Experimental breakthrough curves of **ZNU-6** for $C_2H_2/CO_2/C_2H_4$ (1/9/90). Flow rate: 5 mL/min.

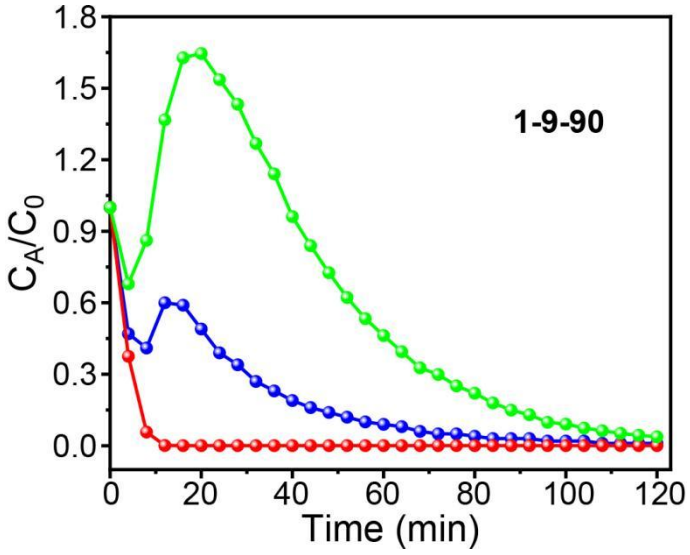

Supplementary Figure 43. Experimental dynamic desorption curves of **ZNU-6** after breakthrough experiment of $C_2H_2/CO_2/C_2H_4$ (1/9/90). Desorption conditions: Ar flow rate 10 mL/min at 75 °C.

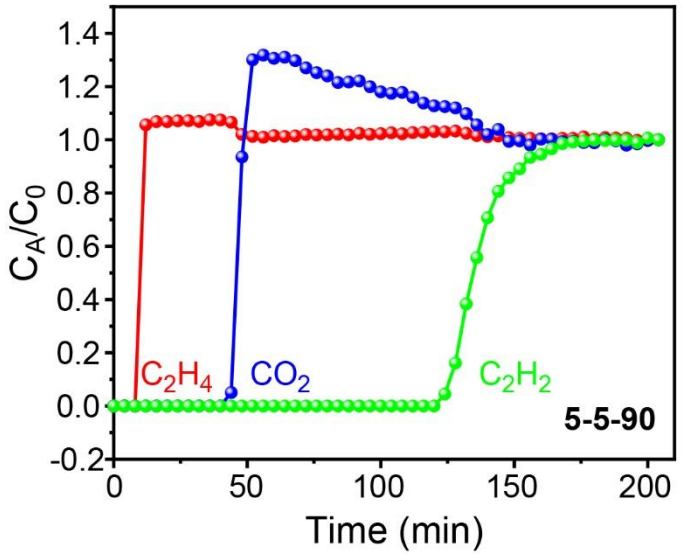

Supplementary Figure 44. Experimental breakthrough curves of **ZNU-6** for $C_2H_2/CO_2/C_2H_4$ (5/5/90). Flow rate: 5 mL/min.

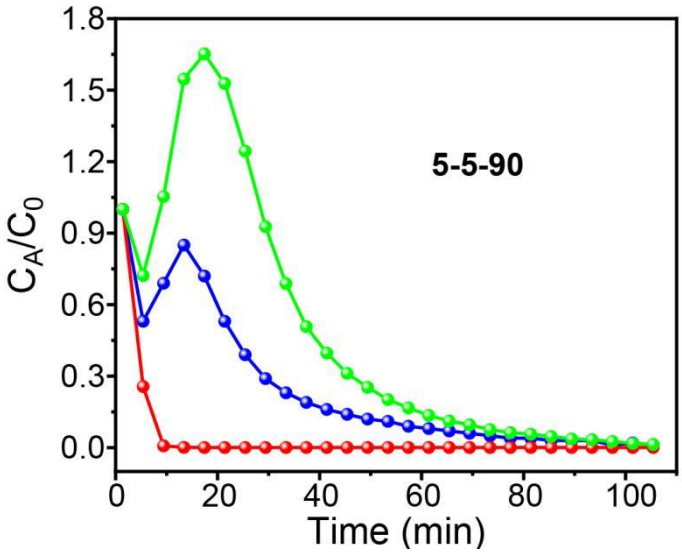

Supplementary Figure 45. Experimental dynamic desorption curves of **ZNU-6** after breakthrough experiment of $C_2H_2/CO_2/C_2H_4$ (5/5/90). Desorption conditions: Ar flow rate 10 mL/min at 75 °C.

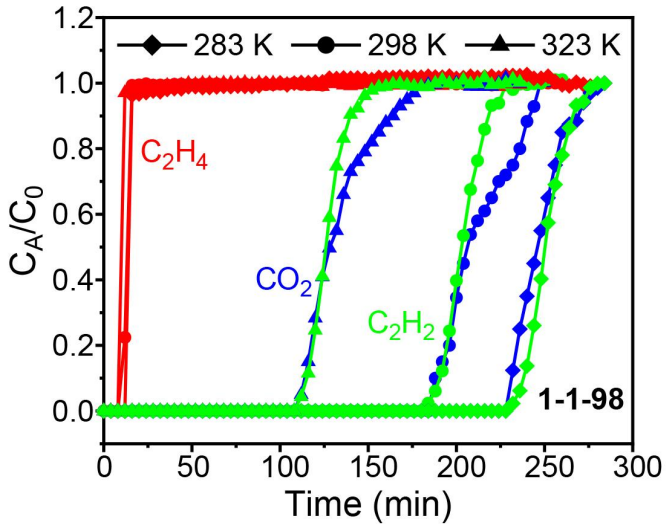

Supplementary Figure 46. Experimental breakthrough curves of **ZNU-6** for $C_2H_2/CO_2/C_2H_4$ (1/1/98) at 283, 298 and 323 K. Flow rate: 5 mL/min.

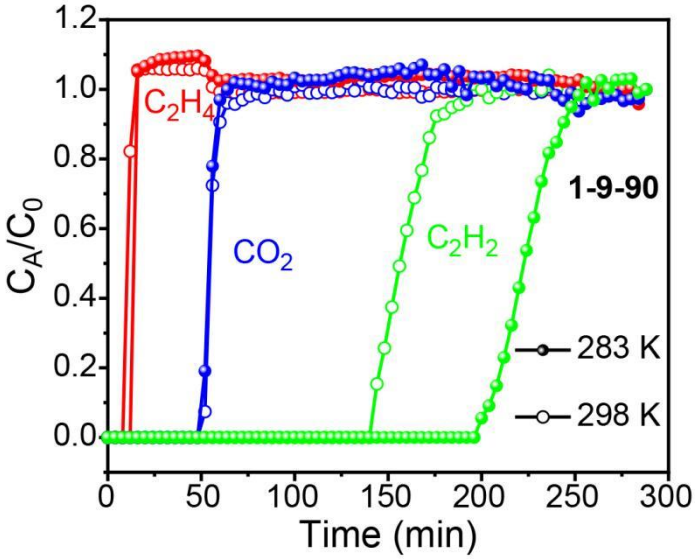

Supplementary Figure 47. Experimental breakthrough curves of **ZNU-6** for $C_2H_2/CO_2/C_2H_4$ (1/9/90) at 283 and 298 K. Flow rate: 5 mL/min.

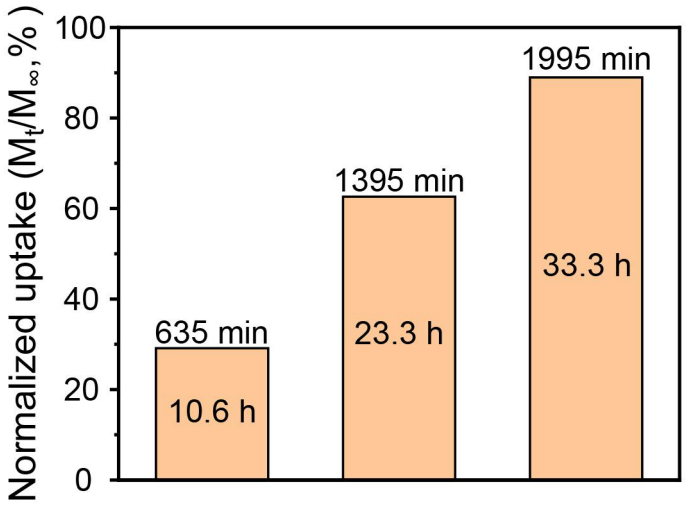

Supplementary Figure 48. H_2O uptake in breakthrough experiments (N_2, RH=100%). Flow rate: 5 mL/min.

Experimental method: The column packed with ZNU-6 was activated completely firstly, and then N_2 with saturated moisture was introduced at a flow rate of 5 mL/min. After each period, the column was picked out and weighted by balance to calculate the adsorbed amount of water. The adsorbed N_2 amount is neglected.

Supplementary Table 9. Experimental dynamic C_2H_4 productivity and captured C_2H_2/CO_2 amount for ZNU-6 from different gas ratios and under different conditions.

Conditions	Experimental C_2H_4 productivity (mol/kg)	Experimental C_2H_2 captured amount (mol/kg)	Experimental CO_2 captured amount (mol/kg)
C_2H_2-CO_2-C_2H_4 (1-1-98) 283 K	80.89	0.96	0.98
C_2H_2-CO_2-C_2H_4 (1-1-98) 298 K	64.42	0.78	0.84
C_2H_2-CO_2-C_2H_4 (1-1-98) 323 K	36.73	0.48	0.53
C_2H_2-CO_2-C_2H_4 (1-5-94) 298 K	21.37	0.60	1.52
C_2H_2-CO_2-C_2H_4 (1-9-90) 298 K (dry)	13.81	0.56	1.97
C_2H_2-CO_2-C_2H_4 (5-5-90) 298 K	11.04	2.65	0.55
C_2H_2-CO_2-C_2H_4 (1-9-90) 298 K (humid)	13.79	-	-

Supplementary Table 10. Experimental dynamic C_2H_4 productivity for different adsorbents.

	$C_2H_2/CO_2/C_2H_4$=1/9/90 (v/v/v) Flow rate: 5 mL/min					
	ZNU-6	NTU-67	Activated carbon	zeolite 5A	SIFSIX-2-Cu-i	SIFSIX-17-Ni
Mass (g)	0.58	1.20	0.98	1.74	0.52	0.82
Time 1[a] (min)	52.00	43.59	21.40	13.18	12.61	12.24
Time 2[b] (min)	196.00	84.38	34.19	45.89	170.08	83.82
Time 1 (min g^{-1})	89.56	36.17	21.84	7.58	24.20	14.96
Time 2 (min g^{-1})	337.58	70.03	34.89	26.40	326.44	102.42
Productivity per adsorption cycle (mol kg^{-1})	13.81	5.42	0.49	0.36	2.40	2.47
Productivity based on Time 1 (mol kg^{-1} h^{-1})	15.93	7.46	1.38	1.62	11.41	12.10
Productivity based on Time 2 (mol kg^{-1} h^{-1})	4.23	3.85	0.86	0.46	0.85	1.77

[a] Time 1 is the time when the second gas can be detected after C_2H_4;

[b] Time 2 is the time when C_A/C_0 reaches 1.0 for all the gases.

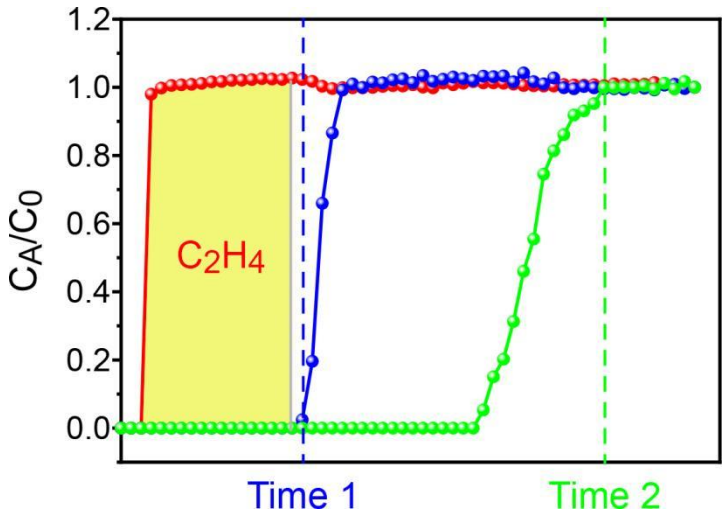

Supplementary Table 11. Experimental dynamic C_2H_4 productivity for ZNU-6 from different gas ratios and under different conditions.

	ZNU-6 Flow rate: 5 mL/min						
$C_2H_2/CO_2/C_2H_4$ (v/v/v)	1-1-98 283 K	1-1-98 298 K	1-1-98 323 K	1-5-94	1-9-90 dry	5-5-90	1-9-90 humid
Time 1 (min)	232.00	184.00	112.00	72.00	52.00	44.00	112.00
Time 2 (min)	284.00	248.00	180.00	192.00	196.00	180.00	180.00
Productivity per adsorption cycle (mol kg^{-1})	80.89	64.42	36.73	21.37	13.81	11.04	13.79
Productivity based on Time 1 (mol kg^{-1} h^{-1})	20.92	21.01	19.68	17.81	15.93	15.05	7.39
Productivity based on Time 2 (mol kg^{-1} h^{-1})	17.09	15.59	12.24	6.68	4.23	3.68	4.60

VI Supplementary References

[1] X.-H. Xiong, L. Zhang, W. Wang, N.-X. Zhu, L.-Z. Qin, H.-F. Huang, L.-L. Meng, Y.-Y. Xiong, M. Barboiu, D. Fenske, P. Hu, Z.-W. Wei, *ACS Appl. Mater. Interfaces* **2022**, *14*, 32105–32111.

[2] Q. Dong, Y. Huang, K. Hyeon-Deuk, I.-Y. Chang, J. Wan, C. Chen, J. Duan, W. Jin, S. Kitagawa, *Adv. Funct. Mater.* **2022**, 2203745.DOI: 10.1002/adfm.202203745.

[3] S. Mukherjee, N. Kumar, A. A. Bezrukov, K. Tan, T. Pham, K. A. Forrest, K. A. Oyekan, O. T. Qazvini, D. G. Madden, B. Space, M. J. Zaworotko, *Angew. Chem. Int. Ed.* **2021**, *60*, 10902–10909.

[4] X. Cui, K. Chen, H. Xing, Q. Yang, R. Krishna, Z. Bao, H. Wu, W. Zhou, X. Dong, Y. Han, B. Li, Q. Ren, M. J. Zaworotko, B. Chen, *Science* **2016**, *353*, 141–144.

[5] X. Cui, Q. Yang, L. Yang, R. Krishna, Z. Zhang, Z. Bao, H. Wu, Q. Ren, W. Zhou, B. Chen, H. Xing, *Adv. Mater.* **2017**, *29*, 1606929.

[6] O. Shekhah, Y. Belmabkhout, Z. Chen, V. Guillerm, A. Cairns, K. Adil, M. Eddaoudi, *Nat. Commun.* **2014**, *5*, 4228.

[7] R.-B. Lin, L. Li, H. Wu, H. Arman, B. Li, R.-G. Lin, W. Zhou, B. Chen, *J. Am. Chem. Soc.* **2017**, *139*, 8022–8028.

[8] Q. Dong, X. Zhang, S. Liu, R.-B. Lin, Y. Guo, Y. Ma, A. Yonezu, R. Krishna, G. Liu, J. Duan, R. Matsuda, W. Jin, B. Chen, *Angew. Chem. Int. Ed.* **2020**, *59*, 22756–22762.

[9] B. Li, X. Cui, D. O'Nolan, H.-M. Wen, M. Jiang, R. Krishna, H. Wu, R.-B. Lin, Y.-S. Chen, D. Yuan, H. Xing, W. Zhou, Q. Ren, G. Qian, M. J. Zaworotko, B. Chen, *Adv. Mater.* **2017**, *29*, 1704210.

[10] M. Jiang, B. Li, X. Cui, Q. Yang, Z. Bao, Y. Yang, H. Wu, W. Zhou, B. Chen, H. Xing, *ACS Appl. Mater. Interfaces* **2018**, *10*, 16628–16635.

[11] Z. Zhang, Q. Ding, J. Cui, H. Xing, *Small* **2020**, *16*, 2005360.

[12] D. O'Nolan, A. Kumar, K.-J. Chen, S. Mukherjee, D. G. Madden, M. J. Zaworotko, *ACS Appl. Nano Mater.* **2018**, *1*, 6000–6004.

[13] N. Xu, J. Hu, L. Wang, D. Luo, W. Sun, Y. Li, Y. Hu, D. Wang, X. Cui, H. Xing, Y. Zhang, *Chem. Eng. J.* **2022**, *450*, 138034.

[14] J. Wang, Y. Zhang, P. Zhang, J. Hu, R.-B. Lin, Q. Deng, Z. Zeng, H. Xing, S. Deng, B. Chen, *J. Am. Chem. Soc.* **2020**, *142*, 9744–9751.

[15] L. Wang, N. Xu, Y. Hu, W. Sun, R. Krishna, J. Li, Y. Jiang, S. Duttwyler, Y. Zhang, *Nano Res.* **2022** (in revision).

[16] H. Li, C. Liu, C. Chen, Z. Di, D. Yuan, J. Pang, W. Wei, M. Wu, M. Hong, *Angew. Chem. Int. Ed.* **2021**, *60*, 7547–7552.

nature portfolio

Peer Review File

Benchmark Single-Step Ethylene Purification from Ternary Mixtures by a Customized Fluorinated Anion Embedded MOF

REVIEWER COMMENTS</B>

Reviewer #1 (Remarks to the Author):

In this work authors reported GeF62- anion incorporated MOF named ZNU-6. The MOF has optimum pore structure and environment for one step ethylene purification and also high selective for carbon di oxide separation as well. This research area is very promising epically today when we need to find better alternative for energy storage and separation. The authors investigated the MOF in different conditions and proved its viability and effectiveness. The chemical approach of this work is strong, and the results are clearly visible from the experiments
However here are some of my questions and concerns
1. The topic of ethylene purification/ separation using MOF is not very new, even incorporation of anions in MOFs has been reported by the authors group recently (Wang et al, Nano Research 2022). It would be great if authors can describe the novelty of this research as suitable of Nature common
2. Its seems that the customized pore environment helps to help achieve higher selectivity however DFT studies, and in-situ X ray have been performed to corroborate the statement. Have the authors performed any in-situ IR to verify the conclusions? This evidence will help strengthen the case
3. Heat of adsorption values and isotherm dependency with temp indicates the physisorption nature of guest /host chemistry. However, the additional interaction with anions and even TPA can provide some chemisorption in CO2. Have the authors performed any Temp programed desorption studies in terms of gases of choice to see the binding behavior?
4. What is the relative humidity used in this study?
5. We can see ZNU-6 is strong water adsorbent however in humid conditions shows negligible deterioration of separation performance. However, the reasoning and data is not very clear, has the authors tried to quantify the effect of humidity in this case,
6. In similar topic, what happen in desorption cases in breakthrough, I mean when the fixed bed is undergoing regeneration, have the authors quantified the effect of humidity in gas desorption cases and in cyclic performance?

Reviewer #2 (Remarks to the Author):

The authors reported a GeF62- anion embedded MOF, ZNU-6, with optimized pore structure and environment for highly efficient C2H4 recovery from various C2H2/CO2/C2H4 ternary mixtures. The material exhibited good recyclability and resistance toward moisture during breakthrough experiments. Ethylene (C2H4) purification from multi-component mixtures by physical adsorption is an important industrial challenging, and this work will be very interesting for the readers. The experiments were well performed and the manuscript has been written well. I agree that this manuscript to be accepted for Nature Communications after some minor revision. The following are the suggestions for the authors to improve the manuscript.
1. Figure 1 Caption, (f) is inconsistent with other numbering.
2. Supplementary Figure 10-11, the authors should provide the pressure of these IAST selectivities.
3. For the in-situ gas-loaded MOF structure, the authors should add a figure to describe the C2H2 gas molecule cluster and the interactions between the molecules, either in main text or SI. A figure illustrating the interaction between adsorbed water and gas molecules should also be added.

Reviewer #3 (Remarks to the Author):

Thanks to its potential to introduce energy-efficient, single-step ethylene purification

approaches, this manuscript by Jiang et al. is of high topical relevance to gas purifications, and MOFs for separations. Considering high importance of the new findings, and their general relevance in controlling the pore electrostatics (F···C=O interactions) driven gas separation/purification properties, I support publication subject to necessary revisions as follows:

● Molecular formulae are missing including that of the new as-synthesised ZNU-6 (although I find this formula in Table S7, should be clearly noted in the manuscript too). All molecular formulae for the gas-loaded phases should be clearly written in the main article, if needed, using a table with analysis of sorbate-sorbent interactions (distances).

● The authors should not be presenting the adsorption data with respect to molecules per GeF62- anion, this makes the data skewed in favour of this adsorbent, ZNU-6. Also, the units for adsorption uptakes and pressure need to be consistent. Right now, with mixed use of cm3/g, mmol/g, mol/mol and mmol/g, these are all mixed up; same mix-up is observed in the units used for pressure, bar and kPa. Collectively, all these mistakes come together in the manuscript Figure 2. I strongly recommend replotting the isotherm-based uptakes in one consistent pair of units: mmol/g and bar. This not only makes this manuscript coherent but also helps the whole community working in this are with regard to comparing performance parameters across different adsorbents.

● Page 2, lines 33-34, the authors need to discuss "Presently, multi-step purification process is adopted for purification of C2H4 from C2H4/C2H2/CO2 mixtures." This needs to take cognisance of the recent reports on single-step C2H4 purification from ternary (1:1:1 for C2H2/C2H4/C2H6) and quaternary (1:1:1:1 for C2H2/C2H4/C2H6/CO2) gas mixtures. Some examples include: Cao, JW. et al., Nat Commun. 2021, 12, 6507. Xu, Z. et al., Nat Commun. 2020, 11, 3163.

● I don't quite agree with the authors use of the word "static" in the heading of Figure 2. Should just be written as "The sorption performance." In another instance, the authors use this phrase "static adsorption" (page 11, line 202), which I object to.

● It is stated that the C2H4 productivity is 309 mL/g, again this unit is far from the standard unit typically used in other literature reports in this area, i.e., mol kg-1 h-1.

● Importantly, the authors have calculated productivity by integrating the effluent flow rate of C2H4 (cm3/min). However, all the breakthrough curves (in Fig. 5) are showed in with the effluent concentration (C/C0). It is obvious that integrating the concentration curve cannot give the amount, although a few references adopt this wrong method. Therefore, it is necessary to show the details for direct measurement and/or indirect calculation of the effluent flow rate and concentration in this study. See Shen, J. et al., Nat Commun. 2020, 11, 6259 as a reference.

● How common / rare is the ith-d topology among the anion-pillared MOF library? It would greatly help the article / future readers, if the authors can address this by a thorough literature-based contextualisation of the structural topology of ZNU-6.

● Section 7 in the supplementary information has a header "Breakthrough simulations and experiments", the following figure captions for Supplementary Figures 28-43 are all including "Experimental" in their figure captions, nonetheless. I wonder where the simulation-derived breakthrough data is?

Overall, an interesting idea executed by the authors that should advance this area in the near future. I will be glad to look at a suitably revised article, when ready.

Reviewer #4 (Remarks to the Author):

This manuscript by Jiang et al, report a metal organic framework (ZNU-6) for the application of simultaneous removal of C2H2 and CO2 from C2H4 stream. This area is of important practical applications and has been extensively investigated in the past few years. The overall quality of this manuscript is high with detailed investigation of the structure characterisation of the MOF, study of its adsorption properties using isotherm and breakthrough experiments, and thorough investigation of the host-guest interactions. Below are some comments and questions from me, and I would recommend the publication of this manuscript after the authors fully address them:

1. I think it is necessary that the authors reference some highly relevant publications in

the inttroduction, e.g. Hexafluorogermanate (GeFSIX) Anion-Functionalized Hybrid Ultramicroporous Materials for Efficiently Trapping Acetylene from Ethylene, Ind. Eng. Chem. Res. 2018, 57, 21, 7266–7274.

2. The cif. File for CO_2 loaded ZNU-6 shows an O-C-O bond angle of CO_2 being 157 ° instead of the theoretical 180°, could the authors please explain this discrepancy.

3. Figure 2f, the Qst for CO_2, why it showed a sudden drop at 2mmol/g coverage?

4. From the isotherms for CO_2 and C_2H_4 (Figure 2b, 2d), the saturation uptake for CO_2 and C_2H_4 are very close; and the kinetic data (supplementary figure 25) of CO_2 and C_2H_4 are also similar with C_2H_4 being slightly faster in adsorption. For Qst, CO_2 started higher than C_2H_4 then fall to be lower than C_2H_4. These three parameters (uptake, kinetic, Qst), all seem indicating the interaction between the gas molecules and the framework is very similar. In this case, how do the authors rationalise the observed separation in breakthrough experiments? what do the authors think is the really reason that ZNU-6 can retain CO_2 from mixtures containing mainly C_2H_4 and small percentage of CO_2.

REVIEWER COMMENTS

Reviewer #1 (Remarks to the Author)

In this work authors reported GeF_6^{2-} anion incorporated MOF named ZNU-6. The MOF has optimum pore structure and environment for one step ethylene purification and also high selective for carbon dioxide separation as well. This research area is very promising especially today when we need to find better alternative for energy storage and separation. The authors investigated the MOF in different conditions and proved its viability and effectiveness. The chemical approach of this work is strong, and the results are clearly visible from the experiments

However here are some of my questions and concerns

1. The topic of ethylene purification/ separation using MOF is not very new, even incorporation of anions in MOFs has been reported by the authors group recently (Wang et al, Nano Research 2022). It would be great if authors can describe the novelty of this research as suitable of Nature common.
2. Its seems that the customized pore environment helps to achieve higher selectivity however DFT studies, and in-situ X ray have been performed to corroborate the statement. Have the authors performed any in-situ IR to verify the conclusions? This evidence will help strengthen the case
3. Heat of adsorption values and isotherm dependency with temp indicates the physisorption nature of guest /host chemistry. However, the additional interaction with anions and even TPA can provide some chemisorption in CO_2. Have the authors performed any Temp programed desorption studies in terms of gases of choice to see the binding behavior?
4. What is the relative humidity used in this study?
5. We can see ZNU-6 is strong water adsorbent however in humid conditions shows negligible deterioration of separation performance. However, the reasoning and data is not very clear, has the authors tried to quantify the effect of humidity in this case.
6. In similar topic, what happen in desorption cases in breakthrough, I mean when the fixed bed is undergoing regeneration, have the authors quantified the effect of humidity in gas desorption cases and in cyclic performance?

Reviewer #2 (Remarks to the Author)

The authors reported a GeF_6^{2-} anion embedded MOF, ZNU-6, with optimized pore structure and environment for highly efficient C_2H_4 recovery from various $C_2H_2/CO_2/C_2H_4$ ternary mixtures. The material exhibited good recyclability and resistance toward moisture during breakthrough experiments. Ethylene (C_2H_4) purification from multi-component mixtures by physical adsorption is an important industrial challenging, and this work will be very interesting for the readers. The experiments were well performed and the manuscript has been written well. I agree that this manuscript to be accepted for Nature Communications after some minor revision. The following are the suggestions for the authors to improve the manuscript.

1. Figure 1 Caption, (f) is inconsistent with other numbering.
2.Supplementary Figure 10-11, the authors should provide the pressure of these IAST

selectivities.
3. For the in-situ gas-loaded MOF structure, the authors should add a figure to describe the C_2H_2 gas molecule cluster and the interactions between the molecules, either in main text or SI. A figure illustrating the interaction between adsorbed water and gas molecules should also be added.

Reviewer #3 (Remarks to the Author)
Thanks to its potential to introduce energy-efficient, single-step ethylene purification approaches, this manuscript by Jiang et al. is of high topical relevance to gas purifications, and MOFs for separations. Considering high importance of the new findings, and their general relevance in controlling the pore electrostatics (F···C=O interactions) driven gas separation/purification properties, I support publication subject to necessary revisions as follows:
1. Molecular formulae are missing including that of the new as-synthesized ZNU-6 (although I find this formula in Table S7, should be clearly noted in the manuscript too). All molecular formulae for the gas-loaded phases should be clearly written in the main article, if needed, using a table with analysis of sorbate-sorbent interactions (distances)
2. The authors should not present the adsorption data with respect to molecules per GeF_6^{2-} anion, this makes the data skewed in favour of this adsorbent, ZNU-6. Also, the units for adsorption uptakes and pressure need to be consistent. Right now, with mixed use of cm^3/g, mmol/g, mol/mol and mmol/g, these are all mixed up; same mix-up is observed in the units used for pressure, bar and kPa. Collectively, all these mistakes come together in the manuscript Figure 2. I strongly recommend replotting the isotherm-based uptakes in one consistent pair of units: mmol/g and bar. This not only makes this manuscript coherent but also helps the whole community working in this area with regard to comparing performance parameters across different adsorbents.
3. Page 2, lines 33-34, the authors need to discuss “Presently, multi-step purification process is adopted for purification of C_2H_4 from $C_2H_4/C_2H_2/CO_2$ mixtures.” This needs to take cognisance of the recent reports on single-step C2H4 purification from ternary (1:1:1 for $C_2H_2/C_2H_4/C_2H_6$) and quaternary (1:1:1:1 for $C_2H_2/C_2H_4/C_2H_6/CO_2$) gas mixtures. Some examples include: Cao, JW. et al., Nat Commun. 2021, 12, 6507. Xu, Z. et al., Nat Commun. 2020, 11, 3163.
4. I don’t quite agree with the authors use of the word “static” in the heading of Figure 2. Should just be written as “The sorption performance.” In another instance, the authors use this phrase “static adsorption” (page 11, line 202), which I object to.
5. It is stated that the C_2H_4 productivity is 309 mL/g, again this unit is far from the standard unit typically used in other literature reports in this area, i.e., mol kg^{-1} h^{-1}
6. Importantly, the authors have calculated productivity by integrating the effluent flow rate of C_2H_4 (cm^3/min). However, all the breakthrough curves (in Fig. 5) are showed in with the effluent concentration (C/C_0). It is obvious that integrating the concentration curve cannot give the amount, although a few references adopt this wrong method. Therefore, it is necessary to show the details for direct measurement and/or indirect calculation of the effluent flow rate and concentration in this study.

See Shen, J. et al., Nat Commun. 2020, 11, 6259 as a reference.
7. How common / rare is the ith-d topology among the anion-pillared MOF library? It would greatly help the article/future readers, if the authors can address this by a thorough literature-based contextualisation of the structural topology of ZNU-6.
8. Section 7 in the supplementary information has a header "Breakthrough simulations and experiments", the following figure captions for Supplementary Figures 28-43 are all including "Experimental" in their figure captions, nonetheless. I wonder where the simulation-derived breakthrough data is?
Overall, an interesting idea executed by the authors that should advance this area in the near future. I will be glad to look at a suitably revised article, when ready.

Reviewer #4 (Remarks to the Author)
This manuscript by Jiang et al, report a metal organic framework (ZNU-6) for the application of simultaneous removal of C_2H_2 and CO_2 from C_2H_4 stream. This area is of important practical applications and has been extensively investigated in the past few years. The overall quality of this manuscript is high with detailed investigation of the structure characterisation of the MOF, study of its adsorption properties using isotherm and breakthrough experiments, and thorough investigation of the host-guest interactions. Below are some comments and questions from me, and I would recommend the publication of this manuscript after the authors fully address them:
1. I think it is necessary that the authors reference some highly relevant publications in the introduction, e.g. Hexafluorogermanate (GeFSIX) Anion-Functionalized Hybrid Ultramicroporous Materials for Efficiently Trapping Acetylene from Ethylene, Ind. Eng. Chem. Res. 2018, 57, 21, 7266–7274.
2. The cif. File for CO_2 loaded ZNU-6 shows an O-C-O bond angle of CO_2 being 157° instead of the theoretical 180°, could the authors please explain this discrepancy.
3. Figure 2f, the Qst for CO_2, why it showed a sudden drop at 2 mmol/g coverage?
4. From the isotherms for CO_2 and C_2H_4 (Figure 2b, 2d), the saturation uptake for CO_2 and C_2H_4 are very close; and the kinetic data (supplementary figure 25) of CO_2 and C_2H_4 are also similar with C_2H_4 being slightly faster in adsorption. For Qst, CO_2 started higher than C_2H_4 then fall to be lower than C_2H_4. These three parameters (uptake, kinetic, Qst), all seem indicating the interaction between the gas molecules and the framework is very similar. In this case, how do the authors rationalise the observed separation in breakthrough experiments? what do the authors think is the really reason that ZNU-6 can retain CO_2 from mixtures containing mainly C_2H_4 and small percentage of CO_2.

Comments from Reviewer 1:

Overall comment. *In this work authors reported* GeF_6^{2-} *anion incorporated MOF named ZNU-6. The MOF has optimum pore structure and environment for one step ethylene purification and also high selective for carbon dioxide separation as well. This research area is very promising especially today when we need to find better alternative for energy storage and separation. The authors investigated the MOF in different conditions and proved its viability and effectiveness. The chemical approach of this work is strong, and the results are clearly visible from the experiments*

However here are some of my questions and concerns

Comment 1. *The topic of ethylene purification/ separation using MOF is not very new, even incorporation of anions in MOFs has been reported by the authors group recently (Wang et al, Nano Research 2022). It would be great if authors can describe the novelty of this research as suitable of Nature common.*

Author response: Thank you for your comment. The topic of using MOFs for ethylene purification is not very new indeed. Presently, ethylene purification from C_2H_2/C_2H_4, C_2H_2/C_2H_4, $C_2H_2/C_2H_4/C_2H_6$ has been realized by a plenty of MOFs materials. Compared with those, the investigation on the single-step C_2H_4 purification from $C_2H_2/CO_2/C_2H_4$ has been investigated much less (no more than 10 materials). The reference mentioned in comment 1 (Wang et al, Nano Research 2022) is for C_2H_2 purification from other mixtures, different from this work. So far, TIFSIX-17-Ni, NTU-65 and NTU-67 are the optimal materials. However, each material has significant drawback. The capacity of C_2H_2 (3.30 mmol/g) and CO_2 (2.20 mmol/g) is relatively low in TIFSIX-17-Ni due to the over-contracted channel. NTU-65 capture C_2H_2 and CO_2 by tuning the gate opening, but the applied temperature must be at 263 K because lower temperatures lead to the adsorption of all the gases while higher temperatures cause the exclusion of CO_2. NTU-67 displays modest C_2H_2 (3.29 mmol/g) and CO_2 (2.04 mmol/g) capacity as well as reduced C_2H_2/C_2H_4 and CO_2/C_2H_4 selectivity compared to TIFSIX-17-Ni. Besides, the separation performance of NTU-67 is deteriorated under

humid conditions. Therefore, the trade-off between adsorption capacity and selectivity in the C_2H_4 purification from $C_2H_2/CO_2/C_2H_4$ is still challenging to overcome by existing porous materials. ZNU-6 reported in this work is a novel MOF with both narrow interlaced channels, large pores and abundant functional sites for record $C_2H_2/CO_2/C_2H_4$ separation. MOFs with such kind of optimal pore chemistry and pore size/shape are rare. Besides, such high stability in humid air and water is difficult to realize in anion pillared MOFs due to the weak Cu-N coordination bonds. Notably, our study include in-situ single crystal structure analysis, in-situ IR spectra analysis and DFT calculation. All the results are consistent and lead to the same conclusion. There has never been a report that provides such detailed mechanism study in $C_2H_2/CO_2/C_2H_4$ separation. Therefore, there are several novel points in this research and all of these can be found in the main text.

Comment 2. *Its seems that the customized pore environment helps to achieve higher selectivity however DFT studies, and in-situ X ray have been performed to corroborate the statement. Have the authors performed any in-situ IR to verify the conclusions? This evidence will help strengthen the case*

Author response: Thank you for your suggestion, the in-situ IR spectroscopy was conducted on gas-loaded and activated samples, and the results have added into supplementary materials. New and obvious stretching bands that belong to C_2H_2 and CO_2 are observed in the C_2H_2 and CO_2 dosed single crystals. The $\nu_{as}(C_2H_2)$ and $\nu(C\equiv C)$ stretching band of adsorbed C_2H_2 down-shifted to 3160 and 1720 cm^{-1} respectively with reference to the gas-phase value at 3287 and 2500-1900 cm^{-1}, indicating the existence of guest-host interactions. Similarity, $\nu(CO_2)$ band also undergoes a downward shift from gas-phase value 2349 cm^{-1} to 2335 cm^{-1}, showing the interactions between CO_2 and framework. In contrast, the stretching band of C_2H_4 is not obvious in C_2H_4@ZNU-6.

Modification:

Supplementary: Page 7 Figure 5

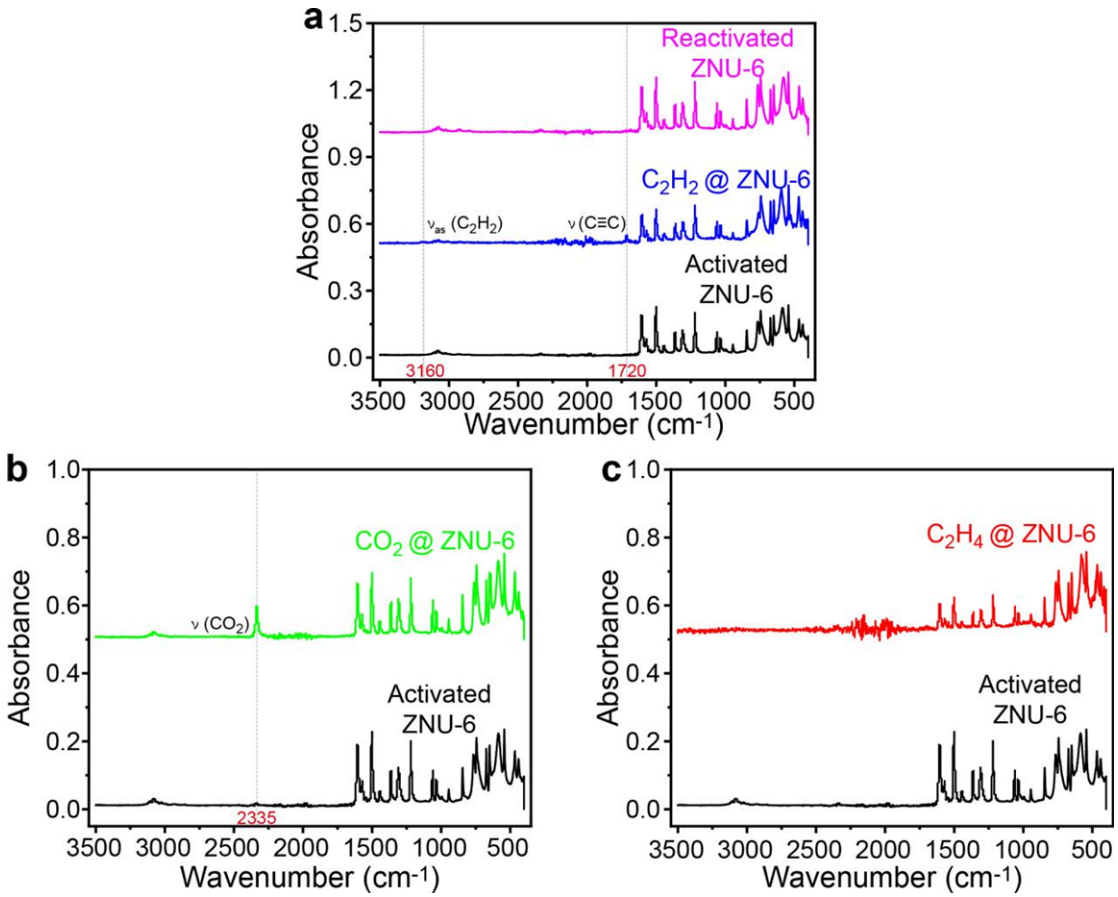

Supplementary Figure 5. In-situ IR spectra for **a.** activated ZNU-6 (black), -C_2H_2@ZNU-6 (blue) and re-activated ZNU-6 (purple); **b.** activated ZNU-6 (black) and CO_2@ZNU-6 (green); **c.** activated ZNU-6 (black) and C_2H_4@ZNU-6 (red).

All the IR spectroscopic data are recorded in a Nicolet iS5 ATR-FTIR spectrometer.

The samples of gas-loaded crystals were prepared by the method described in **Preparation of gas loaded ZNU-6** in manuscript.

As shown in the Supplementary Figure 5, new and obvious stretching bands that belong to C_2H_2 and CO_2 are observed in the C_2H_2 and CO_2 dosed single crystals. The $\nu_{as}(C_2H_2)$ and $\nu(C\equiv C)$ stretching band of adsorbed C_2H_2 down-shifted to 3160 and 1720 cm^{-1} respectively with reference to the gas-phase value at 3287 and 2500-1900 cm^{-1}, indicating the existence of guest-host interactions. Similarity, $\nu(CO_2)$ band also undergoes a downward shift from gas-phase value 2349 cm^{-1} to 2335 cm^{-1}, showing the interactions between CO_2 and framework. In contrast, the stretching band of C_2H_4 is not obvious in C_2H_4@ZNU-6.

Comment 3. *Heat of adsorption values and isotherm dependency with temp indicates the physisorption nature of guest /host chemistry. However, the additional interaction with anions and even TPA can provide some chemisorption in CO_2. Have the authors performed any Temp programed desorption studies in terms of gases of choice to see the binding behavior?*

Author response: Thank you for your suggestion. Firstly, there is no hysteresis in the desorption curves, indicating that the interactions between gas molecules and framework are not too strong. Secondly, we have performed the desorption at room temperature. The reactivation condition between the 5^{th} cycle and 6^{th} cycle adsorption experiment is under dynamic vacuum at room temperature for three hours, as shown in Supplementary Fig. 26, the uptake of 6^{th} cycle is similar with that of 5^{th} cycle. Such mild regeneration condition shows that the interactions between CO_2 and ZNU-6 are relatively week. Thus, it belongs to physisorption rather than chemisorption. Finally, as shown in in-situ crystals, the binding sites of CO_2 are close to GeF_6^{2-} anion in either large cage or small interlaced channel, this shows that the interactions between CO_2 and GeF_6^{2-} anion are stronger than those between CO_2 and TPA. Besides, due to the steric hinderance of pyridine rings, the CO_2 molecules are difficult to approach TPA ligands. In summary, we believe that the whole CO_2 adsorption behavior belongs to physisorption and the strongest interaction is between CO_2 and GeF_6^{2-} anion.

Comment 4. *What is the relative humidity used in this study?*

Author response: The relative humidity used in the breakthrough experiments is 60%.

Comment 5. *We can see ZNU-6 is strong water adsorbent however in humid conditions shows negligible deterioration of separation performance. However, the reasoning and data is not very clear, has the authors tried to quantify the effect of humidity in this case.*

Author response: We have quantified the effect of humidity on the breakthrough by calculating the C_2H_4 productivity. As shown in Table S9 in supplementary, the C_2H_4 productivity is 13.81 and 13.79 mol/kg respectively under dry and humid conditions. The productivity decrease is only 0.14%, in the range of measurement error . The reasons for the negligible deterioration are mainly attributed to the slow diffusion of water molecules in the framework. As shown in supplementary Fig 28 and 48, the H_2O adsorption is very slow. In real breakthrough conditions, less than 30% of saturated H_2O amount is adsorbed within 10.6 h while the gas mixture breakthrough experiments at 298 K are all finished within 200 min. The quite slow diffusion may be resulted from the small hydrophobic widows between large cage and interlaced channel. On the other hands, our in-situ single crystal structure have showed the water can be co-adsorbed in ZNU-6 without the reduction of gas loading. In the original main text (line 226-230), we have showed the reasons: “Although many water molecules can be adsorbed in ZNU-6, as described in in-situ crystals and water adsorption isotherms (Supplementary Fig. 27), the presence of humid has negligible influence on the separation performance (Fig. 5f). This is probably due to the co-adsorption of water and target gases as well as the fast $C_2H_2/CO_2/C_2H_4$ diffusion kinetics (Supplementary Fig. 29-31).”

Modifications:

Supplementary: Page 41 Figure 48

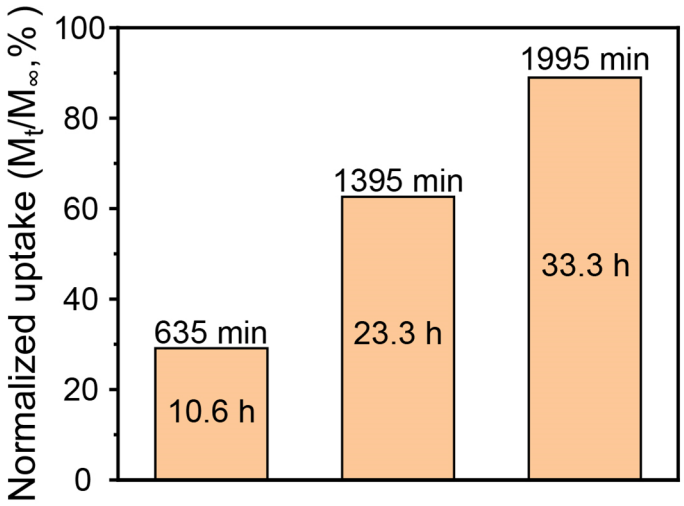

Supplementary Figure 48. H_2O uptake in breakthrough experiments (N_2, RH=100%). Flow rate: 5 mL/min.

Supplementary: Page 42 Table S9

Supplementary Table S9. Experimental dynamic C_2H_4 productivity and captured C_2H_2/CO_2 amount for ZNU-6 from different gas ratios and under different conditions.

Conditions	**Experimental C_2H_4 productivity (mol/kg)**
C_2H_2-CO_2-C_2H_4 (1-9-90) 298 K (dry)	13.81
C_2H_2-CO_2-C_2H_4 (1-9-90) 298 K (humid)	13.79

Comment 6. *In similar topic, what happen in desorption cases in breakthrough, I mean when the fixed bed is undergoing regeneration, have the authors quantified the effect of humidity in gas desorption cases and in cyclic performance?*

Author response: Thank you for your comment. We have conducted the desorption experiments respectively after the breakthrough experiments under dry and humid

conditions, the results are shown in the graph below. It is obviously that the influence of moisture is negligible on the process of the regeneration. This is also reflected by the overlapping (adsorption) breakthrough curves (Fig 5f).

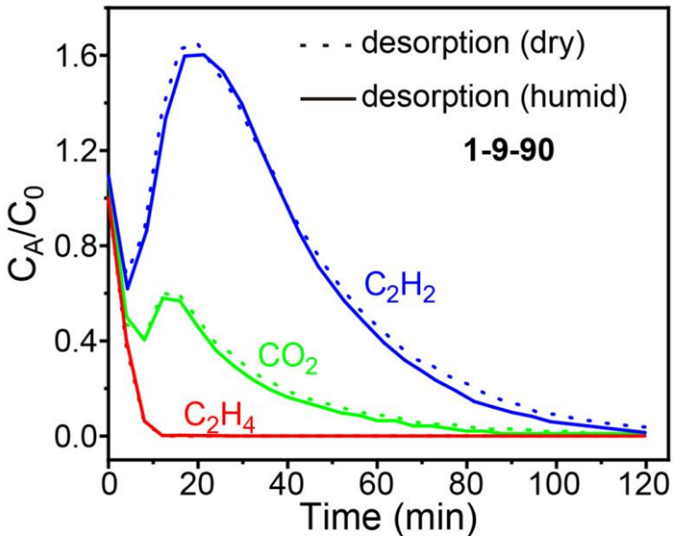

Comments from Reviewer 2:

Overall comment. *The authors reported a GeF_6^{2-} anion embedded MOF, ZNU-6, with optimized pore structure and environment for highly efficient C_2H_4 recovery from various $C_2H_2/CO_2/C_2H_4$ ternary mixtures. The material exhibited good recyclability and resistance toward moisture during breakthrough experiments. Ethylene (C_2H_4) purification from multi-component mixtures by physical adsorption is an important industrial challenging, and this work will be very interesting for the readers. The experiments were well performed and the manuscript has been written well. I agree that this manuscript to be accepted for Nature Communications after some minor revision. The following are the suggestions for the authors to improve the manuscript.*

Comment 1. *Figure 1 Caption, (f) is inconsistent with other numbering.*

Author response: Thanks for your reminder. We have corrected the Figure 1 Caption

Modification:

Manuscript: Page 5 Fig. 1

Fig. 1: a-c Exquisite control of pore size/shape and pore chemistry in ZNU-6 from pillared (3,4)-connected pto network to GeF_6^{2-} embedded ith-d topology framework; **d** Overview of ZNU-6 structure with cage-like pores and interlaced channels. **e** Structure and size of the cage-like pore. **f** Structure and size of the interlaced channel connecting four cages.

Comment 2.*Supplementary Figure 10-11, the authors should provide the pressure of these IAST selectivities.*

Author response: Thanks for your suggestion. We have added the pressure to the Supplementary Figure 13, 14.

Modification:

Supplementary: Page 14 Figure 13, 14

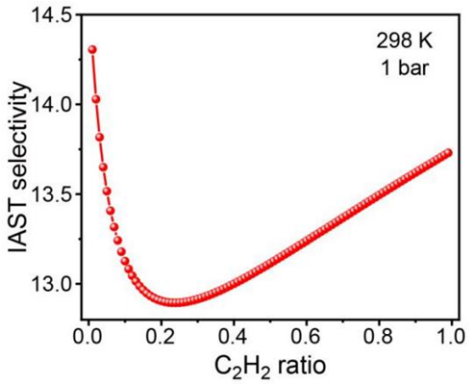

Supplementary Figure 13. IAST selectivity of **ZNU-6** towards gas mixtures of C_2H_2/C_2H_4 with different ratios at 298 K and 1 bar.

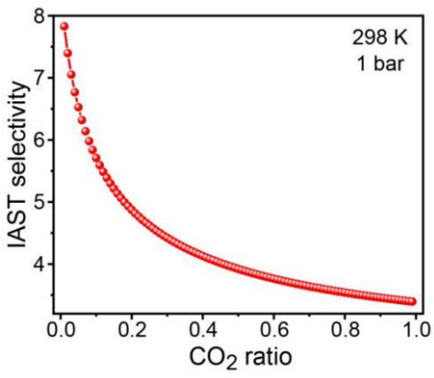

Supplementary Figure 14. IAST selectivity of **ZNU-6** towards gas mixtures of

CO_2/C_2H_4 with different ratios at 298 K and 1 bar.

Comment 3. *For the in-situ gas-loaded MOF structure, the authors should add a figure to describe the C_2H_2 gas molecule cluster and the interactions between the molecules, either in main text or SI. A figure illustrating the interaction between adsorbed water and gas molecules should also be added.*

Author response: Thanks for your suggestion. We have added the figures and the description to SI.

Modifications:

Supplementary: Page 6 Figure 3, 4

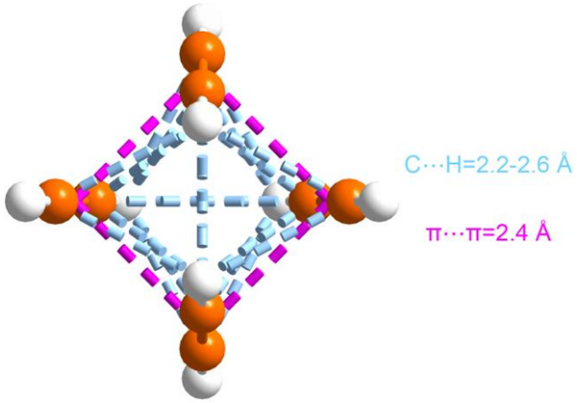

Supplementary Figure 3. The adsorption configuration of C_2H_2 moleucles inside the norrow channel (site I) of ZNU-6 with the formation of rare C_2H_2 clusters.The C-H interaction and π···π packing distance is highlighted.

There are two kinds of interactions between C_2H_2 molecules in the site I. One is the C···H interactions, whose distances are between 2.2 and 2.6 Å, and the other is π···π interactions between C≡C bonds, which are all in the distance of 2.4 Å.

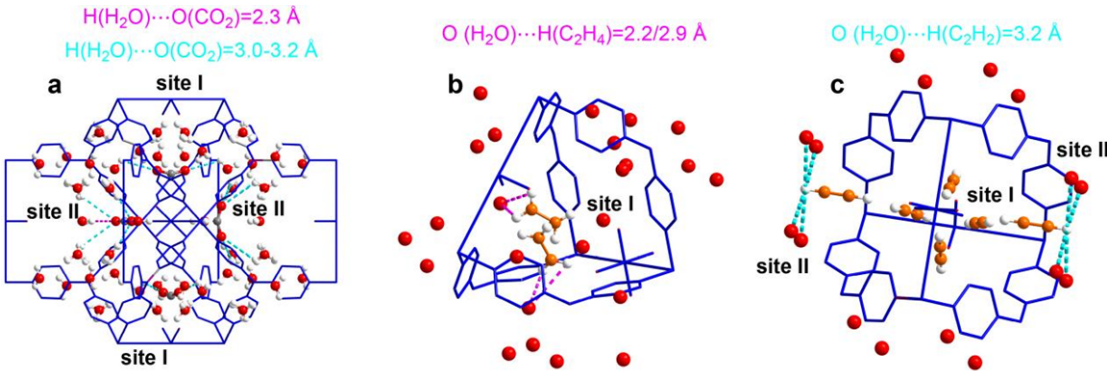

Supplementary Figure 4. Single crystals structure of gas loaded ZNU-6. a. $CuGeF_6C_{20}H_{16}N_{5.33}$ $(CO_2)_3$ $(H_2O)_{3.274}$. b. $CuGeF_6C_{20}H_{16}N_{5.33}$ $(C_2H_4)_{2.178}$ $(O)_{1.137}$. c. $CuGeF_6C_{20}H_{16}N_{5.33}$ $(C_2H_2)_{4.296}(O)_{0.517}$.

Due to the serious disorder of H atoms of H_2O molecules, we haven't solve the H atoms in C_2H_2 and C_2H_4 loaded ZNU-6. In CO_2 loaded crystal, besides 18 CO_2 molecules, there are 19.644 water molecules in each unit cell (sum formula $Cu_6Ge_6F_{36}C_{120}H_{96}N_{32}$). As to C_2H_4 loaded crystals, there are 13.068 C_2H_4 molecules and 6.822 H_2O molecules in an unit cell. In the C_2H_2 loaded crystals, the number of H_2O (3.102) is much lower than that of CO_2 or C_2H_4 loaded crystals. These H_2O vapor molecules don't occupy the adsorption site of targeted gas molecules. Instead, some weak interactions between H_2O and targeted gas molecules were observed. As shown above, The distances of H (H_2O) and O (CO_2) are 2.3-3.2 Å, those of O (H_2O) and H (C_2H_4) are 2.2 and 2.9 Å, and those of O (H_2O) and H (C_2H_2) are 3.2 Å.

Comments from Reviewer 3:

Thanks to its potential to introduce energy-efficient, single-step ethylene purification approaches, this manuscript by Jiang et al. is of high topical relevance to gas purifications, and MOFs for separations. Considering high importance of the new findings, and their general relevance in controlling the pore electrostatics (F···C=O interactions) driven gas separation/purification properties, I support publication subject to necessary revisions as follows:

Comment 1. *Molecular formulae are missing including that of the new as-synthesized*

ZNU-6 (although I find this formula in Table S7, should be clearly noted in the manuscript too). All molecular formulae for the gas-loaded phases should be clearly written in the main article, if needed, using a table with analysis of sorbate-sorbent interactions (distances).

Author response: Thank you for you valuable suggestion, we have added the formulae to the table and the corresponding places in the manuscript.

Modifications:

Manuscript: Page 4 Line 78-79

X-ray crystal analysis revealed that ZNU-6 ($Cu_6Ge_6F_{36}C_{120}H_{96}N_{32}$) crystallizes in a three-dimensional (3D) framework in the cubic Pm-3n space group.

Manuscript: Page 11 **Fig. 4**.

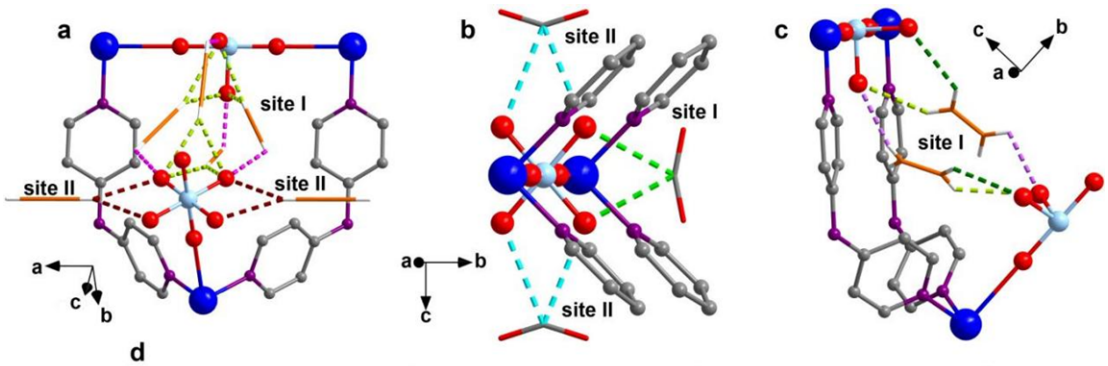

d

	Site I	Site II
25.78 C_2H_2 @ ZNU-6	1.97/2.55 Å (C-H···F)	2.51 Å (C-H···F)
18 CO_2 @ ZNU-6	2.64 Å (C···F)	2.80 Å (C···F)
13.07 C_2H_4 @ ZNU-6	2.31/2.54/2.64 Å (C-H···F)	--

Fig. 4: Single crystal structure of gas-loaded ZNU-6. a C_2H_2 @ ZNU-6 [$Cu_6Ge_6F_{36}C_{120}H_{96}N_{32}$ $(C_2H_2)_{25.78}$]; **b** CO_2 @ ZNU-6 [$Cu_6Ge_6F_{36}C_{120}H_{96}N_{32}$ $(CO_2)_{18}$]; **c** C_2H_4 @ ZNU-6 [$Cu_6Ge_6F_{36}C_{120}H_{96}N_{32}$ $(C_2H_4)_{13.07}$]; **d** Table of the distances of the host-guest interactions.

Comment 2. *The authors should not present the adsorption data with respect to*

molecules per GeF_6^{2-} anion, this makes the data skewed in favour of this adsorbent, ZNU-6. Also, the units for adsorption uptakes and pressure need to be consistent. Right now, with mixed use of cm^3/g, mmol/g, mol/mol and mmol/g, these are all mixed up; same mix-up is observed in the units used for pressure, bar and kPa. Collectively, all these mistakes come together in the manuscript Figure 2. I strongly recommend replotting the isotherm-based uptakes in one consistent pair of units: mmol/g and bar. This not only makes this manuscript coherent but also helps the whole community working in this area with regard to comparing performance parameters across different adsorbents.

Author response: Thanks for your suggestion, to make the manuscript coherent and also helps the whole community working in this area with regard to comparing performance parameters across different adsorbents. we have unified the pressure units to bar, and the uptake units to mmol/g in the manuscript, especially in the Fig. 2. The Fig. 2c that was the adsorption data with respect to molecules per anion before has been replaced by the adsorption data in the units of mmol/g as suggested and the origin Fig.2c has been moved to supplementary. However, we want to make an interpretation why we chose different units to present the adsorption data at first. Different units have different significance, mmol/g (or STP cm^3/g) is the basic uptake unit, the data in this units can be straightly obtained from the adsorption equilibrium measurements. While the density of single crystal is identified, the uptake data in cm^3/g can be converted to that in cm^3/cm^3 to evaluate the uptake of the adsorbent at a certain volume which is more useful for industrial application. To evaluate the influence of anions on the adsorption accurately, and to eliminate the effect brought by density and molecular mass simultaneously, mol/mol was chosen to be the uptake unit. The uptake data in mol/mol represents the number of the gas molecules those are adsorbed by per anion.

Modifications:

Manuscript: Page 2 Line 17

ZNU-6 exhibits significantly high C_2H_2 (1.53 mmol/g) and CO_2 (1.46 mmol/g) capacity at 0.01 bar.

Manuscript: Page 3 Line 47

However, the capacity of C_2H_2 (3.30 mmol/g) and CO_2 (2.20 mmol/g) is relatively low due to the over-contracted channel.

Manuscript: Page 3 Line 50-53

similar C_2H_2 (3.29 mmol/g) and CO_2 (2.04 mmol/g) capacity, but the C_2H_2/C_2H_4 and CO_2/C_2H_4 selectivity is greatly reduced as the C_2H_4 capacity (1.41 mmol/g) is relatively high.

Manuscript: Page 3 Line 58-61

Static gas adsorption isotherms showed that ZNU-6 takes up 1.53/8.06 mmol/g of C_2H_2 and 1.46/4.76 mmol/g of CO_2 at 0.01 and 1.0 bar (298 K), respectively. The calculated IAST selectivities for C_2H_2/C_2H_4 (1/99) and CO_2/C_2H_4 (1/99) are 43.8-14.3 and 52.6-7.8 (0.0001-1.0 bar), respectively.

Manuscript: Page 6 Line 104-106

At 1.0 bar, the C_2H_2 and CO_2 uptakes are 8.06 and 4.76 mmol/g (Fig 2c), higher than those of most APMOFs. The capacities are equal to 4.68 and 2.77 gas molecules per GeF_6^{2-} anion.

Manuscript: Page 6 Line 112-120

Notably, the uptakes of C_2H_2 and CO_2 on ZNU-6 at 0.01 bar are as high as 1.53 and 1.46 mmol/g, superior to those of all the porous materials in the context of ternary $C_2H_2/CO_2/C_2H_4$ separation, such as TIFSIX-17-Ni (1.38/0.32 mmol/g),[36] SIFSIX-17-Ni (0.91/0.20 mmol/g),[36] NTU-67 (0.47/0.65 mmol/g)[38] and TpPa-NO_2 (0.17/0.03 mmol/g)[39]. At 0.1 bar, the capacities of C_2H_2 and CO_2 reach up to 4.64 and 2.21 mmol/g (Fig. 2b), even higher than the uptakes of many porous materials at 1 bar and 298 K, for example, TIFSIX-17-Ni (3.30/2.20 mmol/g).[36] In the meantime, the

C_2H_4 uptakes on ZNU-6 at 0.01 and 0.1 bar are only 0.15 and 1.07 mmol/g, much lower than those of C_2H_2 and CO_2 under the same conditions. The C_2H_2, CO_2 and C_2H_4 adsorption isotherms were further collected at 278 and 308 K (Fig. 2d). The adsorption capacities of C_2H_2 and CO_2 at 1 bar increase to 8.74 and 6.26 mmol/g at 278 K.

Manuscript: Page 7 Fig.2

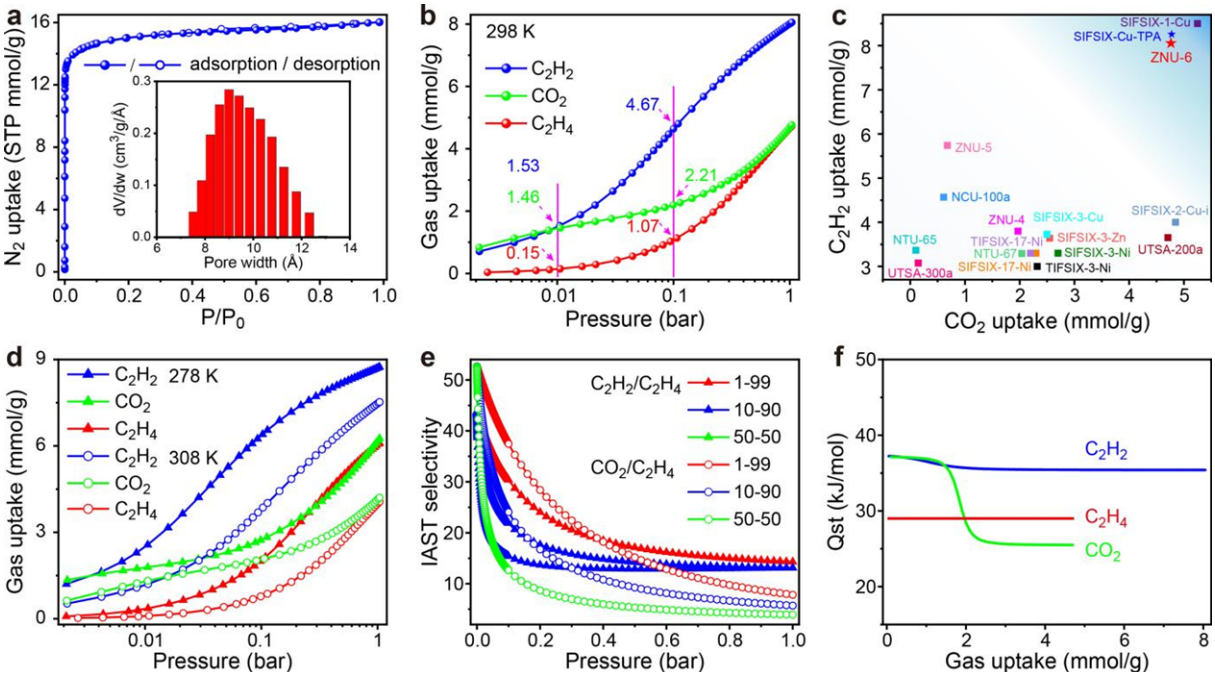

Fig. 2: The sorption performance. a N_2 adsorption and desorption isotherms for ZNU-6 and the calculated pore size distribution. **b** C_2H_2, CO_2 and C_2H_4 adsorption isotherms of ZNU-6 at 298 K. **c** Comparison of the saturated C_2H_2 and CO_2 uptake (1 bar, 298 K) among anion pillared MOFs. **d** C_2H_2, CO_2 and C_2H_4 adsorption isotherms of ZNU-6 at 278/308 K. **e** C_2H_2/C_2H_4 and CO_2/C_2H_4 IAST selectivity of ZNU-6 at 298 K. **f** Q_{st} of C_2H_2, CO_2 and C_2H_4 in ZNU-6.

Comment 3. *Page 2, lines 33-34, the authors need to discuss "Presently, multi-step purification process is adopted for purification of C_2H_4 from $C_2H_4/C_2H_2/CO_2$ mixtures." This needs to take cognisance of the recent reports on single-step C_2H_4 purification from ternary (1:1:1 for $C_2H_2/C_2H_4/C_2H_6$) and quaternary (1:1:1:1 for $C_2H_2/C_2H_4/C_2H_6/CO_2$) gas mixtures. Some examples include: Cao, JW. et al., Nat*

Commun. 2021, 12, 6507. Xu, Z. et al., Nat Commun. 2020, 11, 3163.

Author response: Thanks for your suggestion. However, we have to make a clarity: lines 33-34 in page 2 shows the industrial situation instead of the current status of C_2H_4 purification by physical adsorption. To avoid misunderstanding, we have modified the manuscript according to your advice, and we have added the references to the corresponding places in page 3 line 41-42.

Modifications:

Manuscript: Page 2 Line 33-34

Presently, multi-step purification process is adopted for purification of C_2H_4 from $C_2H_4/C_2H_2/CO_2$ mixtures in industry.

Manuscript: Page 3 Line 41-42

Besides, single-step purification of C_2H_4 from ternary $C_2H_2/C_2H_4/C_2H_6$[33, 34] or quaternary $C_2H_2/C_2H_4/C_2H_6/CO_2$[35] mixtures has also been realized by several porous materials.

Manuscript: Page 22

33. Xu, Z. et al. A robust Th-azole framework for highly efficient purification of C_2H_4 from a $C_2H_4/C_2H_2/C_2H_6$ mixture. *Nat. Commun.* **11**, 3163 (2020).

34. Gu, X.-W. et al. Immobilization of Lewis Basic Sites into a Stable Ethane-Selective MOF Enabling One-Step Separation of Ethylene from a Ternary Mixture. *J. Am. Chem. Soc.* **144**, 2614-2623 (2022).

35. Cao, J. -W. One-step ethylene production from a four-component gas mixture by a single physisorbent. *Nat. Commun.* **12**, 6507 (2021).

Comment 4. *I don't quite agree with the authors use of the word "static" in the heading of Figure 2. Should just be written as "The sorption performance." In another instance, the authors use this phrase "static adsorption" (page 11, line 202),*

which I object to.

Author response: Thank you for your suggestion. We have modified the Figure 2 caption and the sentence in the manuscript.

Modifications:

Manuscript: Page 7-8 Fig.2

Fig. 2: The sorption performance.

Manuscript: Page 11, line 206-207

Motivated by the high adsorption capacity and selectivity in single-component adsorption as well as the in-situ single crystal structure analysis, breakthrough experiments were conducted for C_2H_2/C_2H_4, CO_2/C_2H_4 and $C_2H_2/CO_2/C_2H_4$ mixtures.

Comment 5. *It is stated that the C_2H_4 productivity is 309 mL/g, again this unit is far from the standard unit typically used in other literature reports in this area, i.e., mol kg^{-1} h^{-1}*

Author response: Thank you for the reminder. However, the flow rate play a key role on the time of breakthrough experiment, as shown in Supplementary Fig. 34, 35, it is obvious that although the C_2H_2 captured amount is similar, the break time of C_2H_2 is evidently different under different flow rate. Therefore, it is unable to compare the separation performance with other materials under different flow rate if choosing mol kg^{-1} h^{-1} as the unit. Thus, we modified the units of productivity and captured amount to mol/kg, which is used quite often in literature.

Modifications:

Manuscript: Page 11-12, Line 211-220

For 1/1/98 $C_2H_2/CO_2/C_2H_4$ mixtures, C_2H_2 and CO_2 broke out simultaneously and 64.42 mol/kg of polymer grade C_2H_4 is produced by single adsorption process (Fig. 5b). The productivity is improved to 80.89 mol/kg when decreasing the temperature to

283 K (Supplementary Fig. 42). The CO_2 breakthrough time becomes shortened with the increase of CO_2 ratio, which is 72 and 52 mins for 1/5/94 (Fig. 5c) and 1/9/90 (Fig. 5d) $C_2H_2/CO_2/C_2H_4$ mixtures. The polymer grade C_2H_4 productivity is 21.37 and 13.81 mmol/kg, respectively. As most reported C_2H_4 productivity from $C_2H_2/CO_2/C_2H_4$ mixtures are compared under 1/9/90, a comparison plot of the C_2H_4 productivity and dynamic C_2H_2 capacity from 1/9/90 $C_2H_2/CO_2/C_2H_4$ mixtures is presented in Fig. 5e. ZNU-6 displays the record high C_2H_4 productivity and second highest C_2H_2 dynamic capacity. The C_2H_4 productivity of ZNU-6 is >2.5 folds of the previous benchmark of NTU-67 (5.42 mol/kg).

Manuscript: Page 13, line 245

The C_2H_2/anion and CO_2/anion uptakes are the highest among all the anion pillared MOFs. 64.42, 21.37, 13.81 mol/kg polymer grade C_2H_4 can be produced from $C_2H_2/CO_2/C_2H_4$ (1/1/98, 1/5/94, 1/9/90) mixtures, all superior to the previous benchmarks.

Manuscript: Page 13, Fig. 5e

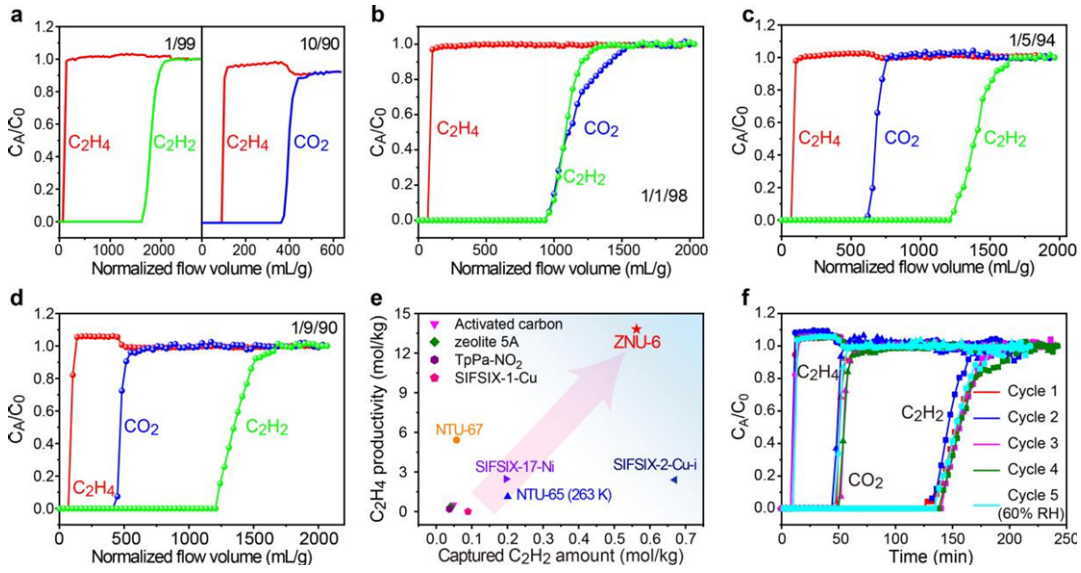

Supplementary: Page 42, Table S9

Supplementary Table S9. Experimental dynamic C_2H_4 productivity and captured C_2H_2/CO_2 amount for ZNU-6 from different gas ratios and under different conditions.

Conditions	Experimental C_2H_4 productivity (mol/kg)	Experimental C_2H_2 captured amount (mol/kg)	Experimental CO_2 captured amount (mol/kg)
C_2H_2-CO_2-C_2H_4 (1-1-98) 283 K	80.89	0.96	0.98
C_2H_2-CO_2-C_2H_4 (1-1-98) 298 K	64.42	0.78	0.84
C_2H_2-CO_2-C_2H_4 (1-1-98) 323 K	36.73	0.48	0.53
C_2H_2-CO_2-C_2H_4 (1-5-94) 298 K	21.37	0.60	1.52
C_2H_2-CO_2-C_2H_4 (1-9-90) 298 K	13.81	0.56	1.97
C_2H_2-CO_2-C_2H_4 (5-5-90) 298 K	11.04	2.65	0.55
C_2H_2-CO_2-C_2H_4 (1-9-90) 298 K (humid)	13.79	-	-

Comment 6. *Importantly, the authors have calculated productivity by integrating the effluent flow rate of C_2H_4 (cm^3/min). However, all the breakthrough curves (in Fig. 5) are showed in with the effluent concentration (C/C_0). It is obvious that integrating the concentration curve cannot give the amount, although a few references adopt this wrong method. Therefore, it is necessary to show the details for direct measurement and/or indirect calculation of the effluent flow rate and concentration in this study.*

See Shen, J. et al., Nat Commun. 2020, 11, 6259 as a reference.

Author response: Thank you for your question. However, we need to clarify one point that we choose mL/g as the unit of x-axis instead of cm^3/min, the normalized flow volume is calculated by the formula "Flow volume (mL/g)= flowrate (mL/min) × time (min) /sample weight (g)". The real flow rates and original figures of experiments with time (min) as x-axis had been presented in the supplementary. According to formula and the figure below, the flow rates have been considered in the calculation of C_2H_4 productivity. Therefore, the productivity can be straightly calculated out by the y-axis which represents effluent concentration (C/C_0).

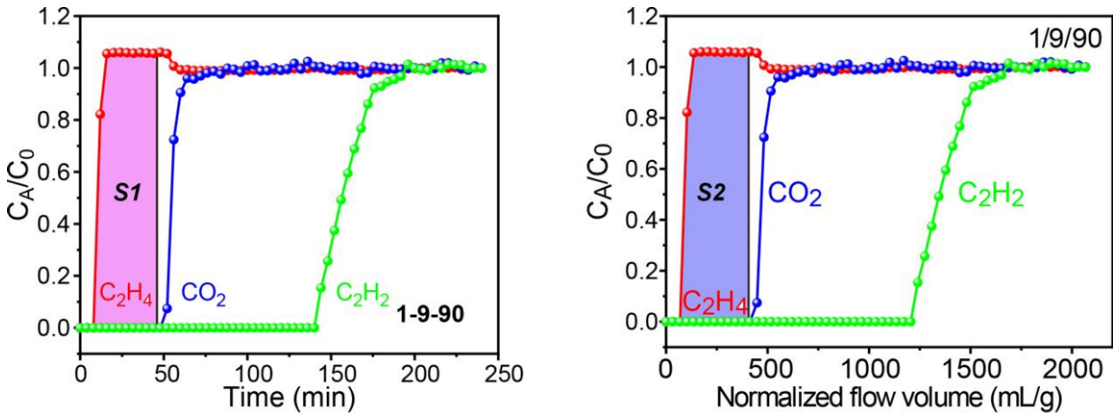

Flow volume (mL/g)= flowrate (mL/min) × time (min) /sample weight (g)

C_2H_4 productivity=S1 (min) x flowrate (mL/min) × time (min) /sample weight (g) = S2 (mL/g)

Comment 7. *How common / rare is the ith-d topology among the anion-pillared MOF library? It would greatly help the article/future readers, if the authors can address this by a thorough literature-based contextualisation of the structural topology of ZNU-6.*

Author response: Thank you for your reminder. To help the article/future readers understand clearly, we will give an introduction. According to the previous research papers and reviews [Li, Xu. et al. *Coord. Chem. Rev.* **470**, 214714 (2022)], among the APMOFs, just two MOFs with ith-d topology have been reported previously, namely SIFSIX-Cu-TPA [Li, H. et al. *Angew. Chem. Int. Ed.* **60**, 7547-7552 (2021)], ZNU-2

[TIFSIX-Cu-TPA, Jiang, Y. et al. *Angew. Chem. Int. Ed.* **61**, e202200947 (2022)].

Comment 8. *Section 7 in the supplementary information has a header "Breakthrough simulations and experiments", the following figure captions for Supplementary Figures 28-43 are all including "Experimental" in their figure captions, nonetheless. I wonder where the simulation-derived breakthrough data is?*

Author response: Thank you for your kind reminder, we have corrected the header of section 7.

Modification:

Supplementary: Page 33

V Breakthrough experiments

Overall, an interesting idea executed by the authors that should advance this area in the near future. I will be glad to look at a suitably revised article, when ready.

Comments from Reviewer 4:

This manuscript by Jiang et al, report a metal organic framework (ZNU-6) for the application of simultaneous removal of C_2H_2 and CO_2 from C_2H_4 stream. This area is of important practical applications and has been extensively investigated in the past few years. The overall quality of this manuscript is high with detailed investigation of the structure characterisation of the MOF, study of its adsorption properties using isotherm and breakthrough experiments, and thorough investigation of the host-guest interactions. Below are some comments and questions from me, and I would recommend the publication of this manuscript after the authors fully address them:

Comment 1. *I think it is necessary that the authors reference some highly relevant publications in the introduction, e.g. Hexafluorogermanate (GeFSIX)*

Anion-Functionalized Hybrid Ultramicroporous Materials for Efficiently Trapping Acetylene from Ethylene, Ind. Eng. Chem. Res. 2018, 57, 21, 7266–7274.

Author response: Thank you for your suggestion, we have added some references to the introduction, such as ref. 25, 26.

Modifications:

Manuscript: Page 21

25. Zhang, Z.-Q. et al. Hexafluorogermanate (GeFSIX) Anion-Functionalized Hybrid Ultramicroporous Materials for Efficiently Trapping Acetylene from Ethylene. *Ind. Eng. Chem. Res.* **57**, 7266-7274 (2018).

26. Ke, Tian. et al. Molecular Sieving of C_2-C_3 Alkene from Alkyne with Tuned Threshold Pressure in Robust Layered Metal-Organic Frameworks. *Angew.Chem. Int. Ed.* **59**, 12725-12730 (2020).

Comment 2. *The cif. File for CO_2 loaded ZNU-6 shows an O-C-O bond angle of CO_2 being 157° instead of the theoretical 180°, could the authors please explain this discrepancy.*

Author response: Thank you for your valuable comment. The slight distortion of CO_2 is caused by the relatively strong interaction between F atoms and C atom of CO_2. Similar phenomena have been observed in other research papers [*Chem. Commun.* **41**, 5125-5127 (2008), *Chem* **5**, 950-963 (2019)].

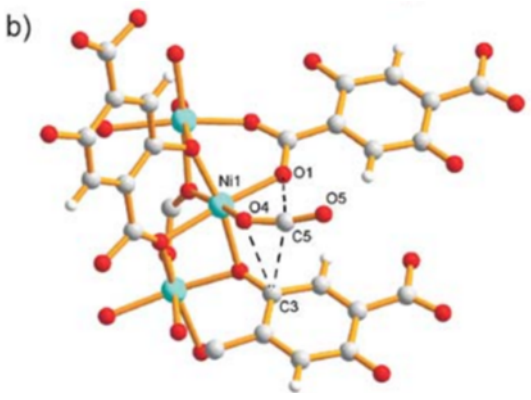

CO_2 @ CPO-27-Ni [*Chem. Commun.* **41**, 5125-5127 (2008)] The angle of C-O-C is 162°

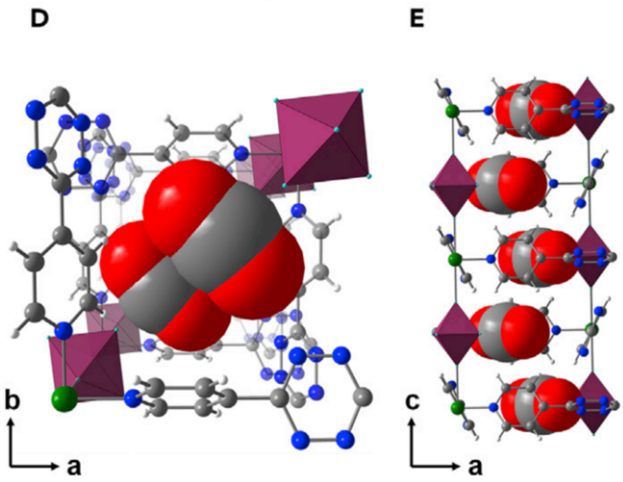

CO_2 @ dptz-$CuTiF_6$ [Chem 5, 950-963 (2019)] The angle of C-O-C is 167°

Comment 3. *Figure 2f, the Qst for CO_2, why it showed a sudden drop at 2 mmol/g coverage?*

Author response: Thank you for your comment. From in-situ crystal CO_2 @ ZNU-6，two binding sites can be observed, and the ratio of the number of CO_2 molecules adsorbed in the site I/II is 1:2. According to the DFT calculations, the binding energy in site I is stronger than that in site II, so CO_2 prefer to be adsorbed in site I. Therefore, at the first stage of the whole adsorption, CO_2 is adsorbed in site I until the uptake in site I reach to saturated point (≈1.72 mmol/g), at the following stage, CO_2 begin to be adsorbed in the site II, while the binding energy in site II is lower, so the whole Q_{st} begins to decrease. Because the ratio of CO_2 molecules adsorbed in site I/II is 1:2, the decrease of Q_{st} is sharp. Line 173-174 has described the phenomenon.

Comment 4. *From the isotherms for CO_2 and C_2H_4 (Figure 2b, 2d), the saturation uptake for CO_2 and C_2H_4 are very close; and the kinetic data (supplementary figure 25) of CO_2 and C_2H_4 are also similar with C_2H_4 being slightly faster in adsorption. For Qst, CO_2 started higher than C_2H_4 then fall to be lower than C_2H_4. These three parameters (uptake, kinetic, Qst), all seem indicating the interaction between the gas*

molecules and the framework is very similar. In this case, how do the authors rationalise the observed separation in breakthrough experiments? what do the authors think is the really reason that ZNU-6 can retain CO_2 from mixtures containing mainly C_2H_4 and small percentage of CO_2.

Author response: Thank you for your valuable comment. The near-zero loading Qst is more important to distinguish the adsorption affinity. Thus, CO_2 and C_2H_2 are more favored to be adsorbed in ZNU-6. Besides, according to the DFT calculations, C_2H_2, CO_2 and C_2H_4 are all preferentially adsorbed in the site I, and according to the binding energy, the affinity sequence in site I is also C_2H_2~CO_2>C_2H_4. From the in-situ crystals, nearly all C_2H_4 molecules are adsorbed in the site I. So the Q_{st} of C_2H_4 calculated from single-component adsorption isotherms reflects the isosteric enthalpy of C_2H_4 in the interlaced channel. However, when the single-component C_2H_4 adsorption changes to competitive C_2H_2/CO_2/C_2H_4 mixture adsorption, the situation will become different. Because the affinity towards C_2H_2 and CO_2 in site I is higher than that towards C_2H_4, the C_2H_2 and CO_2 gases will occupy the interlaced channel (site I) and C_2H_4 adsorption sites will have to be changed to the large cage (site II). While in site II, the binding energy of C_2H_4 is much lower. In brief, it is mainly the much higher Q_{st} of CO_2 at near-zero loading that distinguishes CO_2 from C_2H_4.

REVIEWERS' COMMENTS

Reviewer #1 (Remarks to the Author):

The authors in this manuscript have very reasonably addressed all of my and other reviewers' comments and made/performed the necessary changes and experiments required for the quality of the manuscript. I agree with the technical soundness of this paper. I have no other concerns or reservations about this manuscript.

Reviewer #2 (Remarks to the Author):

The authors have done a good job of improving the manuscript by performing necessacry experiments and analyses. And they have answered the all questions of the reviewers. I agree that this manuscript now can be published on Nature Communications.

Reviewer #3 (Remarks to the Author):

I will be glad to see a revised article published, below are my revision comments:
• Regarding the molecular formula, the authors write Cu6Ge6F36C120H96N32 as the formula. This is not the right way of writing formula for MOFs, the authors need to revise all these places having formula with something like [Cun(TPA)x(GeF6)y], where, n, x and y are integers suites to the molecular formula of ZNU-6.
• Regarding the use of units mmol/g and bar, I am satisfied with the revisions done by the authors.
• Glad about the authors edits on including a few updated citations from 2020, 2021, and 2022.
• I appreciate the authors omitting the word “static” before “adsorption”.
• I do not quite agree with the authors arguing that use of the more commonly used unit for productivity, mol kg-1 h-1 will neglect flow rate. The calculation of productivity with respect to this unit takes into account the flow rate used, and therefore, the authors are again advised to use the unit mol kg-1 h-1 for quantifying the C2H4 productivity.
• I am glad about the authors argument on the productivity calculations based on the plots presented in C/C0 vs. time (min).
• The authors’ response (in the revised introduction) on quantifying the rarity of ith-d topology among anion-pillared family of MOFs is satisfactory.
Overall, I will be glad to look at a suitably revised article, when ready.

Reviewer #4 (Remarks to the Author):

The authors have fully addressed my comments, and I feel the manuscript is ready for publication.

Reviewer #3 (Remarks to the Author):

I will be glad to see a revised article published, below are my revision comments:

1. Regarding the molecular formula, the authors write $Cu_6Ge_6F_{36}C_{120}H_{96}N_{32}$ as the formula. This is not the right way of writing formula for MOFs, the authors need to revise all these places having formula with something like $[Cu_n(TPA)_x(GeF_6)_y]$, where, n, x and y are integers suites to the molecular formula of ZNU-6.

2. Regarding the use of units mmol/g and bar, I am satisfied with the revisions done by the authors.

3. Glad about the authors edits on including a few updated citations from 2020, 2021, and 2022.

4. I appreciate the authors omitting the word “static” before “adsorption”.

5. I do not quite agree with the authors arguing that use of the more commonly used unit for productivity, mol kg-1 h-1 will neglect flow rate. The calculation of productivity with respect to this unit takes into account the flow rate used, and therefore, the authors are again advised to use the unit mol kg-1 h-1 for quantifying the C_2H_4 productivity.

6. I am glad about the authors argument on the productivity calculations based on the plots presented in C/C_0 vs. time (min).

7 The authors’ response (in the revised introduction) on quantifying the rarity of ith-d topology among anion-pillared family of MOFs is satisfactory.

Overall, I will be glad to look at a suitably revised article, when ready.

I will be glad to see a revised article published, below are my revision comments:

Comment 1 *Regarding the molecular formula, the authors write* $Cu_6Ge_6F_{36}C_{120}H_{96}N_{32}$ *as the formula. This is not the right way of writing formula for MOFs, the authors need to revise all these places having formula with something like* $[Cu_n(TPA)_x(GeF6)_y]$*, where, n, x and y are integers suites to the molecular formula of ZNU-6.*

Author response: Thank you for your suggestion. We have modified the molecular formula in the manuscript and supplementary material.

Modification:

Manuscript: Page 4 Line 78-79

X-ray crystal analysis revealed that ZNU-6 $[Cu_6(GeF_6)_6(TPA)_8]$ crystallizes in a three-dimensional (3D) framework in the cubic Pm-3n space group.

Supplementary: Table S1.

Formula	$C_{20}H_{16}Cu$ $F_6GeN_{5.33}$ $Cu(GeF_6)(TPA)_{1.33}$	$C_{20}H_{16}CuGeF_6$ $N_{5.33}\cdot 4.296C_2H_2$ $Cu(GeF_6)(TPA)_{1.33}$ $(C_2H_2)_{4.296}$	$C_{20}H_{16}CuGeF_6$ $N_{5.33}\cdot 2.178C_2H_4$ $Cu(GeF_6)(TPA)_{1.33}$ $(C_2H_4)_{2.178}$	$C_{20}H_{16}CuGeF_6$ $N_{5.33}\cdot 3CO_2$ $Cu(GeF_6)(TPA)_{1.33}$ $(CO_2)_3$

Comment 2 *Regarding the use of units mmol/g and bar, I am satisfied with the revisions done by the authors.*

Author response: Thank you for your positive comment.

Comment 3 *Glad about the authors edits on including a few updated citations from 2020, 2021, and 2022.*

Author response: Thank you for your positive comment.

Comment 4 *I appreciate the authors omitting the word "static" before "adsorption".*

Author response: Thank you for your positive comment.

Comment 5 *I do not quite agree with the authors arguing that use of the more commonly used unit for productivity, mol* kg^{-1} h^{-1} *will neglect flow rate. The calculation of productivity with respect to this unit takes into account the flow rate used, and therefore, the authors are again advised to use the unit mol* kg^{-1} h^{-1} *for quantifying the* C_2H_4 *productivity.*

Author response: Thank you for your suggestion. We have added the productivity in the unit of mol kg^{-1} h^{-1} to the corresponding places. We have chose two time period, one is from 0 to **Time 1**, and the other is from 0 to **Time 2** as shown in Supplementary Table 10..

Modification:

Manuscript: Page 12 Line 220-222

C_2H_4 productivity with the unit of mol/kg/h is also calculated for comparison (Supplementary Table S10). ZNU-6 with the productivity of 15.93 mol/kg/h is still the best material.

Supplementary: Table 10/11

Supplementary Table S10. Experimental dynamic C_2H_4 productivity for different adsorbents.

	$C_2H_2/CO_2/C_2H_4$=1/9/90 (v/v/v) Flow rate: 5 mL/min					
	ZNU-6	NTU-67	Activated carbon	zeolite 5A	SIFSIX-2-Cu-i	SIFSIX-17-Ni
Mass (g)	0.58	1.20	0.98	1.74	0.52	0.82
Time 1[a] (min)	52.00	43.59	21.40	13.18	12.61	12.24
Time 2[b] (min)	196.00	84.38	34.19	45.89	170.08	83.82
Time 1 (min g^{-1})	89.56	36.17	21.84	7.58	24.20	14.96
Time 2 (min g^{-1})	337.58	70.03	34.89	26.40	326.44	102.42
Productivity per adsorption cycle (mol kg^{-1})	13.81	5.42	0.49	0.36	2.40	2.47
Productivity based on Time 1 (mol kg^{-1} h^{-1})	15.93	7.46	1.38	1.62	11.41	12.10
Productivity based on Time 2 (mol kg^{-1} h^{-1})	4.23	3.85	0.86	0.46	0.85	1.77

[a] Time 1 is the time when the second gas can be detected after C_2H_4;

[b] Time 2 is the time when C_A/C_0 reaches 1.0 for all the gases.

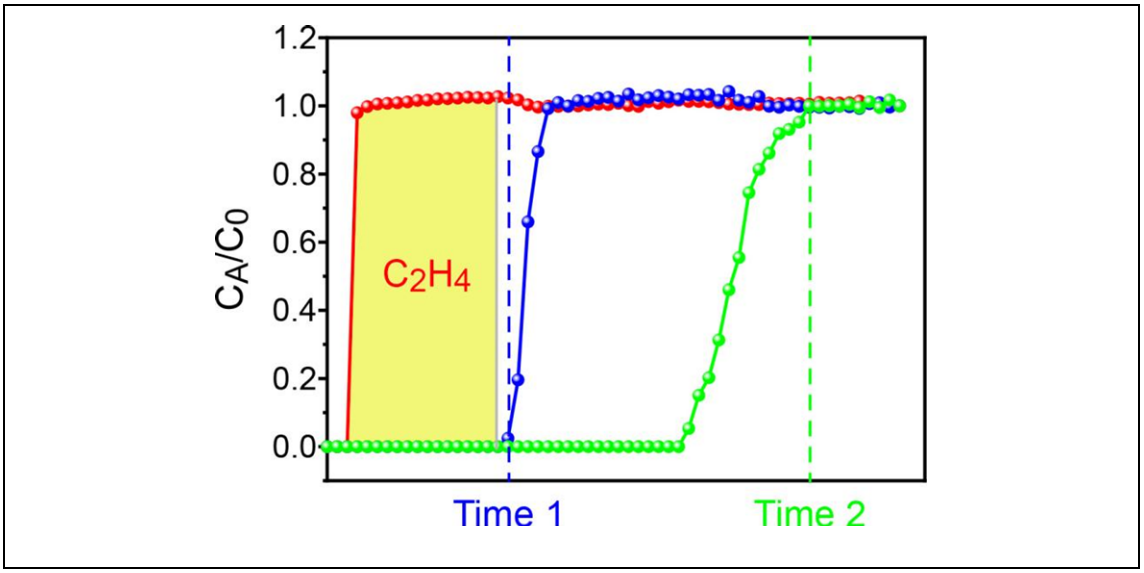

Supplementary Table S11. Experimental dynamic C_2H_4 productivity for ZNU-6 from different gas ratios and under different conditions.

	ZNU-6 Flow rate: 5 mL/min						
$C_2H_2/CO_2/C_2H_4$ (v/v/v)	1-1-98 283 K	1-1-98 298 K	1-1-98 323 K	1-5-94	1-9-90 dry	5-5-90	1-9-90 humid
Time 1 (min)	232.00	184.00	112.00	72.00	52.00	44.00	112.00
Time 2 (min)	284.00	248.00	180.00	192.00	196.00	180.00	180.00
Productivity per adsorption cycle (mol kg^{-1})	80.89	64.42	36.73	21.37	13.81	11.04	13.79
Productivity based on Time 1 (mol kg^{-1} h^{-1})	20.92	21.01	19.68	17.81	15.93	15.05	7.39
Productivity based on Time 2 (mol kg^{-1} h^{-1})	17.09	15.59	12.24	6.68	4.23	3.68	4.60

Comment 6 *I am glad about the authors argument on the productivity calculations based on the plots presented in C/C_0 vs. time (min).*

Author response: Thank you for your positive comment.

Comment 7 *The authors' response (in the revised introduction) on quantifying the rarity of* ***ith-d*** *topology among anion-pillared family of MOFs is satisfactory.*

Author response: Thank you for your positive comment.

Overall, I will be glad to look at a suitably revised article, when ready